CONTROLLING THERMAL PROPERTIES OF ASPHALT CONCRETE AND ITS MULTIFUNCTIONAL APPLICATIONS

A Thesis

by

XIJUN SHI

Submitted to the Office of Graduate and Professional Studies of
Texas A&M University
in partial fulfillment of the requirements for the degree of

MASTER OF SCIENCE

Chair of Committee,	Philip Park
Co-Chair of Committee,	Dallas Little
Committee Member,	Partha Mukherjee
Head of Department,	Robin Autenrieth

August 2014

Major Subject: Civil Engineering

ABSTRACT

Controlling infrastructure temperature, especially flexible pavement, has attracted attention in both industrial and academic societies because: 1) material properties of asphalt, and corresponding structural responses and distresses are temperature dependent and 2) pavement surface temperature directly relates to various environmental or safety problems. This study investigates the feasibility of mitigating the temperature-related problems of civil infrastructures (especially asphalt pavement) by controlling thermal properties of the construction materials. To change thermal properties of asphalt concrete, expanded polypropylene (EPP) pellet and graphite were selected as the additives and mixed into asphalt concrete. Experimental tests are classified into two categories: 1) physical and thermal characterizations of raw materials including Scanning Electron Microscope and heat susceptibility tests, and 2) mechanical and thermal properties of the modified asphalt mixtures via indirect tensile test and hot disk test, respectively. The heat susceptibility test results show that use of EPP as an aggregate replacement is a better choice than the use of the melted-EPP as a binder modifier because it has a good heat susceptibility and is hard to melt at the HMA working temperature. The mechanical performances and thermal properties evaluation results show that by replacing the aggregate with EPP to have 18% by volume of total mixture, the indirect tensile strength was reduced by 17%, and the thermal conductivity and volumetric heat capacity decreased by 32% and 27%, respectively. By adding 4.8 vol. % of graphite, the indirect tensile strength decreased by 20%, and an increase of 43% in thermal conductivity was obtained.

To simulate the effect of the thermally modified asphalt mixtures on the surface temperature of pavements and bridges, a series of heat transfer analysis were conducted using the finite difference heat transfer model. In addition, a case study of a building using EPP modified cement concrete was carried out to investigate the benefits of EPP modified concrete as a wall insulation. From the simulation results, it is concluded that adding graphite into asphalt mixture mitigates the urban heat island effect during summer by dropping the maximum surface temperatures of both pavement and bridge (3.1ºC and 1.9ºC, respectively, with 4.8% graphite), and the graphite modified asphalt concrete can reduce the use of deicing agents during winter by increasing the minimum surface temperature by 0.5ºC for pavement and 0.2ºC for bridge. On the other hand, adding EPP increases maximum surface temperature by 0.8ºC for pavement and 1.0ºC for bridge during winter, which show the potential for snow and ice removal application. In addition, the simulation shows that the EPP modified concrete can serve as a wall insulator.

DEDICATION

To My Father, Hantang Shi,

To My Mother, Xiulan Shi

for their kind support, love and patience.

ACKNOWLEDGEMENTS

I would like to express my deepest appreciation to my academic advisor, Dr. Philip Park, for his continued support and encouragement. It is not only his profound knowledge, but also his diligence, his precision, and his whole academic ethic, which guide and motivate me to overcome difficulties in this research. Without his assistance, this thesis would not have been possible.

I owe many thanks to my committee co-chair Dr. Dallas Little and committee member Dr. Partha Mukherjee for their valuable suggestions. Having had a chance to work and learn from them was a wonderful experience that will benefit me my whole life.

I am grateful to my research teammates, Enrique Ivers, Ikkyun Song, Mirmilad Mirsayar, and Younho Rew, as they have spent a great deal of time helping me in the lab. I also sincerely appreciate my friends at the Materials and Pavement division in Texas A&M University, Aishwarya Baranikumar, Abdul Kabbara, Fan Gu, Fan Yin, Lorena Garcia, Shi Chang, and Dr. Yuqing Zhang for their continued assistance and encouragement.

A special thanks to Dr. Robert Lytton and Dr. Chang-Seon Shon. Dr. Lytton is a distinguished and well respected professor, and his comments and suggestions helped guide me to successfully establish the pavement heat transfer model. Dr. Shon is an assistant research scientist in Texas A&M Transportation Institute, and he brought many ideas to this study and prepared the thermal properties of concrete samples for me.

I also take this opportunity to express my gratitude to Dr. Earl Stenger for financial support and trust in this research. Thank you to the JSP Inc., Asbury Carbon Inc., Knife River Corporation, and Jebro Inc. for providing us with expanded polypropylene, aggregate, graphite and asphalt binder, respectively, for the research.

I could never deny the contributions that were made by Texas A&M University facilities to this research. The Materials Characterizations Facility allowed me to take Scanning Electron Microscope images of the additives. The McNew Lab of Texas A&M Transportation Institute provided me with an excellent facility for producing and testing asphalt mixtures. The Materials and Structures Lab of Aerospace Engineering gave me the access to use the TPS 2500S device, from which I obtained thermal properties of multiple asphalt concrete samples.

Finally, I am extremely thankful for all the love, support, and patience from my family. Though thousands miles away from each other, I believe our hearts have been always connected firmly.

TABLE OF CONTENTS

Page

Page

LIST OF FIGURES

Page

Page

Page

Page

Page

LIST OF TABLES

Page

Page

1. INTRODUCTION

Asphalt concrete is a mixture primarily containing aggregate, asphalt binder, and air void. An asphalt concrete pavement is not just a thin cover over soil, but an engineered structure being deteriorated under various loading and environment conditions. To ensure a good mechanical performance, the asphalt pavement requires various structural performances including rutting, fatigue, and thermal cracking resistance, moisture susceptibility and so on.

Besides, non-structural functions of pavements and their applications have been attracting a lot of attentions in both academic and industrial societies recently. The pavement system can be designed to have multifunctional properties including electrical and thermal conductivity, sensing and actuation, energy harvesting/storage, self-healing capability, electromagnetic interference (EIM) shielding, recyclability, and biodegradability (Gibson 2010).

Various additives like polymer, conductive fillers, and fibers could be added into asphalt concrete to impart non-structural functions. Among the various non-structural properties, the utilization of the electrical and thermal properties of paving materials have huge potentials to provide sustainable solutions to the pavement systems, and the related papers have been continuously published during the past few decades. The probable non-structural functions of asphalt concrete containing different additives is listed in Figure 1.

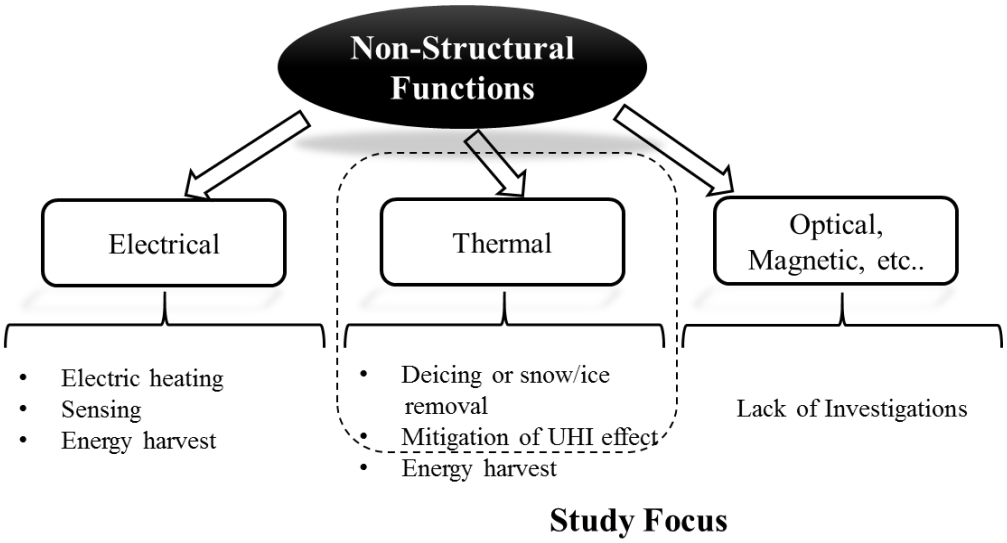

Figure 1. Non-structural properties of asphalt concrete and the probable applications

1.1 Problem Statement

Overall performances of the flexible pavements are highly affected by the pavement temperature. It is widely accepted that asphalt is time and temperature dependent material, and temperature has a significant influence on the mechanical performance of pavements. The different pavement temperatures induce the different structural responses, so that the corresponding distresses will be different. Meanwhile, pavement temperature also directly affects to various environmental or safety problems. Asphalt pavement covering the large area of cities, is considered to be one of the major causes of Urban Heat Island (UHI) effect. During the summer time, the asphalt pavement surface can be heated up to around 60ºC. The pavement stores heat, and radiates back to the surrounding environment. The UHI effect causes the problems of air quality and additional use of energy to cool buildings (Mallick et al. 2009). Conversely, in the cold

climate, the pavements may reach a very low temperature so that the ice layer is formed on the surface. The slippery and wet surface of pavements will threaten the traffic safety.

This study aims to evaluate the feasibility of mitigating the above temperature-related problems of pavements by changing thermal properties of asphalt concrete. To change thermal properties of asphalt concrete, two additives - expanded polypropylene (EPP) with low thermal conductivity and graphite with high thermal conductivity - are employed and their thermal and mechanical effects are investigated.

1.2 Research Objectives

The objective of this study is to investigate the feasibility of mitigating the temperature-related problems of civil infrastructures by changing thermal properties of construction materials especially focusing on asphalt concrete. The EPP and graphite are used as additives to change thermal properties of asphalt concrete. In the first phase, their effects on thermal and mechanical properties are evaluated experimentally. Then, the changes in the temperature distributions in pavement structures, bridge decks, and concrete walls of buildings are simulated by using a heat transfer model. The flow chart of the research plan is shown in Figure 2. Following topics are investigated in this study:

1. The mixing and compaction properties of EPP and graphite modified asphalt concrete

2. The mechanical performance of EPP and graphite modified asphalt concrete (through indirect tensile test)

3. The changes in thermal properties (e.g., heat capacity and thermal conductivity) by adding EPP and graphite

4. The effects of the thermally modified construction materials on the temperature of typical civil structures

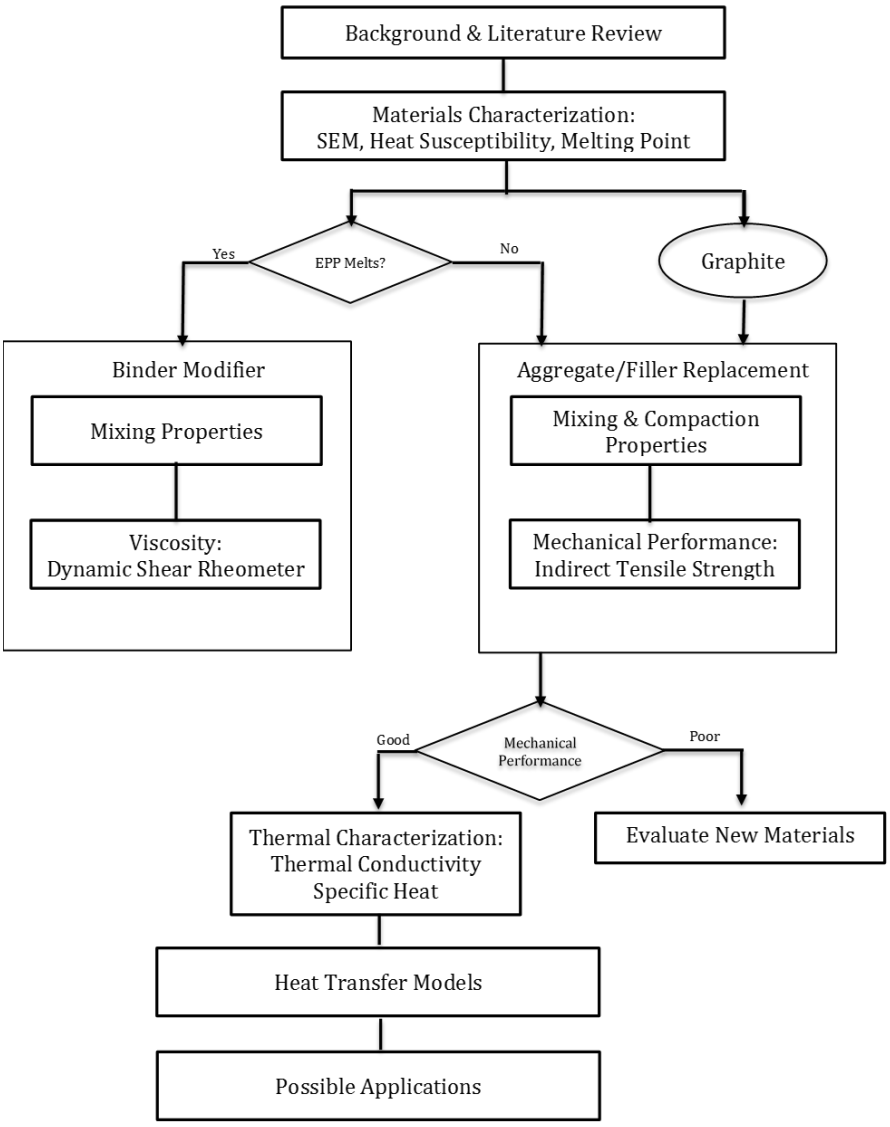

Figure 2. Flow of the research

1.3 Methodology and Thermal Additives

In this study, the EPP pellets and graphite powder (Figure 3) are added into asphalt concrete as an aggregate replacement and filler replacement, respectively. The EPP pellets are small particles with average diameter of 3.3mm, which is the size of No. 8 aggregates (aggregates passing No.4 sieve but remaining on No.8 sieve), and the graphite powder has the size smaller than 0.212 mm. To modify asphalt concrete, No.8 aggregates are replaced by EPP with different volume contents, while graphite specimens are made by replacing fillers by different weight percent of mastic (mixture of filler and asphalt).

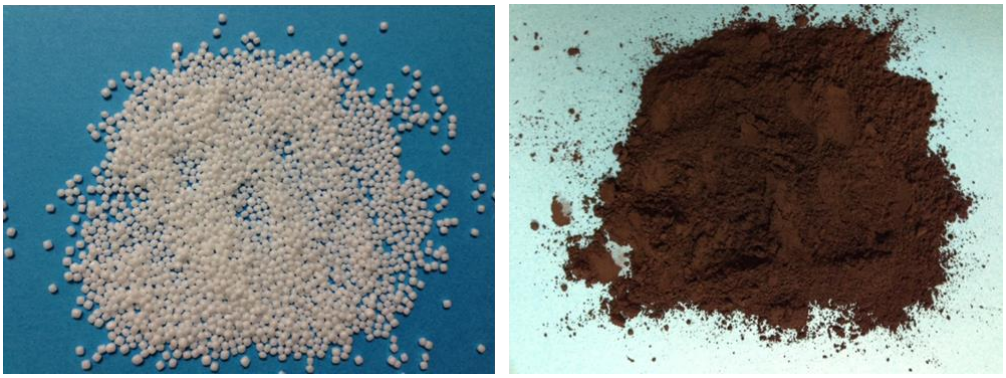

Figure 3. Expanded polypropylene (left) and graphite (right)

The melting point of EPP used in this study is reported as 170ºC by manufacturer. Since the mixing temperature of hot mix asphalt (HMA) in the field is the range from 135ºC to 177ºC, there is chance that the EPP particles melt into asphalt during the mixing process. The melted EPP and the solid EPP pellets will cause different influences on performance of asphalt concrete, and hence, the heat stability of EPP in the asphalt mixing temperature range are investigated.

The mechanical performances of both EPP and graphite modified asphalt concrete are very important factors in considering the field application. Because of the small particle size and small content (up to 4.8% by total volume of mixture), the graphite is expected not to cause significant damage in asphalt concrete. However, EPP pellets are much bigger in size, and added higher volume percent (up to 18% by total volume of mixture). Moreover, the air bubble inside EPP as well as lacking of surface angularity may change the mechanical performance of the modified asphalt concrete dramatically.

Once the mechanical performances are qualified, the thermal properties of the modified asphalt concrete will be evaluated from the test. The EPP and graphite may lead the changes of thermal properties in two different directions. The EPP pellets have low thermal conductivity, and may serve as a barrier for the heat transfer within the asphalt specimens. Conversely, the graphite has a higher thermal conductivity ($24.0\ \mathrm{W/m \times K}$) than Portland cement ($0.530\ \mathrm{W/m \times K}$) (www.matweb.com), the modified asphalt concrete is expected to have a higher thermal conductivity.

The changes in the temperature of a pavement and bridge by using thermally modified asphalt concrete are investigated via a model based on finite difference approximation method of heat transfer. The effect of the additives on construction wall of buildings is evaluated as a case study using steady state heat transfer theory. Figure 3 summarizes the flow of the research.

1.4 Thesis Outline

This thesis consists of six sections, and their contents are as follows:

Section 1 gives the introduction of the study topic. Problems are stated and the objectives of the research are stated.

Section 2 presents a comprehensive literature review related to the study. Previous publications focusing on the use of polypropylene and graphite as pavement additives are summarized. Approaches to mitigate thermal problems caused by hot and cold weather conditions (e.g., the urban heat island effect during summer and the formation of ice and snow during winter) are reviewed. Publications regarding heat transfer models to predict pavement temperature distribution are also included.

Section 3 explains the theoretical background of the heat transfer theory. The physical and mathematical equations for developing the heat transfer model are given in this section.

Section 4 presents the experimental set-ups and test results. Experimental methodologies evaluating mechanical performance and thermal properties of the thermally modified asphalt concrete are described. Indirect tensile strengths and thermal properties of the modified asphalt concrete are obtained and compared to the control specimens.

Section 5 describes simulation studies for different infrastructures. Feasibility of the thermally modified asphalt concrete to mitigate temperature-related problems in pavement and bridge are evaluated. A case study on the use of EPP modified cement concrete as insulation for building wall is also included.

Section 6 gives conclusions from the study and illuminates the future research that need to be done.

2. LITERATURE REVIEW

A literature survey is carried out to illuminate the current trend of temperature-related problems of civil infrastructures focusing on asphalt pavements, as summarized as follows:

2.1 Use of Additives for Asphalt Concrete

Mixing various additives is considered as an effective way to improve structural performances of flexible pavements. Table 1 lists some common additives and their general structural purposes (Roberts et al. 1996). In the meantime, some additives are also added into asphalt concrete to impart non-structural functions including electrical, thermal, optical, and magnetic functions to make pavement more sustainable. This section reviews the previous investigations using polypropylene and graphite as asphalt concrete additives.

Table 1. Common pavement additives and their structural purposes (Roberts et al. 1996)

Type	General Purpose or Use	Generic Examples
Rubber	Increase HMA stiffness at high service temperatures Increase HMA elasticity at medium service temperatures to resist fatigue cracking Decrease HMA stiffness at low temperatures to resist thermal cracking	Natural latex Synthetic latex (e.g., Polychloroprene latex) Block copolymer (e.g., Styrene-butadiene-styrene (SBS)) Reclaimed rubber (e.g., crumb rubber from old tires)
Plastic		Polyethylene/polypropylene Ethylene acrylate copolymer Ethyl-vinyl-acetate (EVA) Polyvinyl chloride (PVC) Ethylene propylene or EPDM Polyolefins
Rubber-Plastic Combinations		Blends of rubber and plastic
Fiber	Improving tensile strength of HMA mixtures Improving cohesion of HMA mixtures Permit higher asphalt content without significant increase in draindown	Natural: Asbestos Rock wool Manufactured: Polypropylene Polyester Fiberglass Mineral
Oxidant	Increase HMA stiffness after the HMA is placed	Manganese salts
Antioxidant	Increase the durability of HMA mixtures by retarding their oxidation	Lead compounds Carbon Calcium salts
Hydrocarbon	Restore aged asphalt cements to current specifications Increase HMA stiffness in general	Recycling and rejuvenating oils Hard and natural asphalts
Antistripping Agents	Minimize stripping of asphalt cement from aggregates	Amines Lime
Waste Materials	Replace aggregate or asphalt volume with a cheaper waste product	Roofing shingles Recycled tires Glass

2.1.1 Use of Polypropylene as Asphalt Concrete Additive

Generally, polymers are widely used as the asphalt modifier. Since the asphalt has viscoelastic properties, it will have a high stiffness at low temperature or fast loading rate and low stiffness at high temperature or slow loading rate. Styrene-butadiene-styrene (SBS), styrene-butadiene rubber (SBR), ethylene vinyl acetate (EVA), and polyethylene are commonly used polymers to improve asphalt rheological properties, so that modified asphalt will have (1) higher stiffness at high service temperatures to reduce rutting distress and (2) lower stiffness at low and intermediate temperatures to obtain good fatigue resistance. The effect of polymer modifiers on the asphalt binder viscosity is shown in Figure 4.

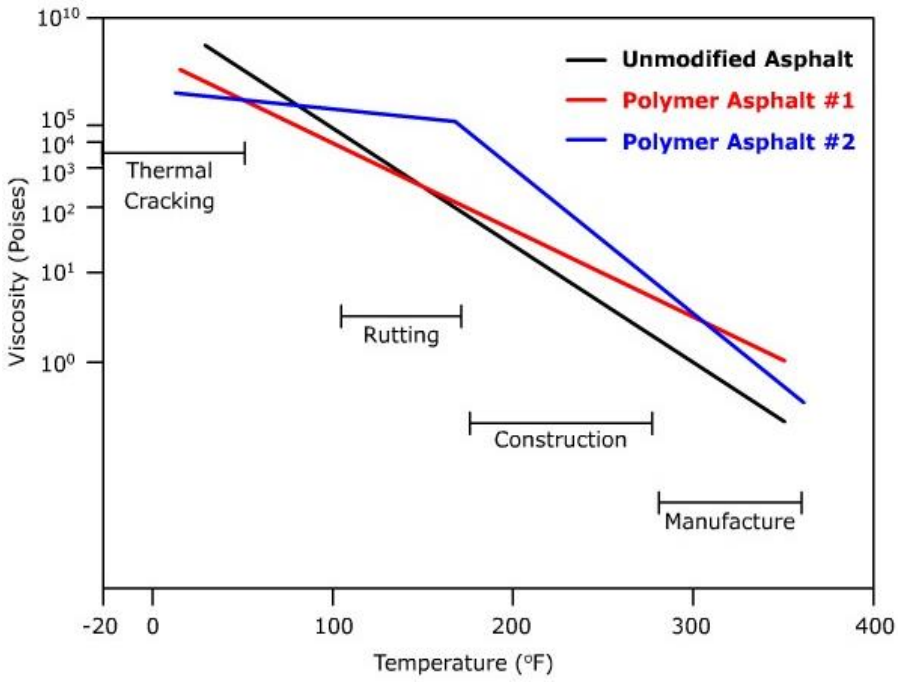

Figure 4. Effect of polymer modifier on asphalt binder viscosity (Sebaaly et al. 2002)

Nowadays, fibers are expected to take on an increasingly prominent role in reinforcing asphalt concrete. During the recent years, many research groups around the world conducted different investigations on various types of fibers use (Fan et al. 2010; Gui-juan 2010; Song et al. 2011; Xiong et al. 2011; Zhao et al. 2011). Among the various fibers involved in the tests, basalt fiber, polyester fiber, polyacrylonitrile fiber, brucite fiber, graphite fiber, carbon fiber, and mineral fiber are the most popular choices. Besides reinforcement effect, mineral and cellulose fibers are widely used as a stabilizer to prevent asphalt draindown, which is a typical distress occurred in open-graded friction courses.

Polypropylene (PP), a thermoplastic polymer, is widely used in both academic and industrial fields, acting as either a binder modifier or fiber reinforcement. However, regarding its non-structural function, very few published papers have been found.

Several researchers used PP materials as asphalt modifiers. Mixing property is a dominant factor that determines modification effect of the polymer. It is fairly hard to blend PP with asphalt not only due to its high melting point (130ºC~171ºC), but also because of its high tendency to crystallize that limits interaction with asphalt (Othman 2010). Yeh et al. (2005) studied asphalt modified by isotactic polypropylene (IPP) and maleated polypropylene (MPP) and found MPP had a better compatibility with asphalt than IPP. To improve efficiency of mixing PP with asphalt, polymer powder has been utilized to ensure a better contact between the two materials. Al-Hadidy and Yi-Qiu (2009) blended 1, 3, 5 and 7 wt. % of PP powder with asphalt at 160ºC. They concluded: 1) Penetration decreased as PP content increased. 2) Softening point of asphalt increased by

adding PP material 3) PP reduced temperature susceptibility of asphalt. These conclusions pretty matched experimental results of (Abtahi et al. 2013).

Due to the difficulty of mixing PP with asphalt, PP fibers are more widely utilized to reinforce asphalt concrete, and more papers were published focusing on PP fiber reinforcement than PP modifier. Abtahi's research team made big contributions in this area. In 2011, they used 6mm and 12mm long PP fibers that were blended with aggregates first at 0.1%, 0.2%, 0.3% and 0.5% by total weight of asphalt concrete to make specimens in accordance with Superpave method. Their results showed adding PP fiber increased Marshall stability, air void and reduced flow properties. In another research of Abtahi et al. (2013), asphalt concrete was reinforced using glass and PP fibers of 12mm by length. The concrete samples were made by adding PP fibers to asphalt at 150ºC while blending glass fibers with aggregates. It was found that combination of 0.1% of glass fiber and 6% PP fiber will have the highest Marshall stability and lowest flow. The authors believed that these benefits were caused by high modulus of glass fibers and good adhesive properties between PP and asphalt binder.

Findings from Tapkin's research studies in the past also showed PP fiber has good reinforcement effects on asphalt concrete. Tapkın (2008) published a paper indicating that Marshall properties of asphalt concrete improved by adding PP fibers. Modified asphalt concrete specimens exhibited good rutting resistance, prolonged fatigue life and less reflection crackings.

Al-Hadidy and Yi-Qiu (2009) studied PP fiber reinforced SMA mixture. Their experiments results manifested that PP fiber had positive effects on Marshall properties

and strengths. According to mechanistic-empirical design software results, they believed that adding PP could reduce the thickness of surface layer.

2.1.2 Use of Graphite as Asphalt Concrete Additive

Graphite, as a typical electrical conductor, was mainly added to asphalt concrete to impart electrical conductivity. The possible non-structural applications of electrically conductive asphalt concrete would include electric heating, sensing, energy harvesting and so on (Baranikumar 2013).

Besides higher electrical conductivity, graphite has a higher thermal conductivity compared to regular pavement materials as well. Several research teams used graphite in order to control the thermal properties of asphalt concrete. As thermal properties differ, asphalt pavement would have different temperature distribution, potential temperature-related problems would be mitigated.

Wu et al. (2008) published a paper investigating the temperature distribution of pavement containing graphite powder modified asphalt concrete. They recorded an increase of thermal conductivity and a decrease of heat capacity of modified asphalt concrete when graphite content increased. Based on a two-dimensional finite element model, they believed the variation of pavement temperature between nighttime and daytime was reduced. Chen et al. (2010) used 18% of graphite by volume of asphalt binder to modify asphalt concrete layer and conducted both simulation analysis and validation tests. They concluded graphite modified asphalt concrete had a higher thermal conductivity compared to unmodified sample. This thermal properties change led to a

decrease of pavement asphalt layer temperature and a reduction of extreme temperature distribution fluctuations in the asphalt pavement.

A summary of literatures using polypropylene and graphite as asphalt concrete additives is shown in Figure 5.

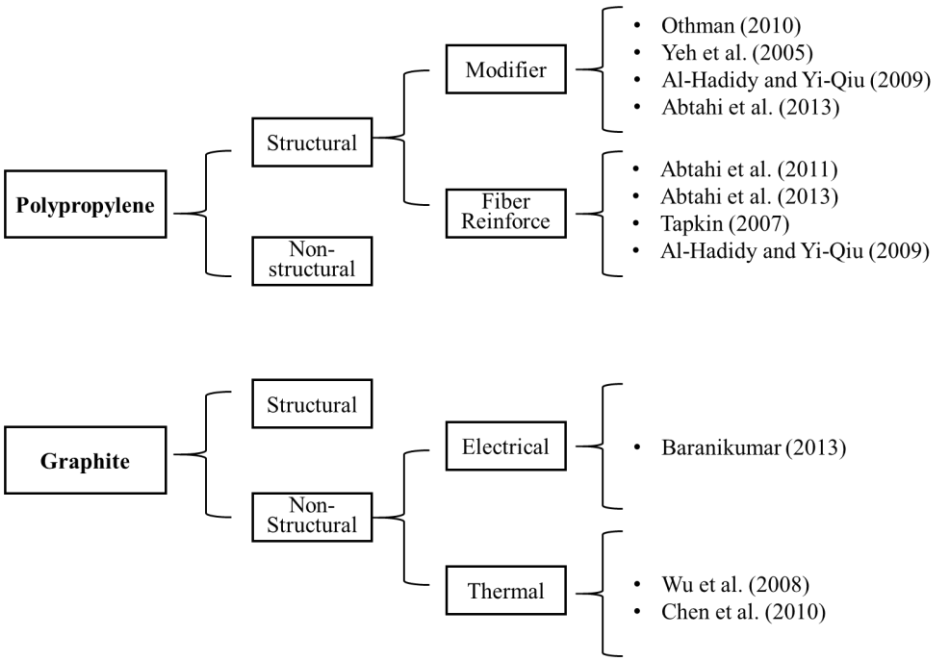

Figure 5. Literatures using polypropylene and graphite as asphalt concrete additives

2.2 Approaches to Control Thermal Properties of Asphalt Concrete

Various approaches were designed to control the thermal properties of asphalt concrete.

Both Chen et al. (2012) and Guan et al. (2011) carried out similar investigations using different phase-change materials to change the thermal properties of asphalt pavement. According to the experimental results, different PCMs had different effects on asphalt pavement, they could either increase or decrease thermal properties of the mixtures.

Lightweight aggregate (LWA) have been found to have lower thermal conductivity and thermal diffusivity compared to conventional asphalt mixture. Khan and Mrawira (2008) investigated the impact of mix design on the thermal behaviors of asphalt pavement consisting of LWA, they found that thermal properties of LWA asphalt mixtures seemed to be insensitive to asphalt binder grade and aggregate gradation.

More comprehensively, Dawson et al. (2012) tried to control the thermal properties of asphalt concrete by replacing limestone with quartzite, cooper slag, Cu fiber and lytag respectively, the mechanical performances of different mixtures were evaluated as well. Their results showed: 1) Adding quartzite in asphalt mixture increased thermal conductivity, improved fatigue performance, but decreased stiffness. 2) Copper fibers increased thermal conductivity slightly, but resulted in a significant improvement of stiffness and fatigue resistance. 3) The use of LWA and copper slag decreased the thermal diffusivity, it is good to heat storage in the pavement, and could reduce the risk of the damage during freeze-thaw cycling. 4) Compared to limestone, quartzite mixture reduced maximum surface temperature by up to 4^{o}C, this could, potentially mitigate rutting distress and Urban Heat Island Effect.

2.3 Mitigation of Pavement Temperature-Related Problems

2.3.1 Efforts on Mitigation of Heat Island Effect

Different methods have been tried to mitigate the urban heat island effect, which is largely contributed by asphalt pavement.

Solar radiation is the major source of heat increasing pavement temperature. Because of good heat absorption of asphalt, pavement surface could be heated up to a very high temperature during the summer time. To mitigate this effect, Chen et al. (2009) applied a solar heat reflective coating on top of the asphalt pavement. The coating was made of resin, pigments, fillings and other additives. According to their investigation, a reduction of 8ºC of asphalt concrete surface temperature as well as better pavement rutting resistance was observed.

Instead of blocking solar energy absorbed by pavement, Guan et al. (2011) added phase change materials (PCM) into asphalt concrete to increase the thermal conductivity and specific heat of the mixture. Using this approach, the found that pavement temperature change rate decreased and the extreme temperature was delayed.

Xie et al. (2011) added infrared powder into asphalt concrete. This powder material is able to absorb heat energy and radiates it into the environment. According to their results, a reduction in the near-earth atmospheric temperature was recorded during their study.

Another famous idea was proposed by Mallick et al. (2009). An appropriate fluid flowing in pipes was installed within the pavement to transfer and store heat. The authors

believed that the concept was feasible according to the results from both laboratory tests and modelling simulation.

Besides, Gui et al. (2007) ran a comprehensive simulation using one dimensional pavement heat transfer model to evaluate the effects and sensitivities of thermo-physical properties on pavement surface temperature. Their results indicated that increasing albedo, emissivity, thermal conductivity and volumetric heat capacity will decrease pavement maximum surface temperature, therefore helping mitigate urban heat island effect during summer.

A summary of approaches for mitigating urban heat island effect is listed in Table 2.

Table 2. Efforts of mitigation of urban heat island effect

Citation	Method	Major Conclusions
Gui et al. (2007)	Pavement heat transfer model simulation	Increasing albedo, emissivity can decrease maximum surface temperature Increasing thermal conductivity and volumetric heat capacity can decrease maximum surface temperature, however increase minimum temperature.
Mallick et al. (2009)	Fluids flowing in pipes	The pavement temperature reduced. Rutting reduced.
Chen et al.(2009)	Solar reflective coating	A reduction of 8ºC of asphalt concrete surface temperature were observed.
Guan et al. (2011)	Add phase change material	Thermal conductivity & specific heat increased. Temperature change rate decreased.
Xie et al. (2011)	Add infrared powder	Temperature of pavement surface & cooling rate decreased with higher powder amount.

2.3.2 Efforts on Mitigation of Snow and Ice Formation

In contrast to mitigate heat island effect, preventing snow and ice formation on the pavement surface during winter has been a significant issue as well, especially in many northern area of United States. A review of recently efforts on pavement snow and ice formation is summarized in this section.

The most conventional approach to remove snow and ice covered on the surface of pavement is to use snow-melting agent. Both inorganic salts and organic compounds would chemically prevent water molecules from binding, therefore decreasing the freezing point. Among all the agents, chloride salt is the most widely used around the world. Zhao and Zhang (2011) added certain proportion of chloride into asphalt mixture and created a chloride-stored asphalt concrete to help pavement delay or even prevent ice formation. According to their investigation, the stored chloride could be released effectively, contributing to a better pavement anti-icing ability. Meanwhile, the mechanical performance of concrete was also improved. Though chloride salts turned out to be a good solution to snow and ice problem, such salts are corrosive and will damage the road and bridge easily. Organic compounds are more environmentally friendly, but their applications are limited because of high prices, and sometimes they will cause refreezing phenomenon.

Porous asphalt pavement is an environmentally friendly choice to help with deicing. According to Houle et al. (2010), Porous asphalt pavement had a very good performance in northern climates. The pavement surface was not only faster to clear ice and snow, but also had a better friction resistance than conventional pavements.

Another interesting investigation was carried out in China by Chen (2013). They used fracture mechanics theory to study ice layer failure. They believed that under repeated traffic load, the cracking of ice layer initialed and propagated, ice failure occurred as long as the cracking density reached to a certain limit. In their research, crumb rubber was added to decrease the modulus of asphalt concrete, therefore the pavement had a larger deformation under the same traffic loading. Both simulation and experiments results indicated larger deformation helped ice layer fail more easily, hence the use of the crumb rubber in asphalt concrete improve the ice and snow removal ability of pavement.

A research team from China developed an asphalt solar collector (ASC) that would be beneficial for melting snow and ice on top of pavement surface during winter. Wu et al. (2008) , Wu et al. (2009) and Chen et al. (2011) conducted a series of studies on ASC. In their device design, pipes circuits were installed below asphalt pavement surface to absorb and transfer solar energy during summer. Graphite powder were utilized as thermal conductive fillers to improve the efficiency. The stored energy is used not only to melt the snow and ice covered on the road, but also to provide heat to the adjacent buildings during winter time.

Approaches on pavement deicing and snow and ice removal are summarized in Table 3.

Table 3. Efforts of pavement deicing and snow and ice removal

Citation	Method	Major Conclusions
Zhao and Zhang (2011)	Create chloride-stored asphalt concrete	Stored chloride could be released effectively, contributing to better anti-icing ability. Mechanical performance was improved.
Houle et al. (2009)	Porous asphalt pavement	The pavement surface was faster to clear snow and ice. A better friction resistance was obtained.
Chen (2013)	Add crumb rubber	Decreased modulus resulted in larger deformation, which was conductive to ice layer failure.
Wu et al.(2008) Wu et al. (2009) Chen et al.(2011)	Asphalt solar collector	Pipe circuits absorbed and transferred solar energy during summer and restored in winter Graphite powder increased thermal conductivity of pavement, improving efficiency of the asphalt collector

2.4 Temperature Distribution Prediction Model

Because of the significance of temperature to the material properties, various researchers exerted a great deal of effort to seek a quick and efficient way to determine pavement temperature. Barber (1957) was one of the first person proposed a method to calculate the pavement maximum temperature. The equations were simple, but the method was not accurate because it used total daily radiation rather than hourly radiation.

To solve the heat transfer problem of pavement system, finite difference approximation method was widely used. The Enhanced Integrated Climatic Model (EICM), initially developed for the FHWA and then adapted for use in the Mechanistic-Empirical Pavement Design Guide (MEPDG), follows finite difference approximation

method for calculating pavement temperature. However, large errors of the prediction results have been found when compared to field data (Ahmed et al. 2005).

Based on formulas for convection, shortwave radiation and long-wave radiation described by Solaimanian and Kennedy (1993), Hermansson (2000) developed a one dimensional pavement temperature prediction model use finite difference theory as well. The accuracy of the model was proved by comparing calculated and measured temperatures using the data from Long-Term Pavement Performance (LTPP) program (Hermansson 2001).

Besides one dimensional model, two-dimensional, transient finite difference approach (Yavuzturk et al. 2005) and three dimensional finite element method (Minhoto et al. 2005) have also been used. Considering the simplicity, a one dimensional temperature prediction model was established by following the formulas explained by (Mrawira and Luca 2002) in this study.

3. THEORETICAL BACKGROUND

3.1 Heat Transfer Terms

Temperature manifests the average randomized kinetic energy of particles in matter, and heat is the transfer of thermal energy across a system boundary into the body or from the body to the environment. Heat capacity, thermal conductivity, and heat diffuse are thermal properties of matter that will directly related to heat transfer.

Heat capacity (c): Heat capacity is defined as the ratio of the amount of heat energy transferred to an object and the corresponding rise in temperature of the object,

$$c \equiv \frac{\Delta q}{\Delta u} \tag{1}$$

In science and engineering, it is more convenient to express heat capacity in relation to a unit mass. Therefore, the specific heat is defined as the heat capacity per unit mass of a material. In engineering area, the volumetric heat is also used. Volumetric heat capacity is one of the two material's thermal properties used in this study.

Thermal conductivity (k): Thermal conductivity is the physical property of a material to conduct heat, defined as thermal energy transferred per unit time and per unit surface area, divided by temperature difference. The higher the thermal conductivity is, the faster the heat will transfer.

Thermal diffusivity (α): Thermal diffusivity is the thermal conductivity divided by density and specific heat. The parameter is used to determine the capacity of a material to conduct thermal energy relative to its capacity to store thermal energy.

$$\alpha = \frac{k}{\rho c_p} \quad (2)$$

Where k is thermal conductivity ($W/(m \times K)$)

ρ is density (kg/m^3)

c_p is specific heat capacity ($J/kg \times K$)

Heat equation: The heat equation is a parabolic partial differential equation that describes the distribution of heat in a given region over time.

The mathematical statement of the equation is

$$\frac{\partial T}{\partial t} - \alpha\left(\frac{\partial^2 T}{\partial x^2} + \frac{\partial^2 T}{\partial y^2} + \frac{\partial^2 T}{\partial z^2}\right) = 0 \quad (3)$$

Where temperature T (x,y,z,t) is a function of three spatial variables (x,y,z) and the time variable t.

α is thermal diffusivity

In this study, the pavement temperature distribution model is simplified as one dimensional problem, gives the heat equation as:

$$\frac{\partial T}{\partial t} - \alpha\left(\frac{\partial^2 T}{\partial z^2}\right) = 0 \quad (4)$$

Where temperature T (z,t) is a function of spatial variable z and the time variable t.

3.2 Heat Transfer Theory for Pavement

The temperature distribution of pavement system is determined by the heat transfer between pavement surface and surrounding environment, and the heat conduction within pavement. The concept is shown in Figure 6:

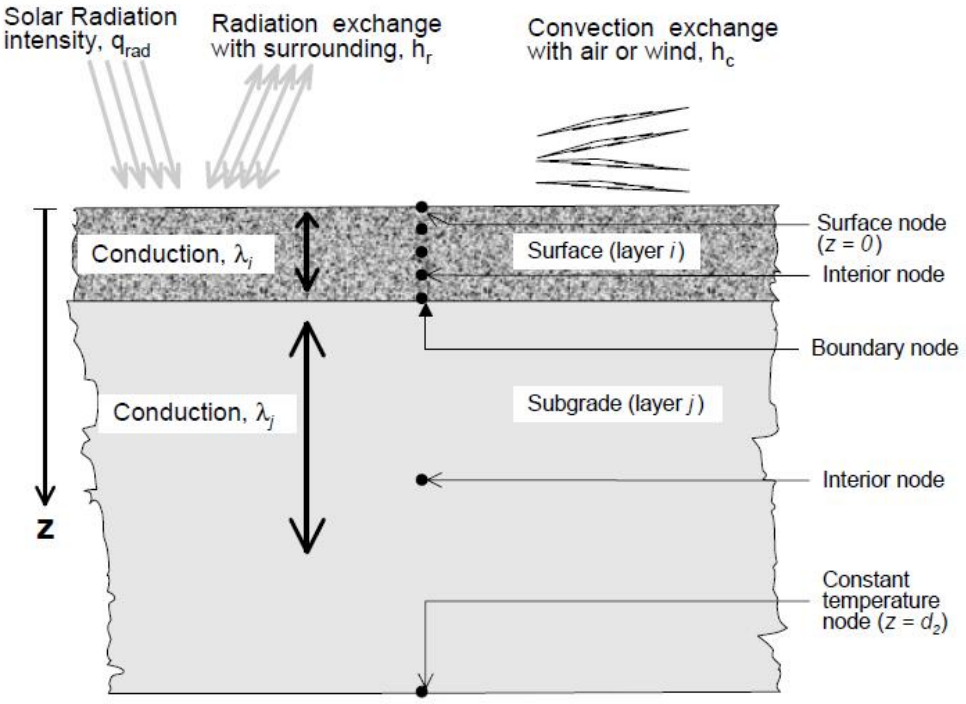

Figure 6. Heat interaction elements and boundary conditions for full-depth AC pavement (Mrawira and Luca 2002)

3.2.1 Heat Transfer on Pavement Surface

The energy interaction between pavement surface and surrounding environment is complicated, mainly including radiation balance and convection.

Radiation

On pavement surface, radiation balance consists of the solar radiation, q_i, reflected thermal radiation of pavement surface, q_f ,and the emitted radiation from pavement surface to the environment, q_e.

In this study, solar radiation q_i is directly obtained from online database.

The reflected thermal radiation of pavement surface is calculated as:

$$q_f = \beta q_i \quad (5)$$

Where

β is reflectivity of the pavement surface

q_i is intensity of solar radiation

q_f is reflected radiation from pavement surface

Calculation of emitted radiation from pavement surface to the environment is:

$$q_e = h_r(T_s - T_{sur}) \quad (6)$$

Where

q_e is emitted radiation from pavement surface to surrounding environment

T_s is pavement surface temperature

T_{sur} is temperature of surroundings

h_r is the radiation transfer coefficient, given by

$$h_r = e\sigma(T_s + T_{sur})(T_s^2 + T_{sur}^2) \quad (7)$$

Where e is the emissivity of pavement surface, and σ is the Stefan-Botlzman constant.

Convection

Convection is a major mode of heat transfer within fluids (e.g., liquids, gases) and rheids. The convection between pavement surface and the air follows:

$$q_c = h_c(T_s - T_{air}) \quad (8)$$

Where

q_c is convection heat transfer

T_{air} is bulk temperature of the air above the pavement surface

h_c is convection heat transfer coefficient calculated as (Hermansson 2001):

$$h_c = 698.24 \times [0.00144 \times \left(\frac{T_s+T_{air}}{2}\right)^{0.3} \times U^{0.7} + 0.00097 \times \text{abs}(T_s - T_{air})^{0.3} \quad (9)$$

Where U denotes the wind velocity in meters per second.

At the pavement surface, the boundary condition can be written as:

$$-k\frac{\partial T}{\partial z} = q_i + q_e + q_f + q_c \quad (10)$$

3.2.2 Heat Conduction within Pavement

Within the pavement domain, the heat conduction follows one dimensional heat equation

$$\frac{\partial T}{\partial t} - \alpha\left(\frac{\partial^2 T}{\partial z^2}\right) = 0 \quad (11)$$

The interlayer boundary condition is:

$$k_1\frac{\partial T_1}{\partial z} = k_2\frac{\partial T_2}{\partial z} \quad (12)$$

At the bottom of the pavement, it is assumed that soil temperature is not changed by the short term weather and remains constant below certain depth.

3.3 Pavement Temperature Prediction Model

In this study, a pavement temperature distribution prediction model is established to investigate the impacts of thermal properties on asphalt pavement temperature. The pavement in the model is assumed as full-depth with a 300-cm deep subgrade layer and a 28-cm deep asphalt concrete layer on top. The system is considered as a semi-infinite

medium, and heat conduction only occurs one dimensionally in vertical direction. At bottom of the pavement (z_2= 328cm), the temperature is assumed to be constant.

A finite difference theory of heat transfer is used to carry out numerical analysis.

The discrete form of equations can be written as (Mrawira and Luca 2002):

$$T_m^{p+1} = k\left(\frac{T_{m-1}^p - 2T_m^p + T_{m+1}^p}{\Delta z^2}\right)\frac{\Delta t}{\rho c} + T_m^p \text{ for } 0<z<d_1 \text{ and } 0<z<d_2 \quad (13)$$

$$T_m^{p+1} = \frac{2\Delta t}{r(\Delta z)^2}\left(k_1 T_{m-1}^p + k_2 T_{m+1}^p\right) + (1 - \frac{2k_1\Delta t}{r(\Delta z)^2} - \frac{2k_2\Delta t}{r(\Delta z)^2})T_m^p \quad \text{for } z=d_1 \quad (14)$$

$$T_0^{P+1} = \frac{2\Delta t(q + k\frac{T_1^p - T_0^p}{\Delta z})}{\rho c \Delta z} + T_0^p \quad \text{for } z=0 \quad (15)$$

$$\text{And } q = h_c\left(T_{air} - T_s^p\right) + h_r\left(T_{air} - T_s^p\right) + (q_i - q_f) \quad (16)$$

Where

T_{air} is air surface temperature during time step p

T_0^P is pavement surface temperature during time step p

T_m^p is pavement temperature at node m during time step p

3.4 Bridge Deck Temperature Prediction Model

Similar to pavement prediction model, heat transfer within bridge deck is considered to be one-dimensional problem in this study. Instead of setting constant temperature as the bottom boundary condition for the pavement, the bottom of the bridge also exposes in the air and transfers energy by convection and emission. By applying similar equations used for the surface of the pavement to the bottom boundary condition of deck, the discrete formed equations can be written as:

$$T_0^{P+1} = \frac{2\Delta t(q+k\frac{T_1^p - T_0^p}{\Delta z})}{\rho c \Delta z} + T_0^p \quad \text{for z=0} \tag{17}$$

Where $q = h_{ct}\left(T_{air} - T_o^p\right) + h_{rt}\left(T_{air} - T_o^p\right) + (q_i - q_f)$ (18)

$$T_m^{p+1} = k\left(\frac{T_{m-1}^p - 2T_m^p + T_{m+1}^p}{\Delta z^2}\right)\frac{\Delta t}{\rho c} + T_m^p \quad \text{for } 0<z<d_1 \text{ and } 0<z<d_2 \tag{19}$$

$$T_m^{p+1} = \frac{2\Delta t}{r(\Delta z)^2}\left(k_1 T_{m-1}^p + k_2 T_{m+1}^p\right) + \left(1 - \frac{2k_1\Delta t}{r(\Delta z)^2} - \frac{2k_2\Delta t}{r(\Delta z)^2}\right)T_m^p \quad \text{For z=}d_1 \tag{20}$$

$$T_b^{P+1} = \frac{2\Delta t(q+k\frac{T_{b-1}^p - T_b^p}{\Delta z})}{\rho c \Delta z} + T_0^p \quad \text{For z=}d_2 \tag{21}$$

Here $q = h_{cb}\left(T_{air} - T_b^p\right) + h_{rb}\left(T_{air} - T_b^p\right)$ (22)

Where

T_{air} is air surface temperature during time step p

T_0^P is pavement upper surface temperature during time step p

T_m^p is pavement temperature at node m during time step p

T_b^P is pavement lower surface temperature during time step p

4. EXPERIMENTAL PROGRAM

Experiments in this study could be classified into two categories: raw material characterization tests and mixture properties investigation tests.

Thermally modified asphalt concrete is a mixture containing different materials including asphalt, aggregate, fillers, and thermal additives. It is very important to characterize raw materials, especially the thermal additives, at the very beginning since their properties will have a direct impact on the structural and thermal behaviors of the mixtures. To have a better understanding of the additive surface topography and composition, Scanning Electron Microscope (SEM) was used to obtain photos of the EPP and graphite samples. Since the EPP beads used in this study have melting point within HMA working temperature, the heat susceptibility tests for the EPP were carried out to ensure the EPP pellets could remain solid and serve as an aggregate replacement during the mixing and compaction process.

Modified asphalt concrete specimens were made through Superpave method. Mechanical performances and thermal properties of the specimens were investigated through the indirect tensile test and hot disk test, respectively.

Detailed experimental procedures and their results are presented in this section.

4.1 Characterization of Raw Materials

Asphalt binder, aggregate and filler: The asphalt binder used in this study is PG 64-22, PG 70-22, provided by Jebro Inc. PG 64-22 asphalt was used for the modified binder test because PG 70-22 asphalt contains polymers that may disturb EPP mixing properties, PG 70-22 was added in the mixture to made asphalt concrete specimens.

The coarse aggregates are limestone from Kniferiver Inc, and the fine aggregates are sieved from Quickcrete®. Portland cement is added as a traditional filler.

Expanded polypropylene: In this study, the expanded polypropylene bead, manufactured by JSP Resins LCC, was served as an aggregate replacement. The EPP material is round shaped, with average diameter of 3.3mm. Because the EPP particles pass No.4 sieve and remain on No.8 sieve, they were added into the asphalt mixture by partially or fully replacing No.8 aggregate based on the volume content.

Due to the air bubbles inside the particle, the EPP has a much lower density ($0.25\ g/cm^3$) compared to regular PP material ($0.946\ g/cm^3$ for crystalline). The melting point of EPP is reported by the manufacture as 170ºC.

Graphite: A flake type graphite F516 produced by Asbury Carbons Inc. was used in this study. The graphite is black fine power, with the density of 2.26 g/cm^3. The graphite asphalt concrete samples were made by adding graphite with various weight fractions.

The properties of raw materials provided by manufactures are listed in Table 4.

Table 4. Manufacture materials data

Material Name	Specific Gravity	Typical Size	Note
PG 64-22 Asphalt	1.035(25ºC)	NA	
PG 70-22 Asphalt	1.031(25ºC)	NA	
Coarse Aggregate	2.575	>=4.75mm	
Fine Aggregate	2.700	<4.75mm	
Cement	3.15	<0.1mm	
Expanded Polypropylene	0.25	~3.3mm	Melts at 170ºC
Graphite	2.26	<0.212mm	Flake type

4.1.1 Scanning Electron Microscope

JEOL JSM-7500F field emission SEM was selected in this study, The configuration is shown in Figure 7 and Figure 8.

Figure 7. JEOL JSM-7500F field emission SEM

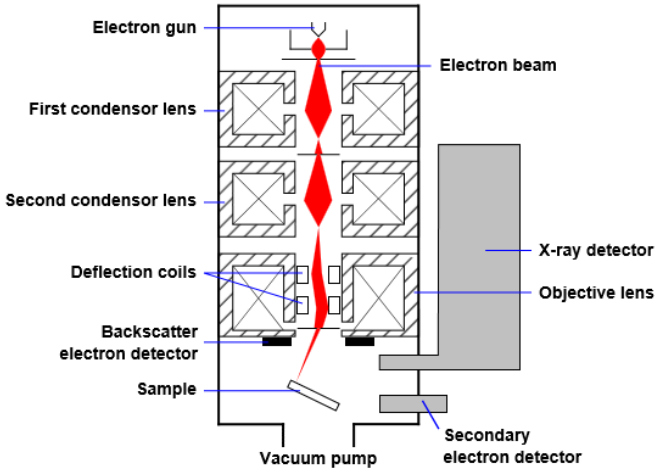

Figure 8. SEM configuration

Figure 9 are SEM images of EPP and graphite. As Figure 9a shows, the surface of EPP is smooth. This may cause a worse absorption of asphalt binder than normal aggregate, and contribute to a differences in compaction level and optimum binder content. Figure 9b and Figure 9c show a close view of EPP surface. Holes on the surface

of EPP were found, indicating EPP particles have lots of air bubbles inside. These air bubbles, on one hand, will act as insulators that change thermal properties of asphalt mixtures, on the other hand, may have negative effect on mechanical performance of the EPP modified asphalt concrete.

As shown in Figure 9d, e, f, the flake type graphite have the shape of a hexagonal plate, which has super-conductivity parallel to the plate surface. Since moving of electrons from one atom to another is one of the fastest way of transferring heat, the graphite has a higher thermal conductivity compared to other components of pavement materials.

4.1.2 EPP Heat Susceptibility

Melting of the EPP during the mixing and compaction process will have a significant effect on the performances of modified asphalt concrete. To have a better evaluation of the heat susceptibility of the EPP, differential scanning calorimeter (DSC) was utilized to verify the melting point of the beats, and a simple oven heat test was carried out to check the physical change of the EPP during heating.

Differential scanning calorimeter

DSC is a device that measures the difference in the amount of heat required to cause the same temperature change between a testing sample and the reference. When the testing sample undergoes a phase transition, more or less heat will be needed than the reference sample to change the same temperature. The DSC can detect the phase transition

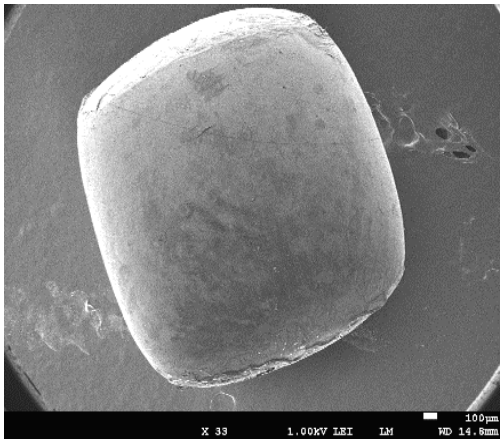

(a) EPP ×33

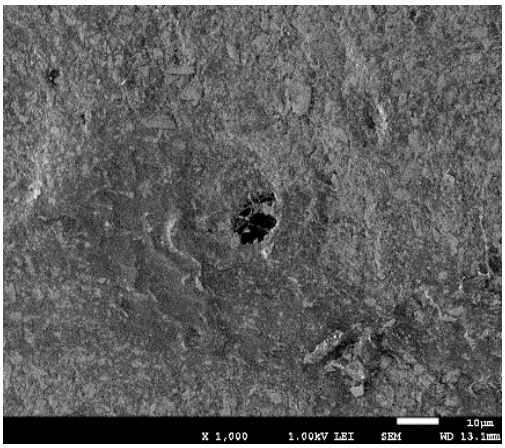

(b) EPP ×1000

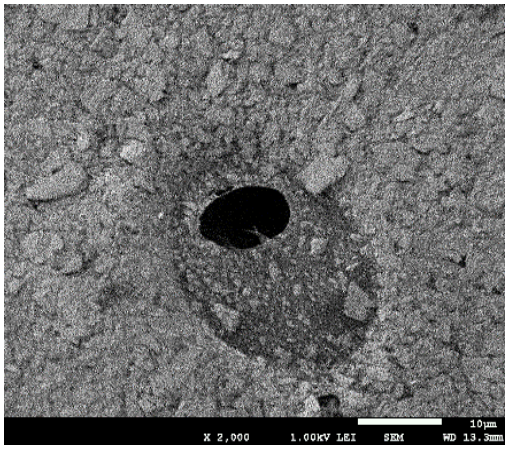

(c) EPP ×3000

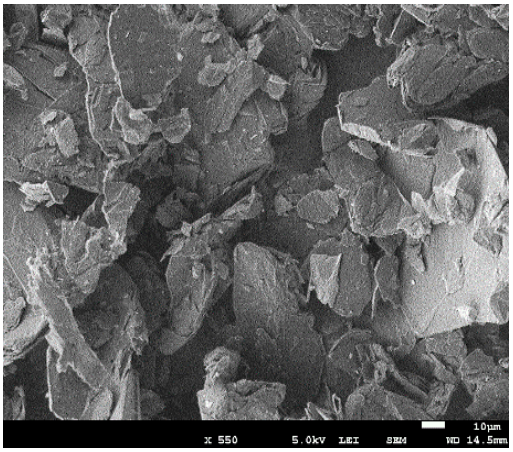

(d) Graphite ×550

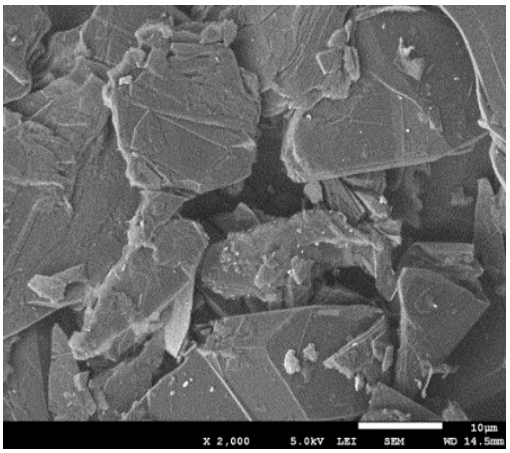

(e) Graphite ×2000

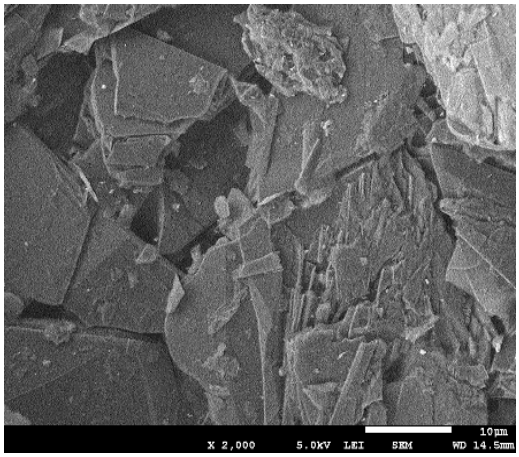

(f) Graphite ×2000

Figure 9. SEM images

of a material from the sudden change of the heat required to cause an unit temperature change. The schematic of the DSC is shown in Figure 10. In the test, TA Instruments SDT Q600 (Figure 11) was used.

The result of DSC test is shown in Figure 12, the peak of heat flow indicated that the difference of heat absorbed between the EPP sample and the reference reached a maximum value at 171.43ºC. The EPP melting process is endothermic, and hence, this temperature point was regarded as measured melting point of EPP sample. 171.43ºC well matched with the melting point (~170ºC) reported by the manufacturer.

Oven heat test

EPP samples were put into oven for heating at 143ºC, the physical changes were recorded every 40 minute. The change after one night was also observed.

The physical changes of EPP after placed in the oven were recorded in Table 5.

Table 5. Oven heat test

Materials	Temperature(ºC)	40mins	80mins	120mins	Overnight
EPP	143	No Change	No Change	No Change	Partially Turned Yellow

As shown in Table 5, EPP were quite stable at 143ºC within 2 hours heating process, no physical changes regarding color and shape were observed. However, after heated during whole night, EPP samples partially turned yellow (Figure 13), this color changed was caused by degradation of polypropylene material from long time exposure to heat. However, EPP shapes kept unchanged, and no melt was found.

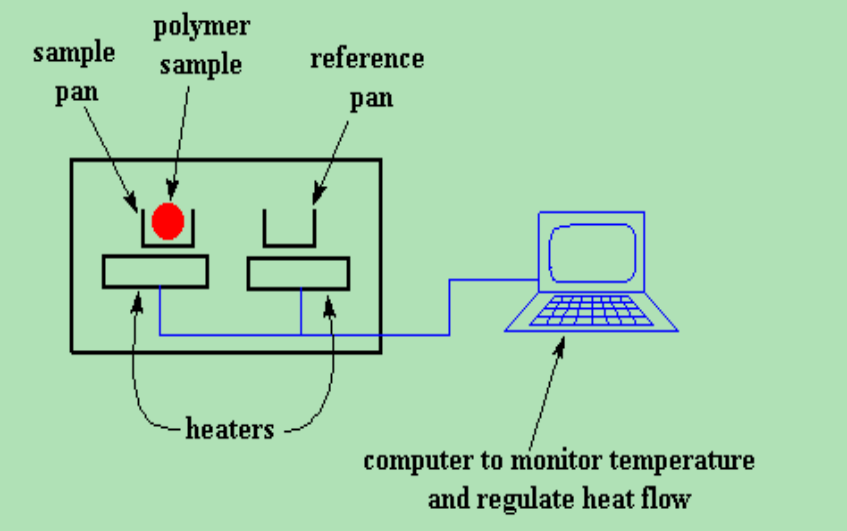

Figure 10. DSC working principle

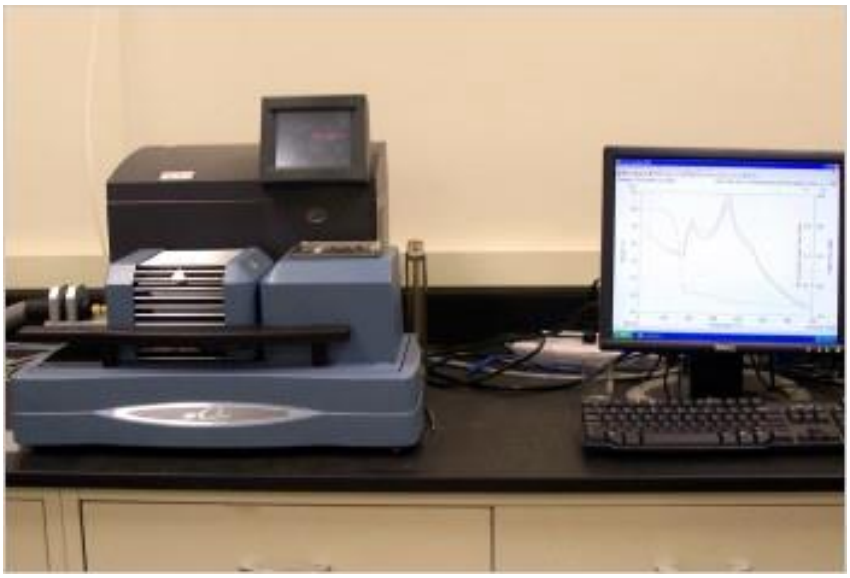

Figure 11. TA Instruments SDT Q600

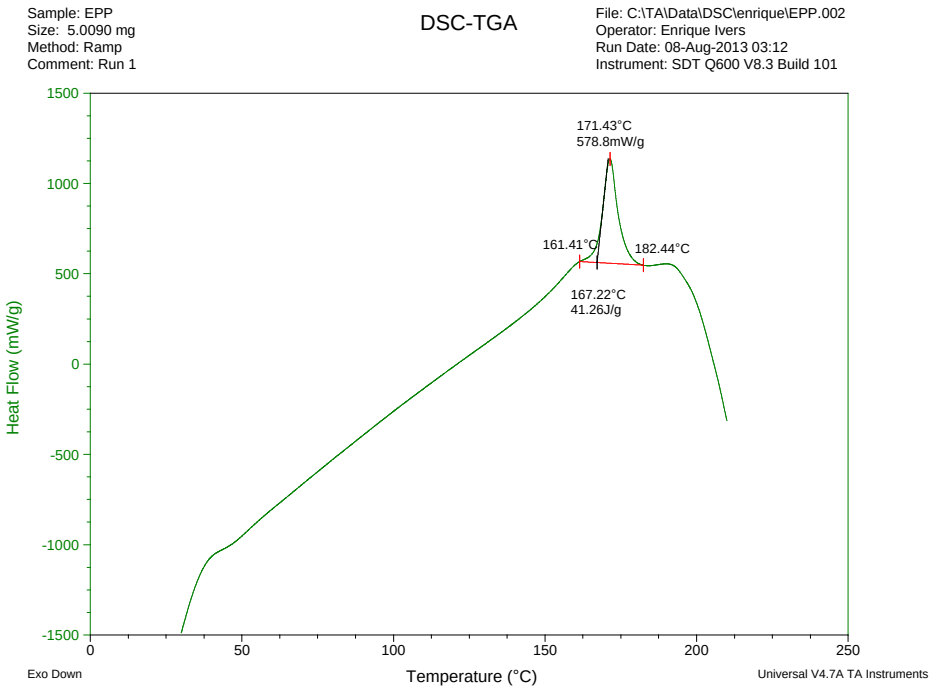

Figure 12. EPP DSC curve

Figure 13. EPP after heated during night

4.2 Properties Tests of Modified Asphalt Mixtures

4.2.1 Asphalt Binder Tests

EPP asphalt mixing test

EPP beads were heated to melted state and mixed with asphalt during two hours at two different temperatures, e.g., 180ºC and 185ºC. After every half an hour, the samples were taken out of the oven and mixed with a mechanical mixer for around 5 minutes.

Observation was recorded during this melting and mixing process. For each temperature, 2%, 4% and 6% of EPP samples by the weight of asphalt (equal to 8.2%, 16.4% and 24.6% vol. %) were mixed. The results are listed as follows:

(1) 180ºC: The EPP still remained un-melted after one hour. After another hour, EPP particles of half original size to nearly full size were found on the top of asphalt (Figure 14a).

(2) 185ºC: EPP formed a film on the top, the 2% EPP sample appeared melted after 90 minutes, and 4% and 6% were found melted after 120 minutes (Figure 14b).

(a) Mixing EPP at 180ºC (b) Mixing EPP at 185ºC

Figure 14. EPP asphalt mixing test

During the mixing process, as time went by, the mixture became stiffer and the polypropylene material reformed some small particles in the mixture (clumps). Even with the mixer, it is difficult for the mixture to become uniform.

Dynamic shear rheometer test

Dynamic shear rheometer (DSR) test was conducted using EPP modified asphalt sample to investigate its rheological property. Tests were carried out at 64ºC and 70 ºC with the oscillation rate at 10 rad/sec using samples of 25mm by diameter and 1mm by thickness. Complex modulus (G*) defined as $G^* = \frac{\tau_{max}}{\gamma_{max}}$ was obtained according to the principles explained as Figure 15.

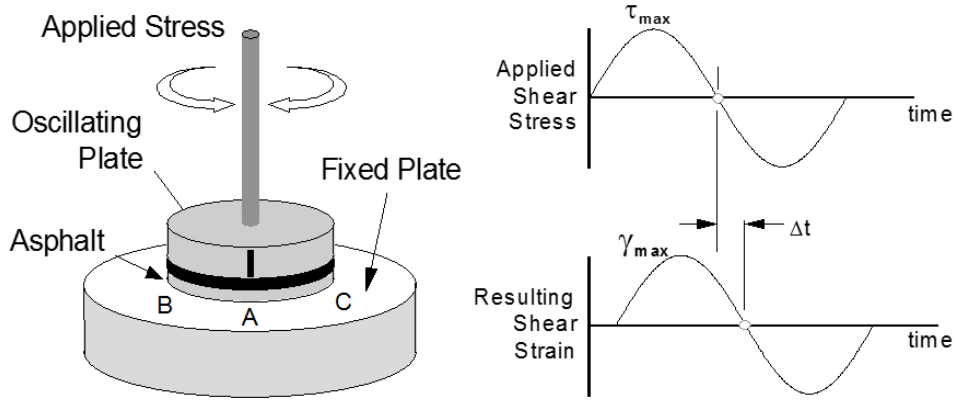

Figure 15. DSR working principles

0, 2%, 4% and 6% EPP beads by weight of asphalt were added into PG 64-22 asphalt, the dynamic modulus (G^*) of these samples were obtained at both 64ºC and 70ºC.

The test result in Figure 16 shows that the complex modulus increased when EPP content increased, this means adding EPP would make asphalt binder stiffer. The irregularity complex modulus regarding 4.0% EPP asphalt sample, as well as pictures (Figure 17) taken after the test, indicated that EPP clumps existed in the mixture.

Based on heat susceptibility tests and DSR test above, it is concluded that EPP has a relatively good heat susceptibility and difficulty was found to melt and mix EPP into asphalt, Therefore, EPP is not considered to be a good asphalt modifier, the research focus moves to the idea that adding EPP into asphalt concrete as aggregate replacement.

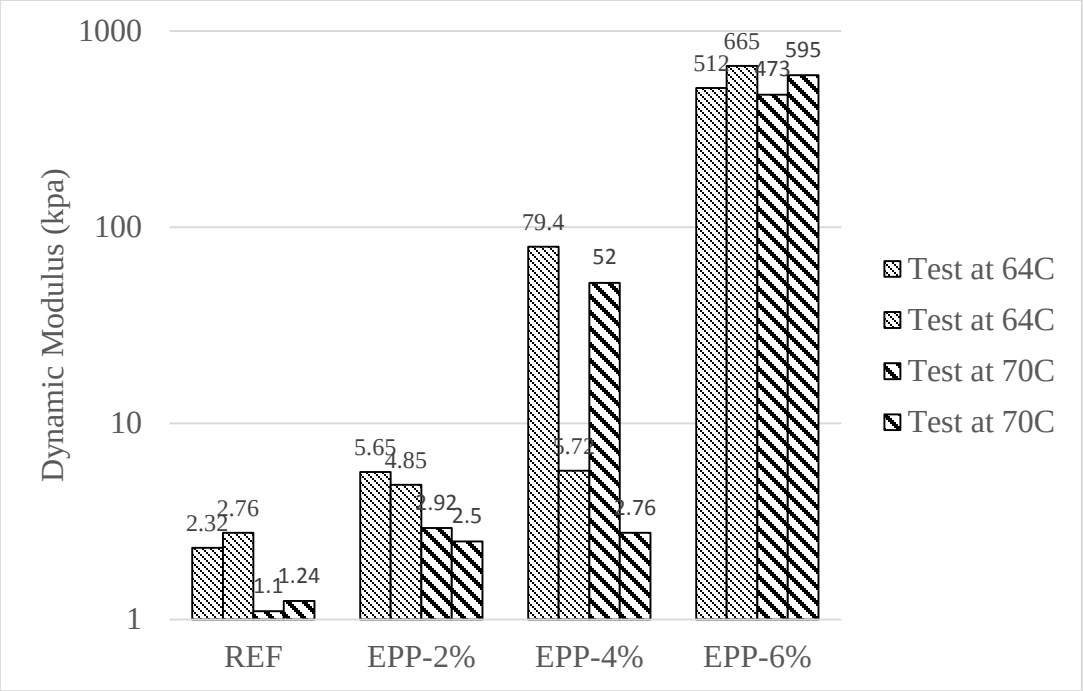

Figure 16. DSR tests results of EPP modified asphalt

Figure 17. EPP clumps attached to DSR device

4.2.2 Asphalt Concrete Tests

Mix design

Asphalt concrete specimens were made in accordance with Superpave Mix Design Method. The aggregates gradation for EPP modified asphalt concrete was selected to satisfy D-5 mixture requirements and D-6 mixture requirements for graphite modified asphalt concrete specified in ASTM D3515. Followed by Superpave Specification, the optimum binder content was determined as 4.37% for D-5 gradation, and 5.3% for D-6 gradation.

The mix designs of D-5 and D-6 are listed in Table 6.

Table 6. Mix designs

Sieve Size (mm)	**19**	**12.5**	**9.5**	**4.75**	**2.36**	**1.18**	**.6**	**.3**	**.15**	**.075**	**Pan**
D-5% passing	100	95	82	55	34	22	16	12	6	5	0
D-6% passing	100	99.9	95.3	68.1	50.8	35.3	21.0	11.5	7.2	6.1	0

Regarding specimens modified by EPP beads, the aggregate gradation was fixed as D-5 specification. 0%, 10%, 20%, 40%, 60%, 80% and 100% of No.8 Aggregates were replaced by EPP beads based on volumetric portion.

For specimens modified by graphite, the aggregate gradation kept unchanged as D-6 specification. Graphite was added into mixture as replacement of fillers, with the content of 0%, 10%, 15%, 20%, 25%, 30%, 35% and 40% by weight of mastic.

Specimens preparation

The specimens were made according to Superpave specification and ASTM standard. Before blending aggregates, coarse aggregates and fine aggregates were heated in the oven through the night to eliminate moisture. Aggregates were then sieved and classified as different sizes, the aggregates blend were obtained by mixing different sized aggregates in accordance with the gradation that has been designed before. Before mixed with asphalt, blended aggregates were put into oven at 149ºC through the night and asphalt binder was heated for 2 hours at the same mixing temperature. A mechanical mixer was used during the mixing process to ensure aggregates would be well coated by asphalt. The mixtures were then conditioned in the oven at 135ºC before compaction.

A Superpave gyratory compactor was used to make asphalt concrete specimens. Two sets of EPP modified asphalt samples were made. One set of samples were made by controlling the gyrations as 115 while the other set were controlled as 4% target percent air void. Graphite asphalt concrete specimens were made only by controlling the target percent air void. For each case, two or three cylindrical specimens of 150mm by diameter and 95mm by height were made, one or two of them were used to test mechanical performance, and the other one was prepared for thermal properties measurement.

A summary of all specimens made is listed in Table 7.

Table 7. Specimens prepared for the tests

Specimen Name	Quantity	Gradation	Binder Content %	Vol. % of Add. by total mixture	Note
REF-D-5-AC	3	D-5	4.37	0	AV:4%
REF-D-5-GC	2	D-5	4.37	0	Gyrations: 115
EPP-20%-AC	3	D-5	4.37	3.7	AV:4%
EPP-60%-AC	3	D-5	4.37	11.1	AV:4%
EPP-100%-AC	3	D-5	4.37	18.5	AV:4%
EPP-10%-GC	3	D-5	4.37	1.8	Gyrations: 115
EPP-20%-GC	3	D-5	4.37	3.7	Gyrations: 115
EPP-40%-GC	3	D-5	4.37	7.4	Gyrations: 115
EPP-60%-GC	3	D-5	4.37	11.1	Gyrations: 115
EPP-80%-GC	3	D-5	4.37	14.8	Gyrations: 115
REF-D-6-AC	3	D-6	5.30	0	AV:4%
GRA-10%-AC	2	D-6	5.30	1.2	AV:4%
GRA-15%-AC	2	D-6	5.30	1.8	AV:4%
GRA-20%-AC	3	D-6	5.30	2.4	AV:4%
GRA-25%-AC	3	D-6	5.30	3.0	AV:4%
GRA-30%-AC	3	D-6	5.30	3.6	AV:4%
GRA-35%-AC	3	D-6	5.30	4.2	AV:4%
GRA-40%-AC	3	D-6	5.30	4.8	AV:4%

Mixing and compaction properties

The mixing temperature was set to 149ºC, EPP beads were blended with aggregates and put into oven during a whole night heating. After this process, it was found that EPP beads formed clumps, turned yellow and had a tendency to stick to the side of

the pans, as shown in Figure 18 . However, no problems regarding asphalt coating EPP particles were observed.

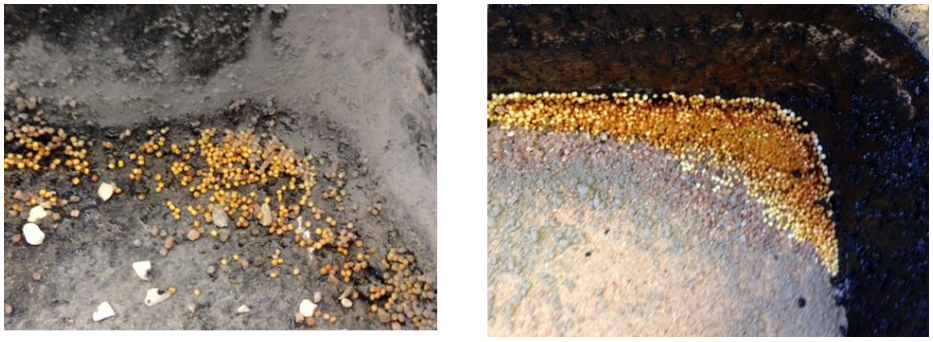

Figure 18. EPP after a whole night heating at 149 ºC

Two sets of EPP specimens were compacted followed by Superpave method. One was to control the compacting gyrations as 115 (Gyration Controlled (GC) samples) while the other required the target air void to be 4.0% (AV Controlled (AC) samples).

For the GC samples, EPP specimens, especially of higher EPP volume content, looked wet and sticky. This phenomenon could be explained as: EPP beads surfaces are round and smooth, they don't have enough angularity to absorb asphalt binder, therefore after loading, the excessive asphalt came out to the surface and caused bleeding problem.

For the AC samples , EPP samples were much easier to be compacted compared to the reference asphalt concrete, the higher the EPP volume content, the lower the gyrations for 4.0% of air void required. This was due to elasticity of EPP modified specimens caused by large amount of air bubble inside. The compaction efforts (gyrations corresponding to 4.0 air void percent of asphalt concrete samples) is plotted in Figure 19.

Graphite specimens were duplicated by controlling target air void as 4.0%. It was not so difficult to mix and compact asphalt concrete containing graphite. Different from cement concrete, the dispersion of graphite in asphalt concrete was much more uniform, but small graphite clumps were still found. Compared to plain asphalt concrete, graphite modified asphalt concrete specimens looked lackluster (Figure 20).

The average number of gyrations required are plotted in Figure 21. As is can be seen, when graphite content increased, the compaction efforts increased. The reason is given as: the specimens became harder to be compacted because graphite has a higher surface area that would absorb more asphalt binder and made the specimens dry.

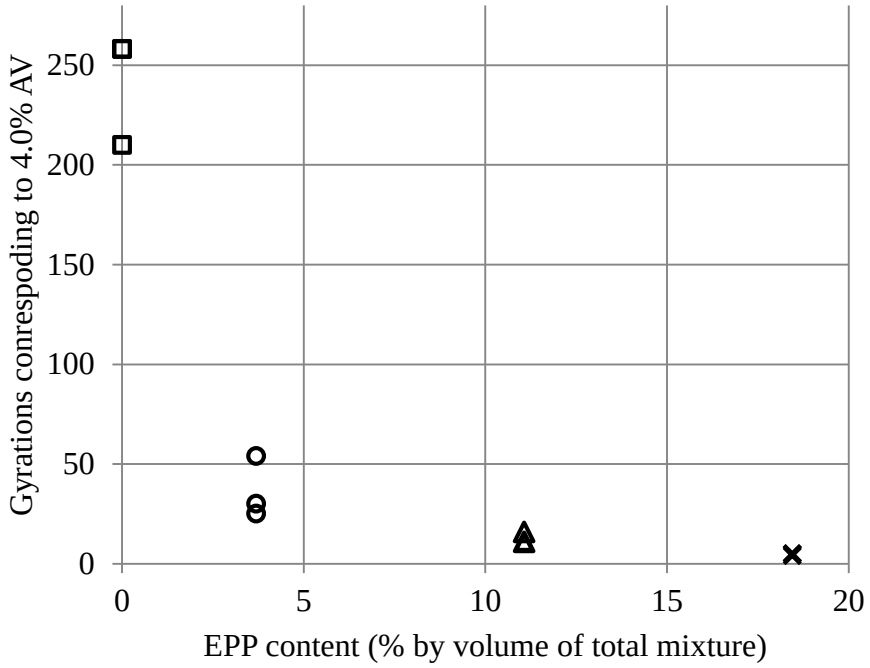

Figure 19. Compaction efforts of EPP modified asphalt concrete by controlling air void

Figure 20. EPP modified asphalt concrete (left) and graphite modified asphalt concrete (right)

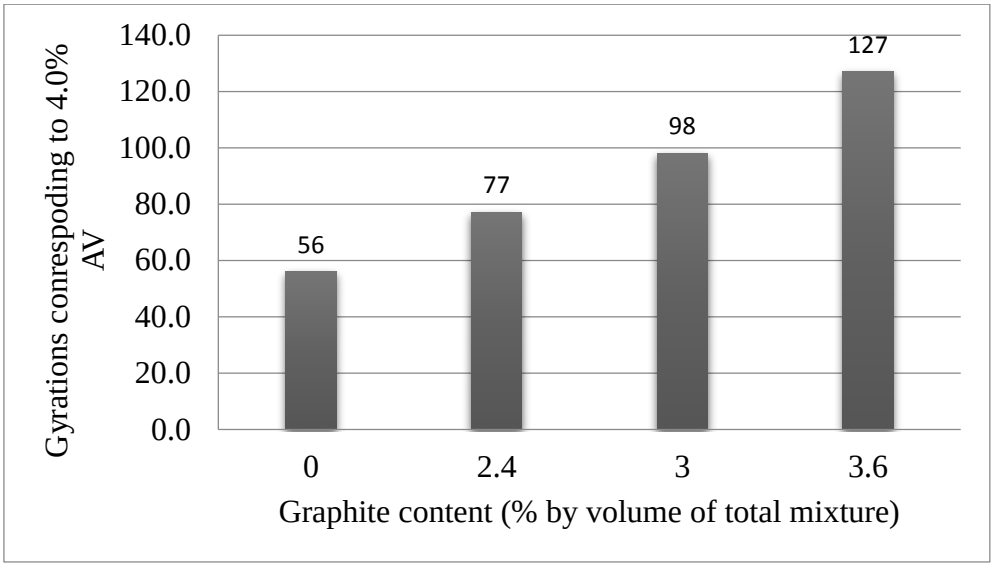

Figure 21. Compaction efforts of graphite modified asphalt concrete by controlling air void

Volumetric properties test

After compaction, the specimens' volumetric parameters (air void (AV), voids in the mineral aggregate (VMA), voids filled with asphalt (VFA)) were checked based on the measured bulk specific gravity (G_{mb}) and theoretical maximum specific gravity (G_{mm}) using the following equations:

$$AV = (1 - \frac{G_{mb}}{G_{mm}}) \times 100 \quad (23)$$

$$VMA = 100 - \frac{G_{mb} \times P_s}{G_{sb}} \quad (24)$$

$$VFA = 100 \times \frac{VMA - AV}{VMA} \quad (25)$$

The volumetric properties of asphalt concrete specimens were checked. The measured and calculated volumetric parameters are summarized in Appendix.

EPP GC samples

GC samples were made by controlling the gyrations as 115. 115 is the N_{max} value corresponding to N_{des} = 75. Specimens compacted to N_{max} were used as a check to help guard against plastic failure caused by excess traffic (Design 1996) . According to the Superpave requirement, the air void content at N_{max} should never be below 2.0%, otherwise the mixtures would be vulnerable to rutting distress. The calculated AV% of gyrations controlled EPP concrete samples is shown in Figure 22.

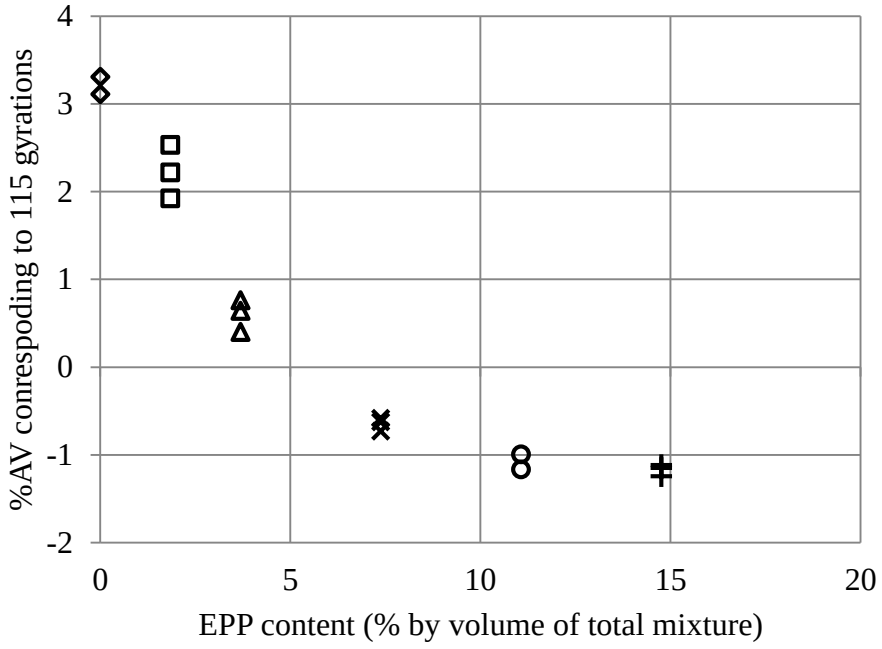

Figure 22. %AV of EPP modified asphalt concrete by controlling gyrations

Figure 22 indicates that the higher the EPP volume content, the lower the air void in the specimens under the same compaction level (115 gyrations). When more than 40 vol. % of No.8 aggregates were replaced (equal to 7.4% by volume of total mixture), the calculated air void percentage even became negative (G_{mb}>G_{mm}). This is because under heavy loading, EPP beads have been compressed seriously, leading to a reduction of volume of the specimens. After unloading process, EPP particles could not restore to the original sizes due to the effect of access asphalt binder, therefore the bulk specific gravity (G_{mb}) of the specimens increased a lot. In high EPP volume content samples, large amount

of EPP particles have been compressed, leading to higher G_{mb} than G_{mm}, hence the negative %AV was calculated.

EPP AC samples

The other set of specimens were made by controlling percent air void as 4.0. The calculated AV% on various content of EPP modified asphalt concrete is plotted in Figure 23.

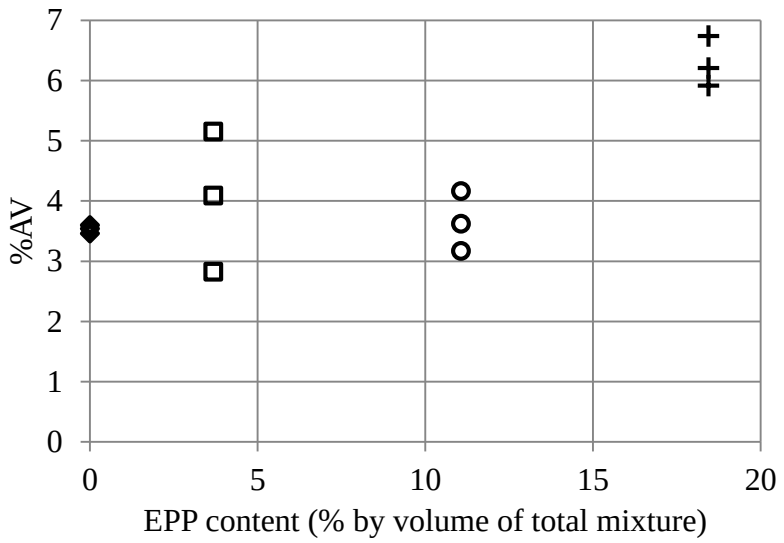

Figure 23. %AV of EPP modified asphalt concrete by controlling air void

As Figure 23 shows, regarding low and intermediate percent of EPP volume content, controlling 4.0 air void percent of specimens seemed easier and feasible, the data scattered around 4.0. However, when EPP volume percent increased to a high level, large amount of EPP had been compressed under loading, and restored after compaction. The recovery process resulted in higher %AV than the target.

Graphite AC samples

Different from EPP samples, controlling air void of graphite modified asphalt concrete seemed to be easy and accurate. Since the amount of graphite added was fairly small compared to the whole mixture, the average air void of the sample was all controlled around 4.0%, as shown in Figure 24.

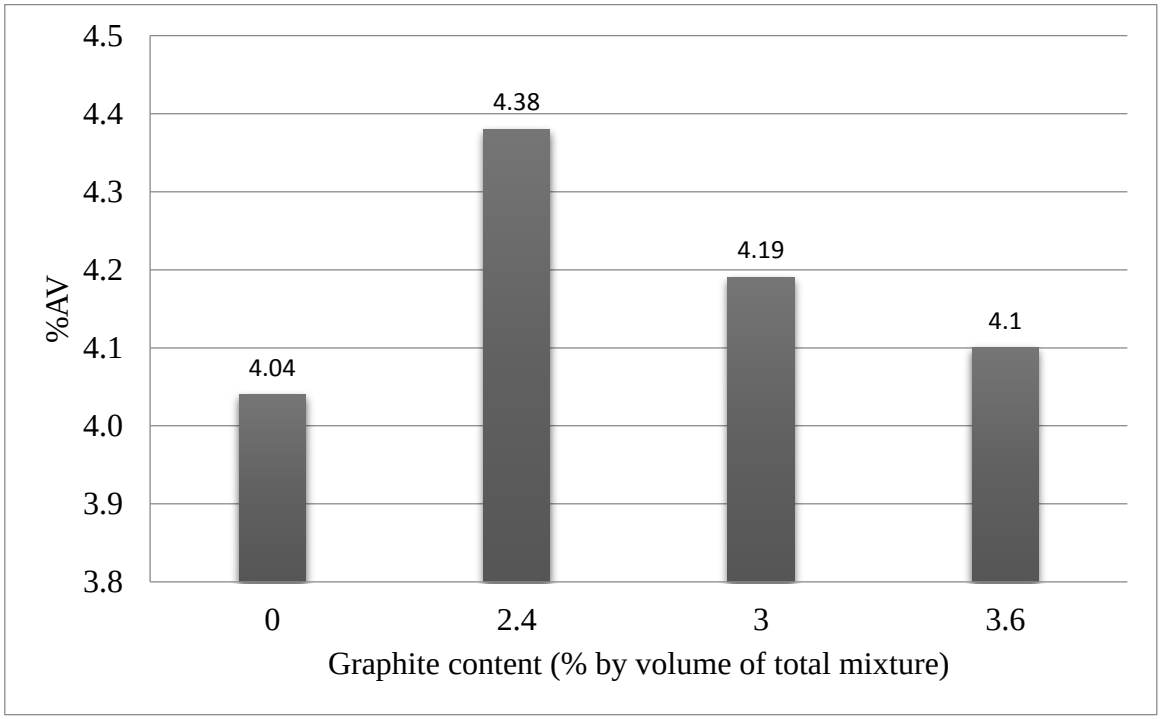

Figure 24. %AV of graphite modified asphalt concrete by controlling air void

Mechanical performance test

Indirect tensile (IDT) test (Figure 25) was selected to evaluate the mechanical performance of asphalt concrete specimens. A higher IDT strength corresponds to a better mechanical strength and higher tensile strength ratio (TSR) means the specimen is less susceptible to moisture damage. In this study, specimens of 95mm by height and 150mm by diameter were conditioned at room temperature, the IDT tests were carried out using Instron 5583. The machine applied compressive load on the specimen at a constant displacement rate of 50.8mm/min (2 inch/min) until the sample was splitted. The load and strain was recorded and the IDT strength was calculated by the following equation, as shown in Figure 26.

$$S_T = \frac{2 \times P}{\pi \times t \times D} \tag{26}$$

Where S_T is the IDT strength in MPa

P is the maximum load in N,

t is the specimen height immediately before test in mm

D is the specimen diameter in mm

Figure 25. IDT test set-up

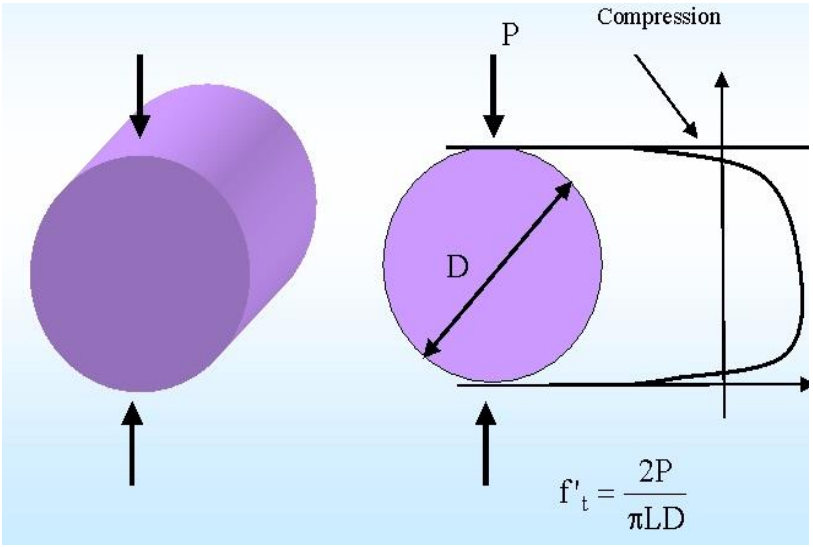

Figure 26. Indirect tensile strength calculation

EPP GC samples

Figure 27 compares IDT strength of different GC samples containing different amount of EPP.

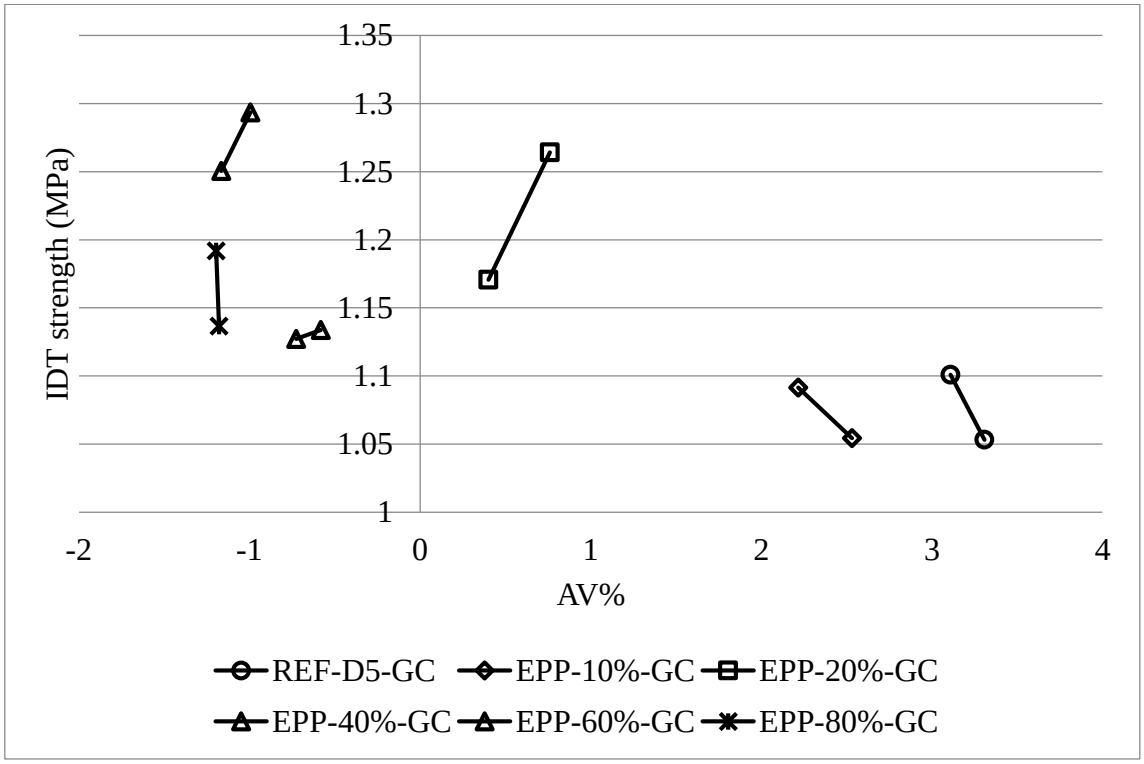

Figure 27. IDT strengths of EPP modified asphalt concrete by controlling gyrations

As shown in Figure 27, the IDT strength increased with addition of EPP compared to un-modified samples. However, this doesn't mean adding EPP would increase strength of asphalt mixture because the samples containing higher EPP content had smaller %AV and IDT strength also increases as air void decreases. Therefore, the IDT strengths of AC

samples would be more meaningful to represent the mechanical performance of modified samples.

EPP AC samples

The IDT strengths of EPP air void controlled samples are shown in Figure 28.

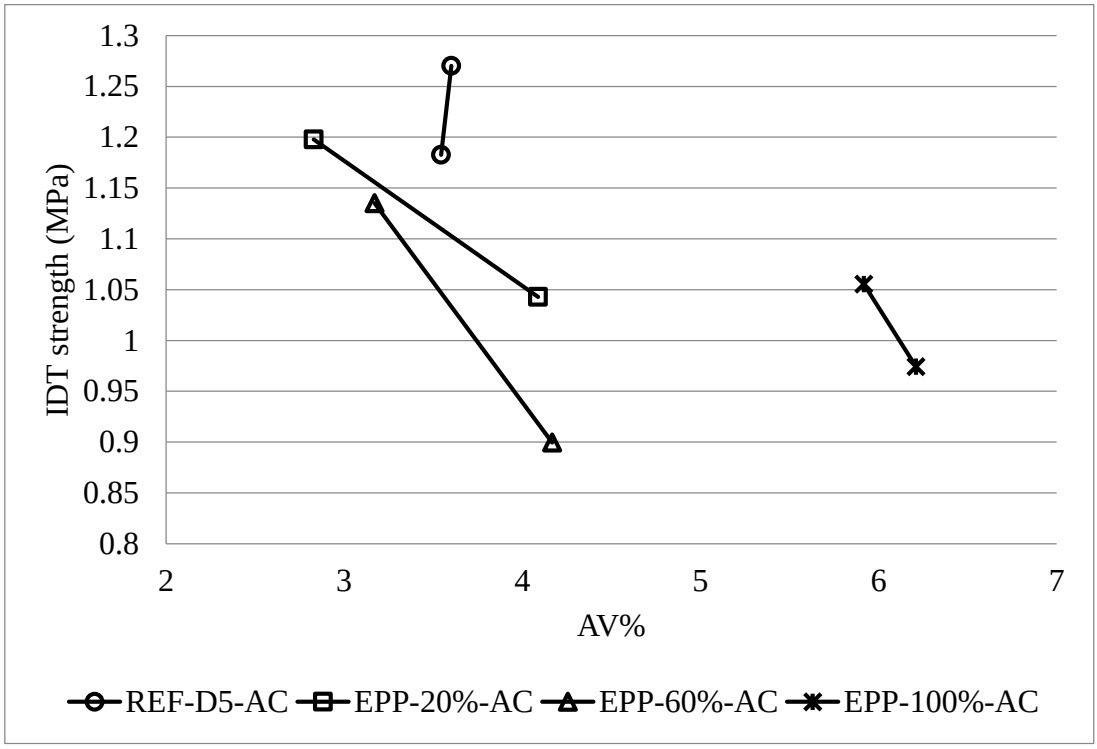

Figure 28. IDT strengths of EPP modified asphalt concrete by controlling air void

The IDT strengths of AC samples were comparable because they had similar air void content. It is clear that adding EPP into asphalt mixture would decrease IDT strengths from Figure 28. However, the strength was not seriously damaged, a 17% reduction in

averaged IDT strength was obtained by comparing EPP-100%-AC sample with REF-D-5-AC sample.

Graphite AC samples

The graphite modified asphalt concrete samples were duplicated by controlling air void. The IDT test were conducted by Park et al. (2014), as shown in Figure 29.

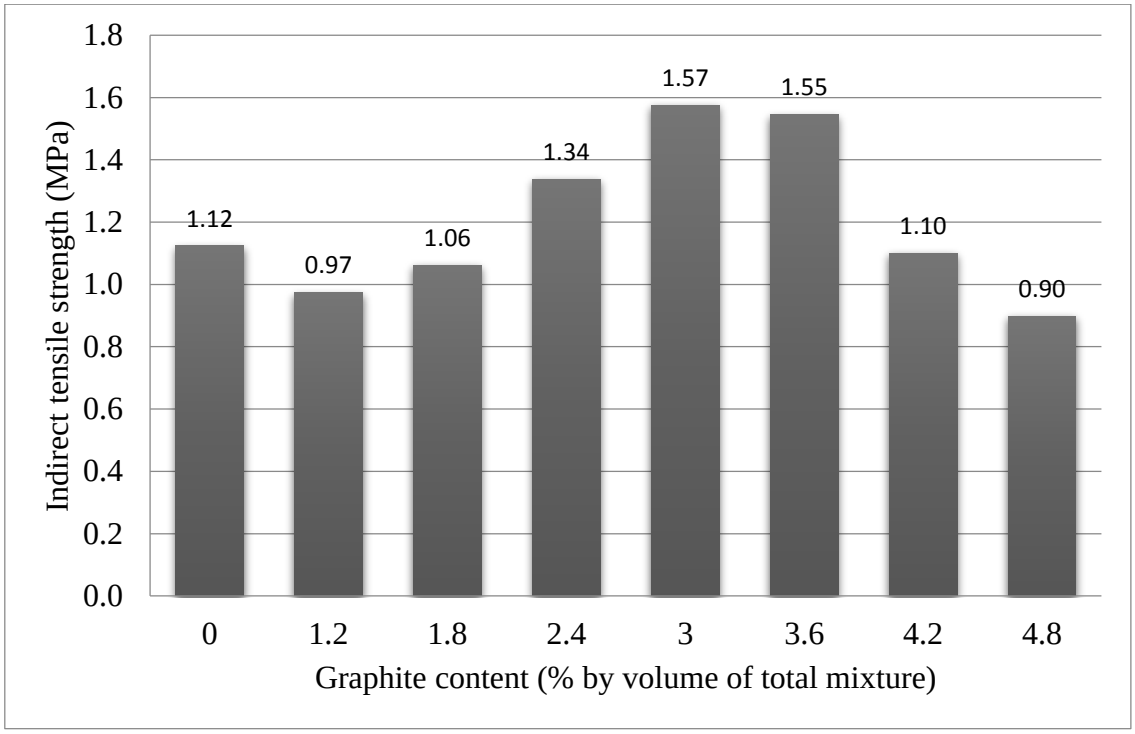

Figure 29. IDT strengths of graphite modified asphalt concrete by controlling air void

It is shown in Figure 29 that by adding slight amount of graphite, IDT strength decreased compared to the un-modified sample. When graphite content increased from

1.2% to 4.8%, the strength at first increased and then decreased. It is recorded that adding 1.8 % to 3.6% of graphite into asphalt concrete would increase IDT strengths, while lower and higher contents would lead to a reduction of mechanical performance compared to the unmodified samples. At the highest graphite content, the IDT strengths reduced by 20%**.**

Thermal properties measurement

Collecting the thermal properties data (thermal conductivity and heat capacity) of the modified and plain asphalt concrete samples is one of the most important task in this study. ASTM C177-85 introduces a standard procedure to measure the thermal properties of asphalt concrete, however, it is practically difficult to meet the slab requirements with the thickness not exceeding 1/5 of the maximum linear dimension of the metered region (Mrawira and Luca 2002). Instead, a hot disk thermal constants analyzer was used in this study. The machine is Transient Plane Source (TPS) 2500S (Figure 30), sold by Thermtest Inc. from Canada.

TPS machine is designed to measure thermal conductivity, heat capacity and thermal diffusivity of various materials including liquids, pastes, solids and powders. The TPS probe comprises of a sensor (Figure 31), made of nickel foil, acting both as heat source and a resistance thermometer to record the time dependent temperature increase. During the measurement, the sensor is sandwiched by two pieces of the samples. An increase in temperature is created by passing a current through the nickel foil. The time and power output need to be adjusted before the test according the characteristics of the

samples. Thermal properties of the samples are calculated automatically by the computer from the recording of the temperature increase versus time response in the sensor.

Thermal properties of plain, EPP modified asphalt concrete and graphite modified asphalt concrete specimens were investigated in this study by TPS 2500S. For each case, one specimen of 150mm by diameter and 95mm by height were made via Superpave gyratory compactor. Each specimen was cored to 50.8mm (2 inch) by diameter and then cut into four pieces from transverse direction (Figure 32). During measuring process, the C5465 sensor was sandwiched between disk shaped samples, as shown in Figure 33.For each specimen type, three pairs of samples were used, and 12 sets of data were obtained when adjusted the location of the sensor between the samples. By averaging 12 sets of data, the thermal properties of different types of samples were collected.

Figure 30. TPS 2500S

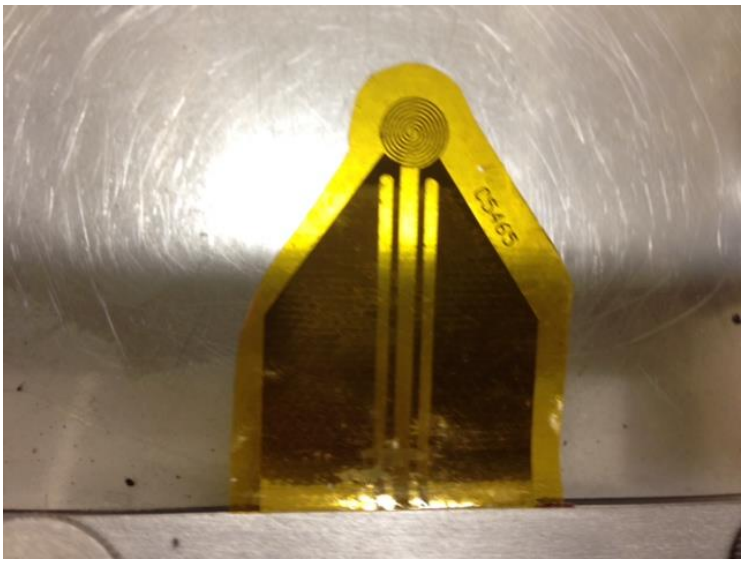

Figure 31. TPS 2500S sensor C5465

Figure 32. TPS 2500S sample preparation

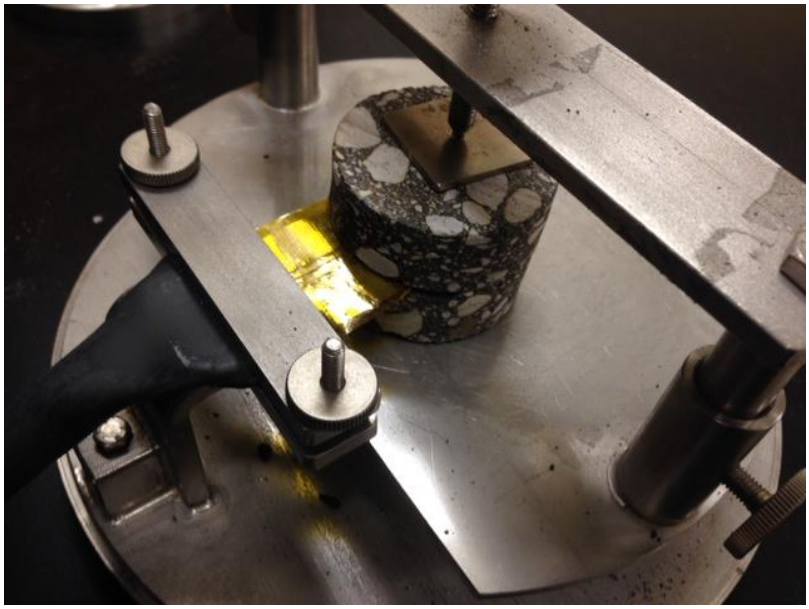

Figure 33. TPS 2500S test set-up

EPP asphalt concrete

Figure 34 shows thermal conductivity of asphalt concrete modified by different volume content of EPP. It is clear that adding EPP decreased the thermal conductivity of asphalt concrete, the higher the EPP amount, the lower the thermal conductivity of the sample. When EPP fully replaced No.8 aggregate, which was equivalent to 18% volume percent of total mixture, the thermal conductivity of modified asphalt concrete decreased by 32% compared to plain asphalt concrete.

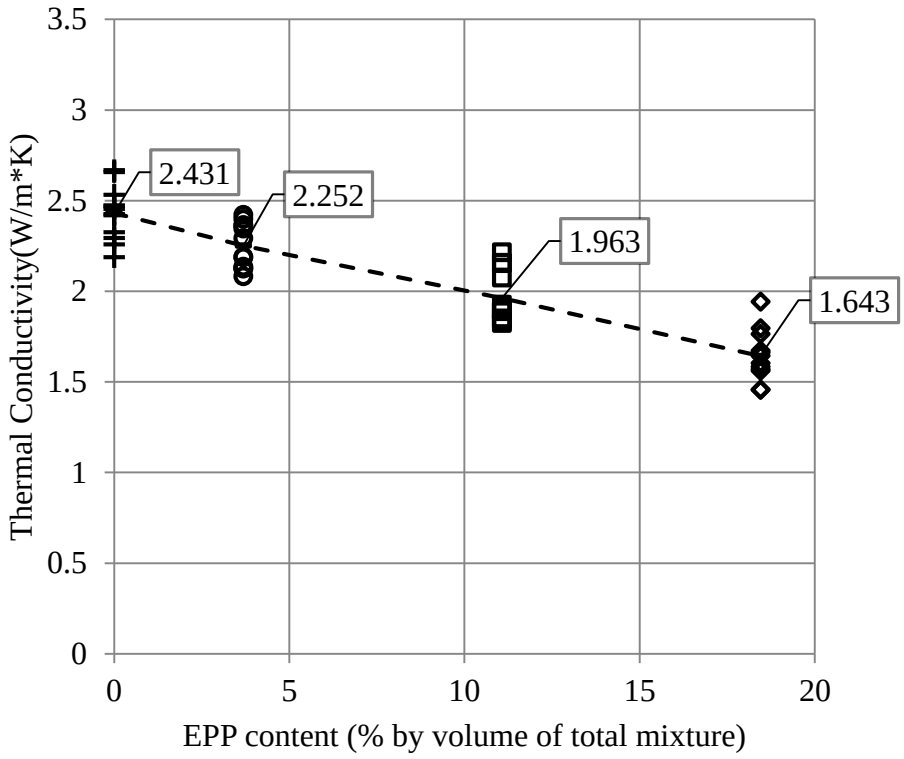

Figure 34. Thermal conductivity of EPP modified asphalt concrete

Figure 35 compares volumetric heat capacity of specimens with various EPP content. The experimental results indicated that heat capacity decreased as EPP volume content increased. It should be noted that when more and more EPP particles were added into the mixture, the heat capacity data became more and more sparse. This is due to small sensor size and inhomogeneous distribution of EPP beads in the modified asphalt concrete. At the content of 18%, a 27% reduction in averaged volumetric heat capacity of EPP modified asphalt concrete was obtained, compared to the un-modified sample.

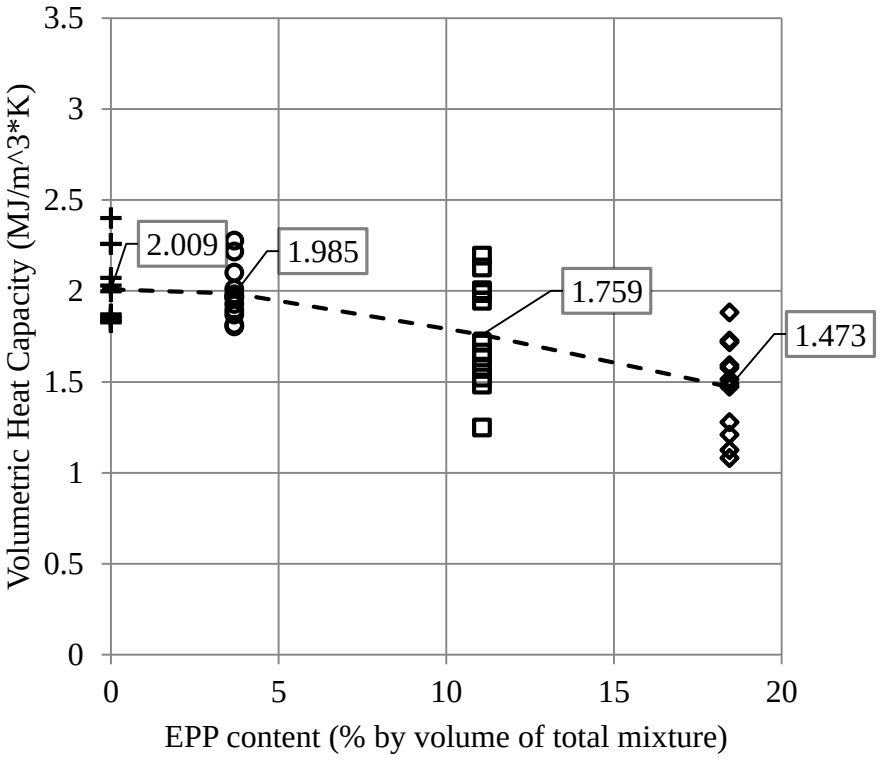

Figure 35. Heat capacity of EPP modified asphalt concrete

Graphite asphalt concrete

Thermal Conductivities of asphalt concrete samples with different content of graphite are compared in Figure 36. Though data was sparse, the trend was still very clear by averaging all the data for one type of samples. The results indicated that the higher the content of the graphite, the higher the thermal conductivity was. The average thermal conductivity of plain asphalt concrete specimen was $1.936\,\mathrm{W/m \times K}$, the maximum improvement in thermal conductivity at the specimens containing 4.8% of graphite was reported as 2.768 $\mathrm{W/m \times K}$, increasing by 43% compared to the reference.

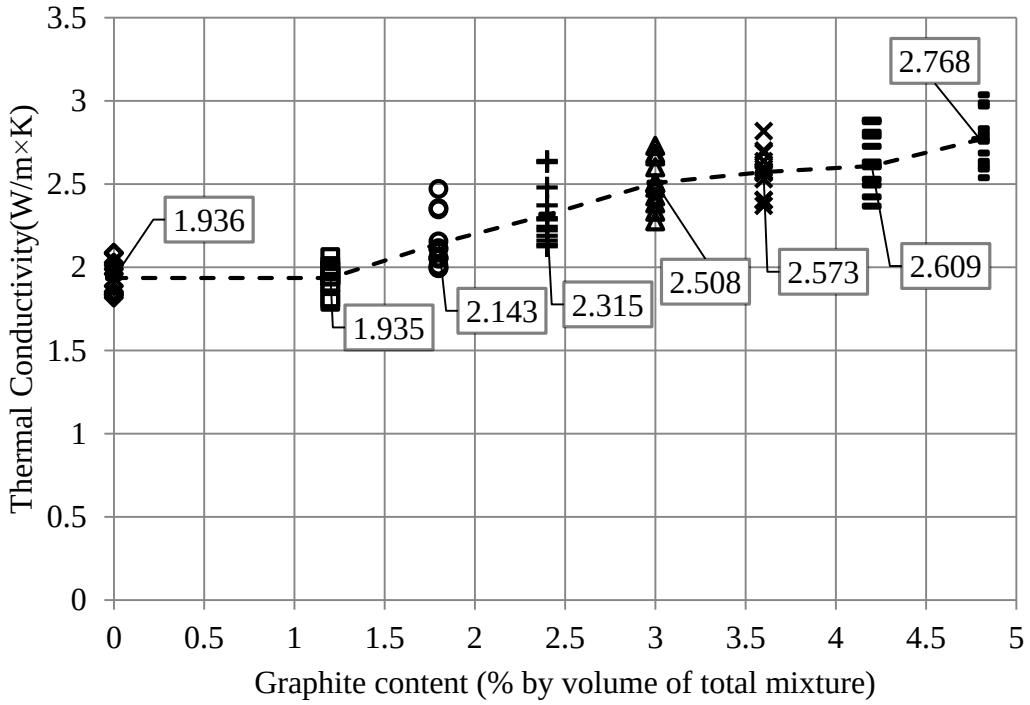

Figure 36. Thermal conductivity of graphite modified asphalt concrete

Unlike EPP modified asphalt concrete, the trend of volumetric heat capacity on various graphite content was not significant, as shown in Figure 37. The data was scattered widely, within the range of 1.119 MJ/m^3 × K and 2.813 MJ/m^3 × K. The reason for the unordered data is that the graphite had the similar heat capacity as other concrete materials, and the amount of graphite added was too small compared to the whole mixture that would not have a very strong effect on changing heat capacity of asphalt concrete.

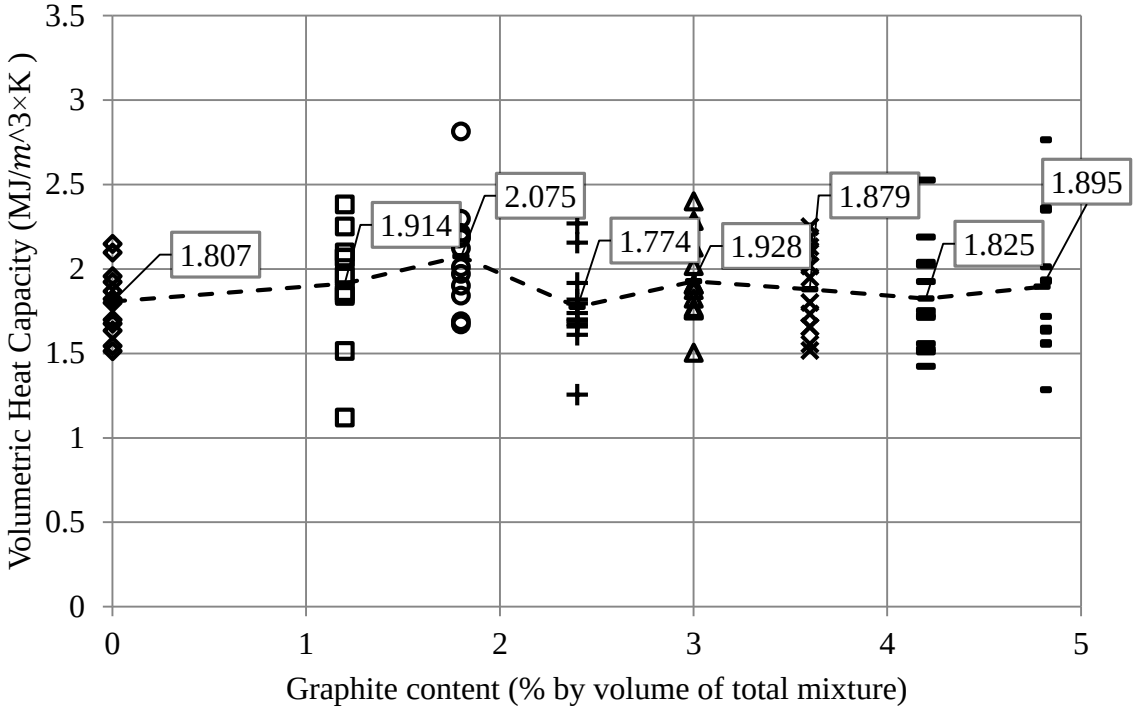

Figure 37. Heat capacity of graphite modified asphalt concrete

4.3 Summary of the Test Results

A summary of experiments results is listed in Table 8.

Table 8. Summary of experimental results

Target	Properties	Test	Samples	Results
Materials Characterization	Surface composition	SEM	EPP, graphite	EPP has rounded porous surface graphite is flake-shaped.
	Heat susceptibility	DSC Oven Heat Test	EPP	EPP melting point was confirmed as 172ºC EPP turned yellow partially after overnight heating at 143ºC.
Asphalt Binder Tests	Mixing & melting	EPP asphalt mixing test	EPP modified asphalt: 0,2.0%,4.0% and 6.0% by weight of asphalt	Difficult to mix EPP with asphalt
	Rheological properties	DSR		Addition of EPP increases viscosity of asphalt

Table 8. Summary of experimental results (continued)

Target	Properties	Test	Samples	Results
Asphalt Concrete Tests	Mechanical Performance	Volumetric & IDT	EPP samples: 0,4%,11% and 18% by vol. of mixture Graphite samples: 0, 1.2, 1.8, 2.4, 3.0, 3.6 ,4.2 and 4.8% by total vol. of mixture	EPP modified concrete sample was easier to compact while compacting graphite modified asphalt concrete required more gyrations. Hard to control %AV of EPP concrete EPP concrete samples had decreased IDT strengths. At 18%, the reduction was 17%. Adding 2.4% to 3.6% of graphite increased IDT strengths, and IDT strengths decreased with lower and higher graphite concrete. At highest volume content, IDT strength decreased by 20%.
	Thermal Properties	TPS		Both thermal conductivity and volumetric heat capacity decreased when EPP content increased, maximum reduction was reported as 32% and 27%, respectively. Thermal conductivity increased when graphite content increased, a maximum increase of 43% was obtained. Volumetric heat capacity did not change very much by adding graphite.

5. HEAT TRANSFER MODELS AND THERMAL APPLICATIONS

This section investigated the probable thermal applications of the thermally modified asphalt or cement concrete materials for various civil structures, including pavement, bridge deck, and concrete walls of buildings. For pavement and bridge deck, a numerical analysis based on a finite difference method of heat transfer was conducted using the data collected from previously published experimental data. The temperature gradients of these infrastructures during a day in the summer and winter were simulated, and the effects of using EPP or graphite as asphalt concrete additive on mitigating temperature-related problems were evaluated. In case of wall, a simple steady-state heat transfer model was used, and the feasibility of EPP as a wall thermal insulator was investigated.

5.1 Numerical Analysis of Pavement

As discussed in *Section 3*, the temperature gradient prediction model is applied to a full-depth asphalt pavement, with 28 cm thick asphalt layer on top of 300 cm thick subgrade. With the assumption that the temperature gradient does not vary with the location, the pavement is modeled as one dimensional problem, i.e., the heat transfer only occurs in vertical direction. The pavement surface has various heat sources involving radiation and convection, while temperature at the bottom of the pavement is assumed to be constant, not affected by the short climate changes. The asphalt layer consists of 29 nodes, dividing the layer into 28 elements with 1 cm thickness. The subgrade layer has

301 nodes that divides it into 300 elements. For different comparison cases, the pavement layer thicknesses and subgrade properties remained unchanged. The pavement model is shown in Figure 38.

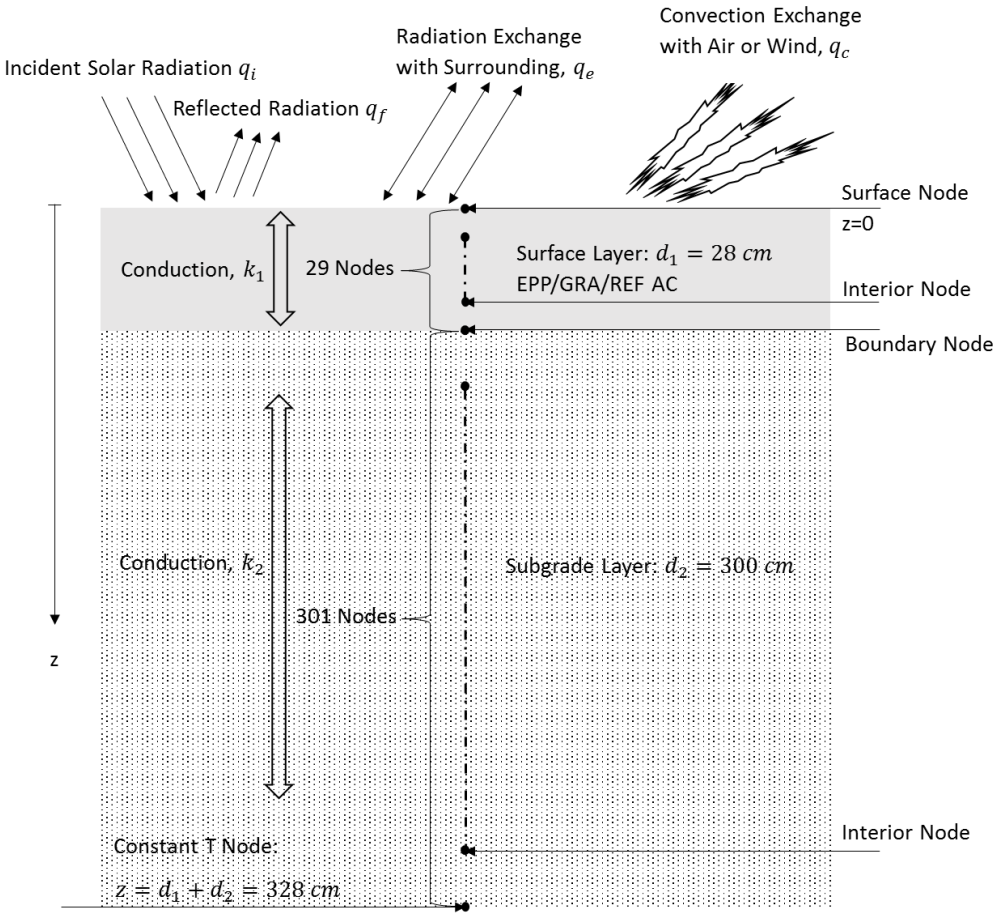

Figure 38. Pavement heat transfer model

Based on the theory introduced at *Section 3*, a Matlab code is developed to carry out the heat transfer analysis. Figure 39 shows the flow chart of the simulation procedure.

5.1.1 Simulation Input

Climatic data

In this model, the solar radiation, wind speed and air temperature at each hour are needed. The pavement surface boundary condition was explained in *Section 3*, the solar radiation is the major heat source of pavement system. The wind speed is the parameter to calculate the convection heat transfer coefficient. The difference between the air temperature and pavement surface temperature is used to compute the convection and emitted radiation.

For the winter case, the solar radiation and wind speed data was obtained from the environment Canada weather station in Fredericton, New Brunswick (Mrawira and Luca 2002). The air temperature data was assumed by the author. In case of summer, solar radiation was measured in Fort Hood, Texas on May 31, 1975 (Rapp and Hoffman 1977). Air temperatures of May 31, 1975 were checked from online temperature history database (www.weathersource.com).

The same wind speed profile is used for the summer and winter simulations. Table 9 lists the hourly wind speeds used in the simulation. The air temperatures and solar radiations of winter and summer are plotted in Figure 40 and Figure 41, respectively.

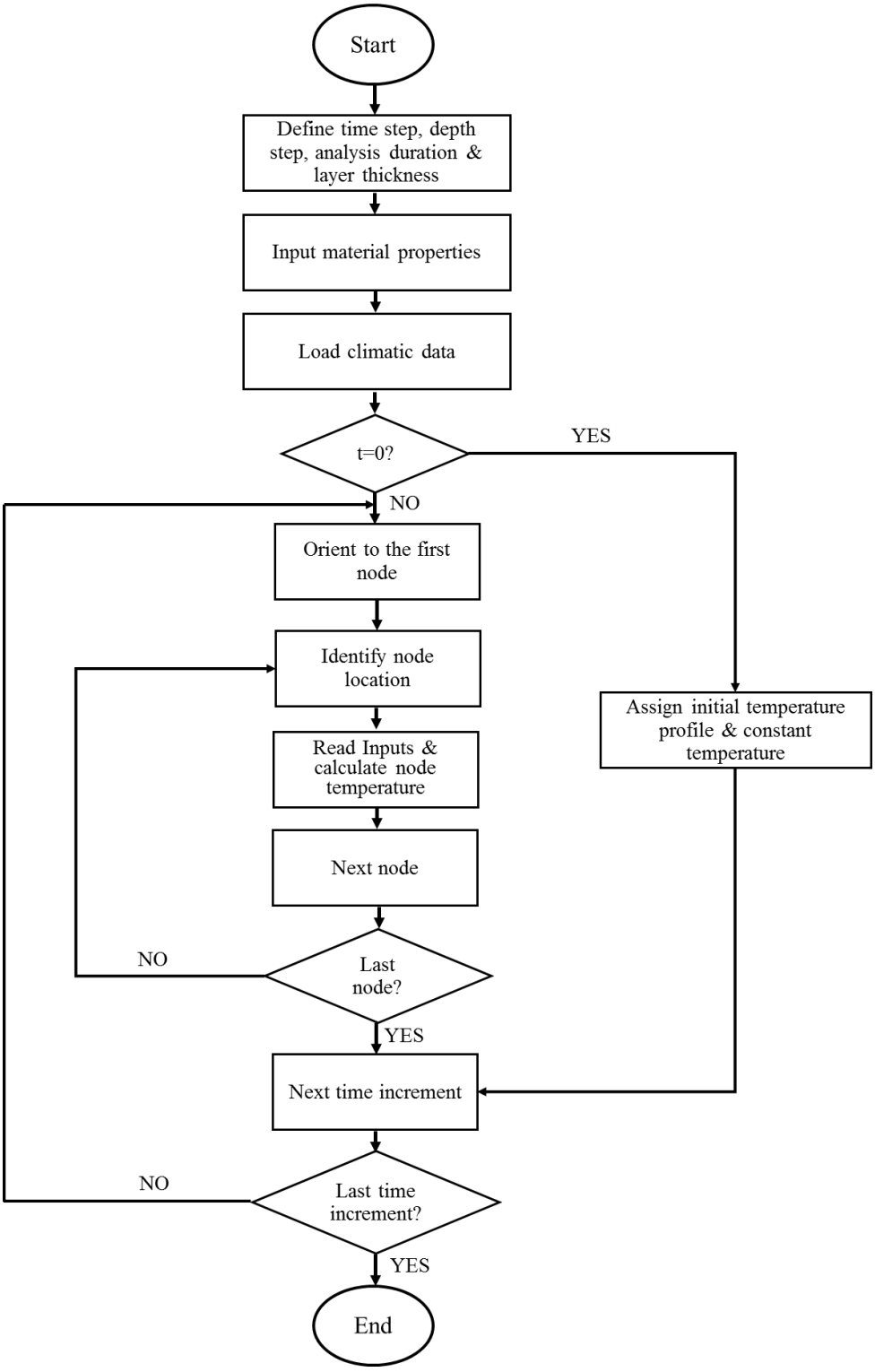

Figure 39. Flow chart of simulation procedure

Table 9. Wind speed for both summer and winter simulations

0:00 ~ 3:00	**4:00**	**6:00 ~ 9:00**	**10:00**	**11:00**	**12:00**	**13:00 ~ 15:00**	**16:00**	**17:00**	**18:00 ~ 22:00**	**23:00**
12 km/h	11 km/h	12 km/h	13 km/h	15 km/h	16 km/h	17 km/h	16 km/h	14 km/h	13 km/h	12 km/h

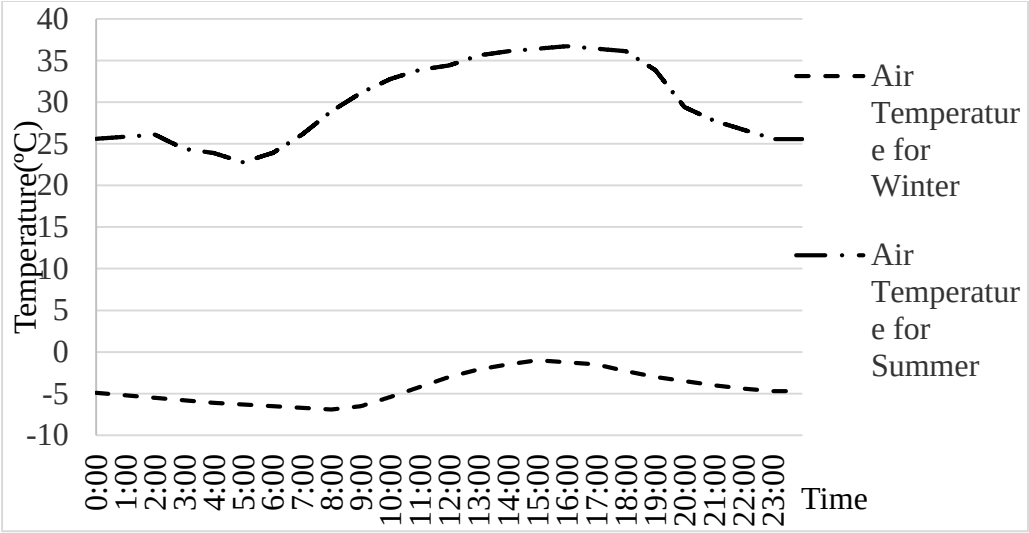

Figure 40. Air temperatures of summer and winter

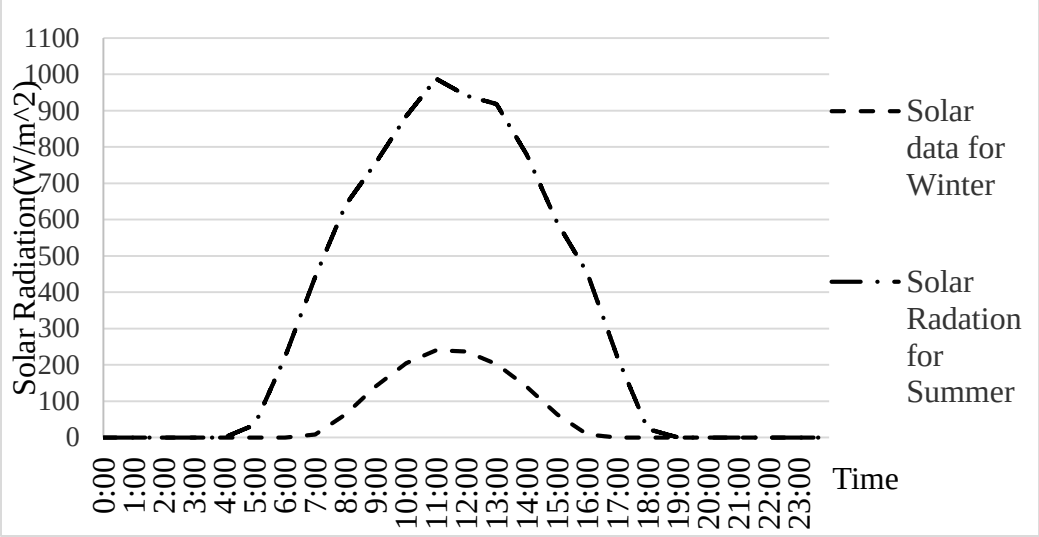

Figure 41. Solar radiations of summer and winter

Material properties

The required material properties are the absorptivity ($\alpha = 1 - \beta$) and emissivity (e) of the surface layer, and thermal conductivity (k) and volumetric heat capacity (c) of the all layers.

The same absorptivity ($\alpha = 0.9$) and emissivity ($e = 0.85$) are used for both reference and modified asphalt concrete. The thermal properties of the reference, EPP modified, and graphite modified asphalt concrete layers are obtained from the measurements described in *Section 4*. The asphalt concrete samples containing highest additives content, EPP-100%-AC (18% EPP by total volume of the mixture) and GRA-40%-AC (4.8% graphite by total volume of the mixture) are selected. Thermal properties of subgrade are obtained from Yunus (2003), and remain constant during the comparative simulations. The material properties are summarized in Table 10.

Table 10. Thermal properties inputs of pavement layers

Case		**Layer**	**Thermal Conductivity ($\mathbf{W/m \times K}$)**	**Volumetric Heat Capacity ($\mathbf{MJ/m^3 \times K}$)**
Comparison 1	#1	D-5 Ref AC	2.431	2.009
	#2	D-5 EPP AC	1.643	1.473
Comparison 2	#3	D-6 Ref AC	1.936	1.807
	#4	D-6 Graphite AC	2.768	1.895
All Pavements		**Subgrade**	**1.00**	**2.85**

Initial condition

Because of the lacking of the field data, the initial temperature gradient for the simulation is assumed in reasonable manner after reviewing the temperature gradient data at other locations.

5.1.2 Prediction Procedures

The simulation uses Equation 13~16 in *Section 3*. Temperature variations during 24-hours (from 0:00 to 24:00) are simulated with 12 second time increment (Δt).

5.1.3 Prediction Results

Summer prediction

Daily temperature variation

The 24-hour temperature variations at surface, 5cm depth and 20cm depth of the pavement for the four cases: the reference D-5 asphalt concrete, EPP modified asphalt concrete, reference D-6 asphalt concrete, and graphite modified asphalt concrete, are shown in Figure 42~45, respectively. From these figures, it is concluded that the temperature at surface is most sensitive to the daily weather changes, and the temperature is less affected by the daily changes as the depth increases. Maximum pavement surface temperature is observed at 13:00pm while minimum temperature occurred at 5:00am. The peak temperatures occur with delay as the depth increases. During the daytime, the surface temperature is much higher than the air temperature because of the strong solar heat, but is similar to air temperature at night.

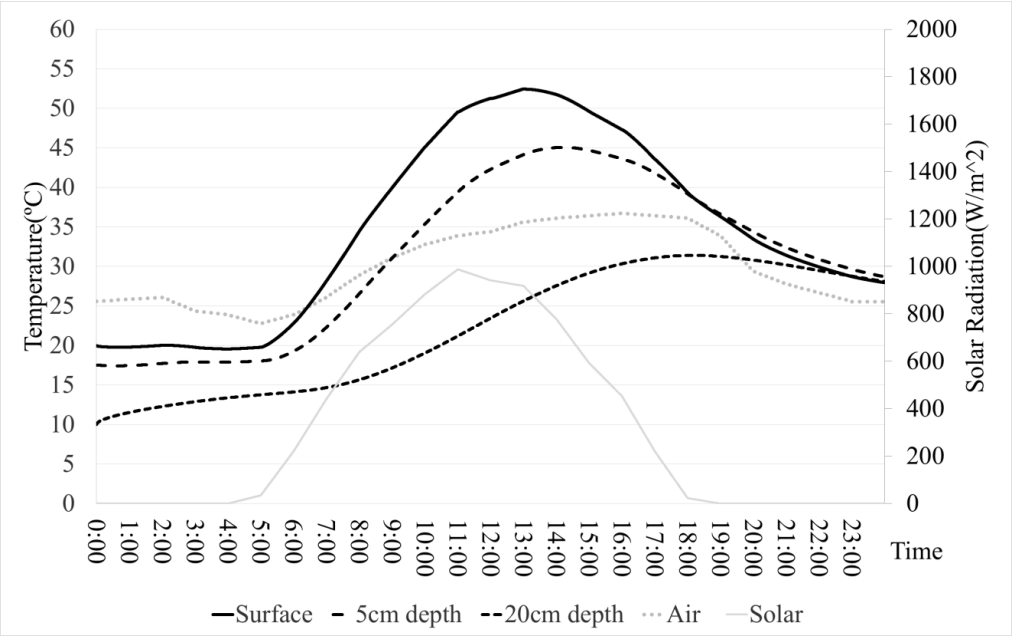

Figure 42. Predicted temperature variation with time in D-5 reference AC pavement (summer)

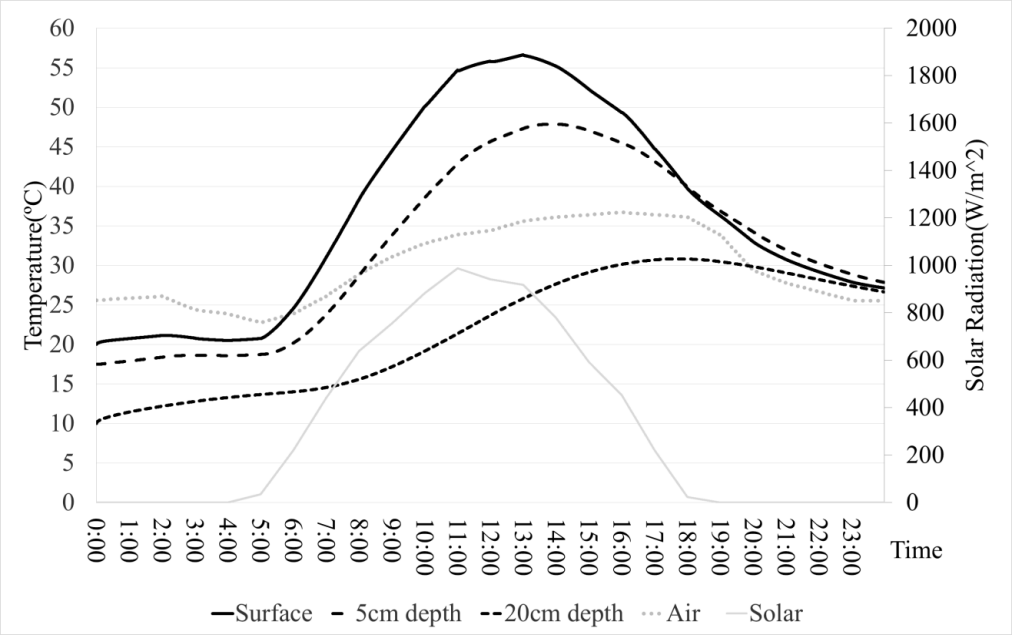

Figure 43. Predicted temperature variation with time in D-5 EPP modified AC pavement (summer)

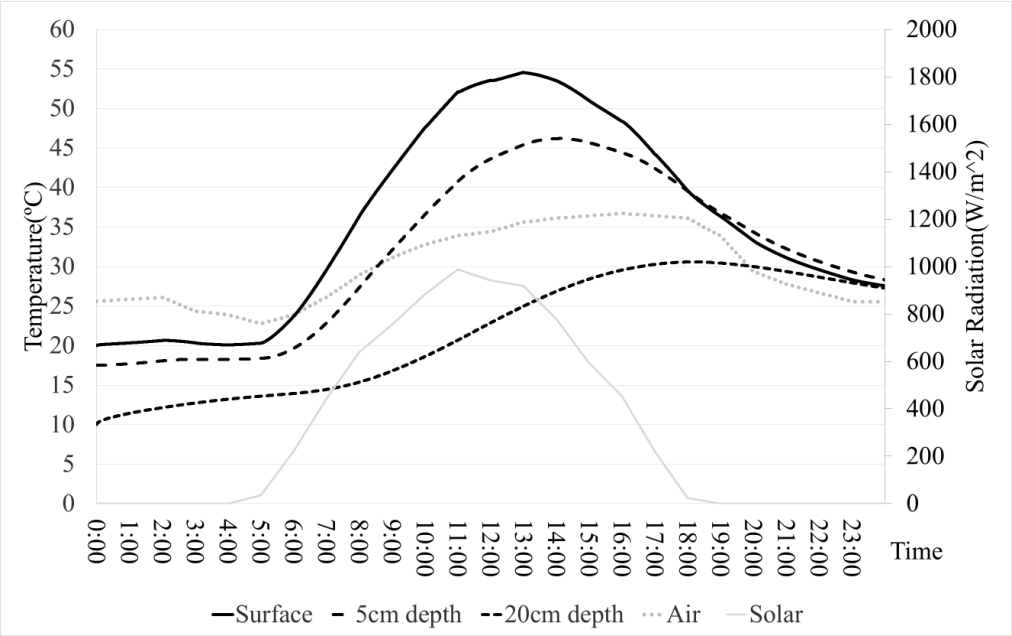

Figure 44. Predicted temperature variation with time in D-6 reference AC pavement (summer)

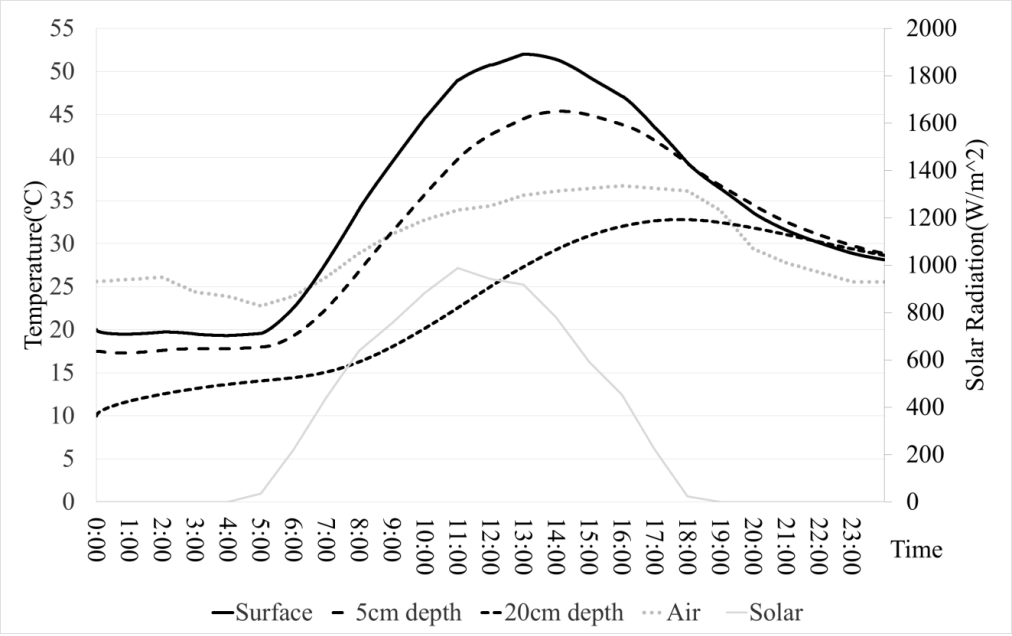

Figure 45. Predicted temperature variation with time in D-6 graphite modified AC pavement (summer)

Temperature gradient

Temperature profiles of pavements containing different kinds of modified/ unmodified asphalt concrete are plotted in Figure 46~49. As shown in the figures, the asphalt concrete layer starts to be heated up by the solar energy, and the surface temperature increases with time. After 16:00pm, the pavement surface begins to cool down, and a reversal in the temperature profile occurred at 20:00pm. The reason for the reversal is explained that after 16:00, the solar energy becomes weak, and the temperature in the top part of asphalt concrete layer dropped rapidly because of the convection and emission on the surface. In the meantime, the temperature at bottom is still high because it takes time to transfer heat through the pavement. As a result, the maximum temperature is observed below the surface at 20:00.

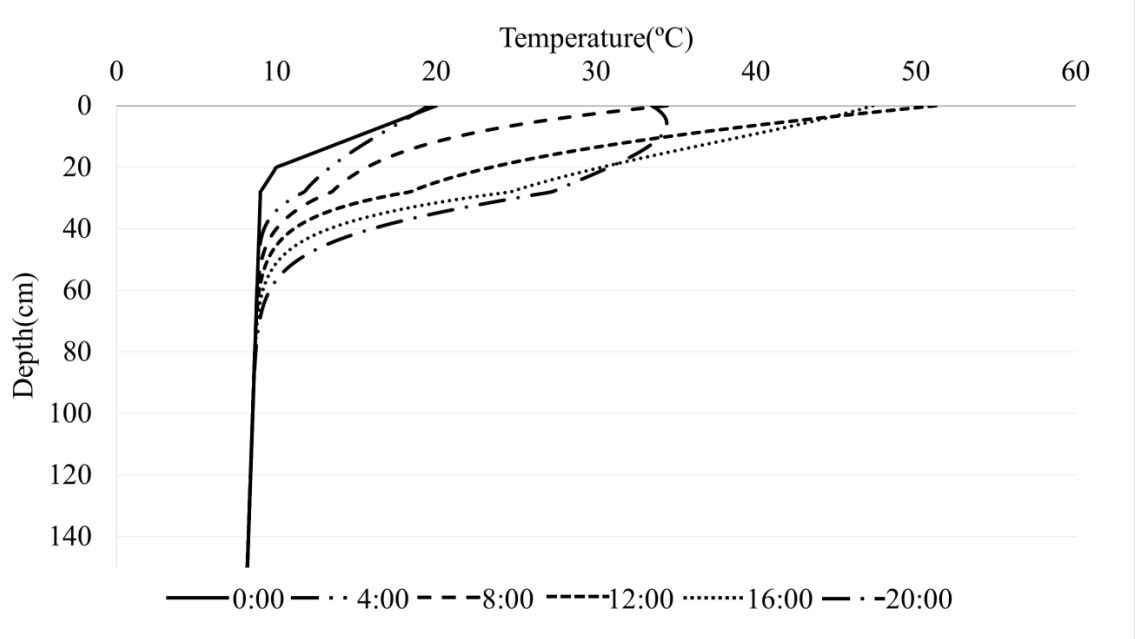

Figure 46. Predicted temperature profile in D-5 reference AC pavement (summer)

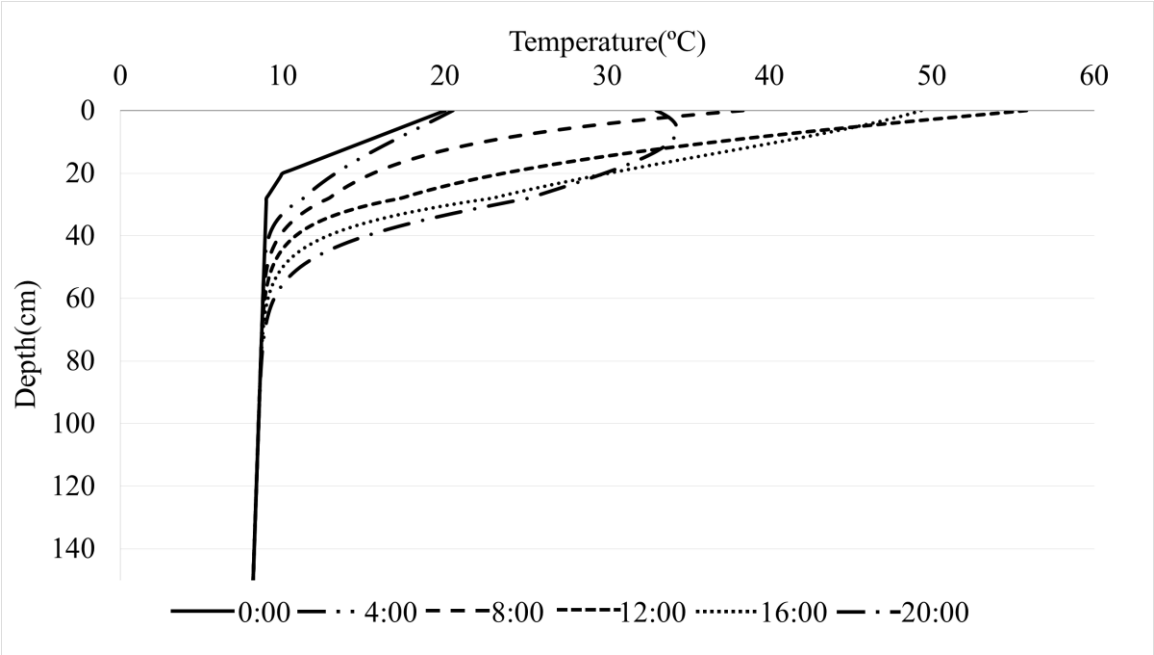

Figure 47. Predicted temperature profile in D-5 EPP AC pavement (summer)

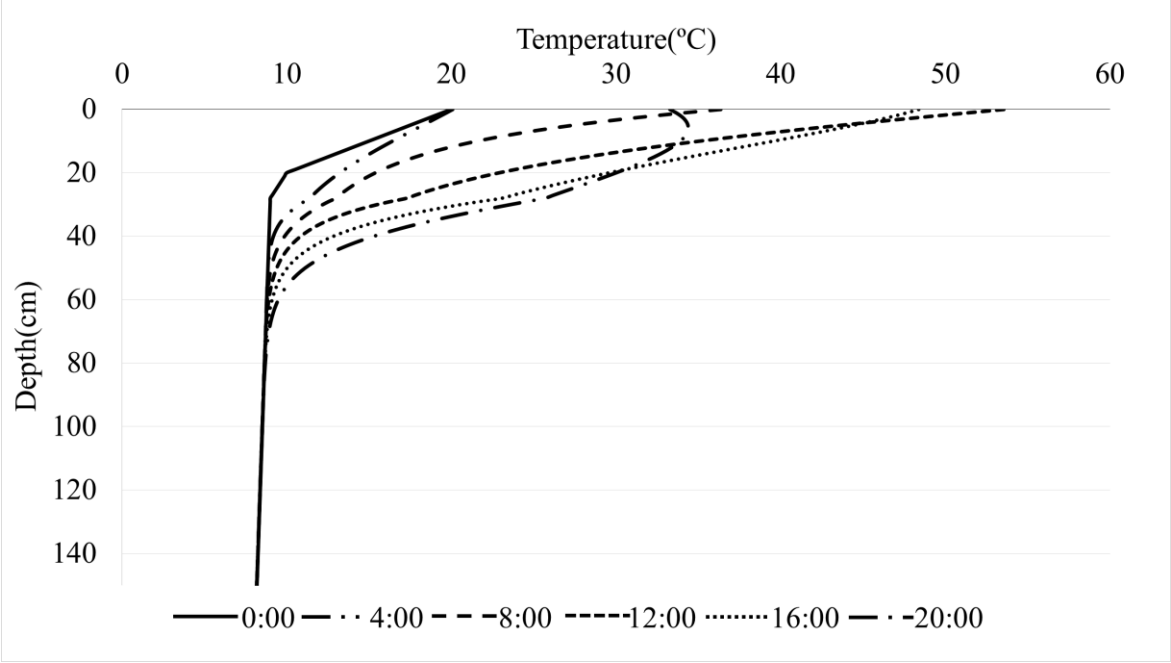

Figure 48. Predicted temperature profile in D-6 reference AC pavement (summer)

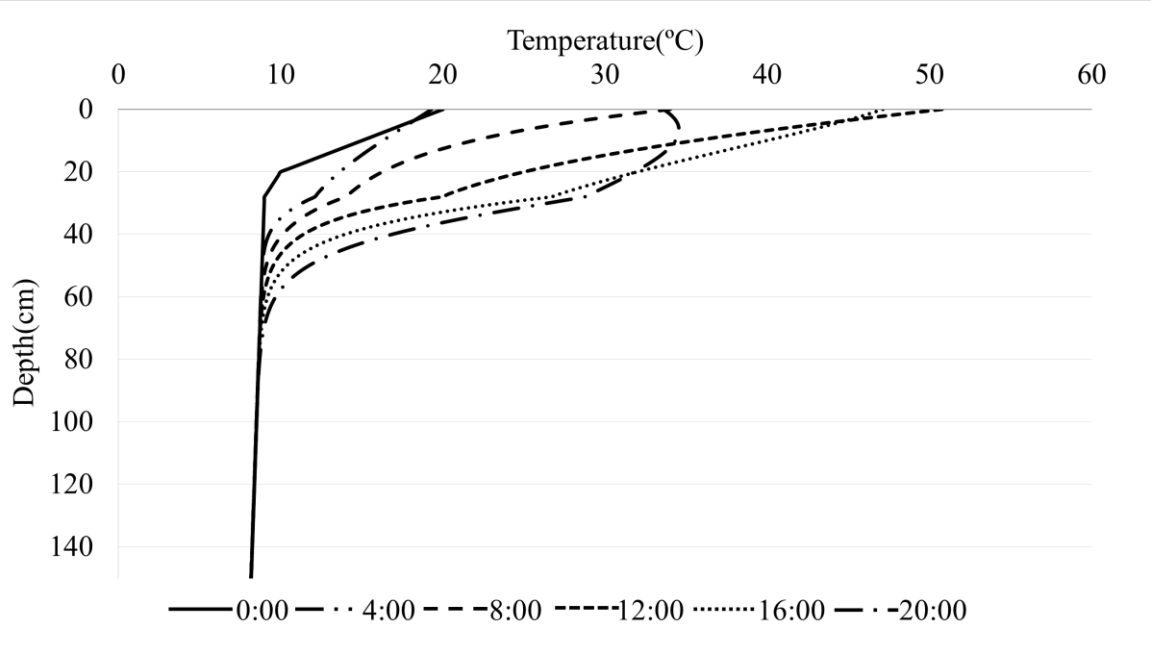

Figure 49. Predicted temperature profile in D-6 graphite AC pavement (summer)

Comparison of pavement surface temperature

The pavement surface temperature in summer is of great interest in this study because it is directly related to the ability of mitigating urban heat island effect. Figure 50 and Figure 51 compare the surface temperatures of the EPP modified pavement and graphite modified pavement with their corresponding reference pavement, respectively. As shown in the figures, adding 18% EPP by volume of total asphalt mixture increases the pavement maximum surface temperature (occurred at 13:00) by 5.2ºC. Conversely, 4.8% graphite decreases the maximum surface temperature by 3.1ºC. It is obvious that graphite modified asphalt concrete is effective for mitigating urban heat island effect while adding EPP could even make the situation worse from the simulation. In addition, because

of lower pavement temperature, the rutting in graphite modified asphalt concrete is expected to be reduced as well.

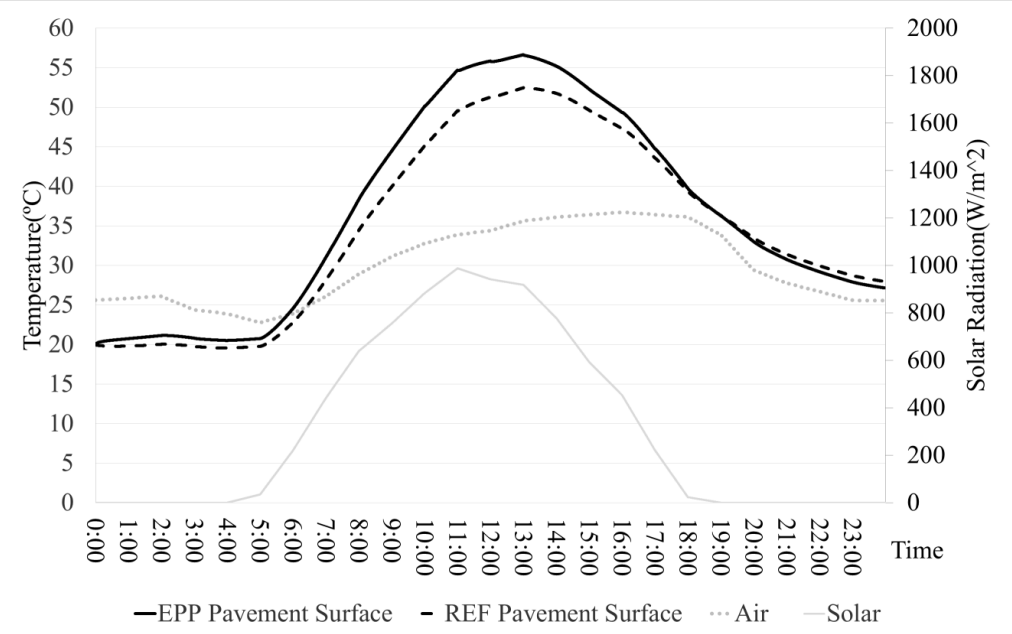

Figure 50. Comparison of surface temperature of EPP and reference AC (summer)

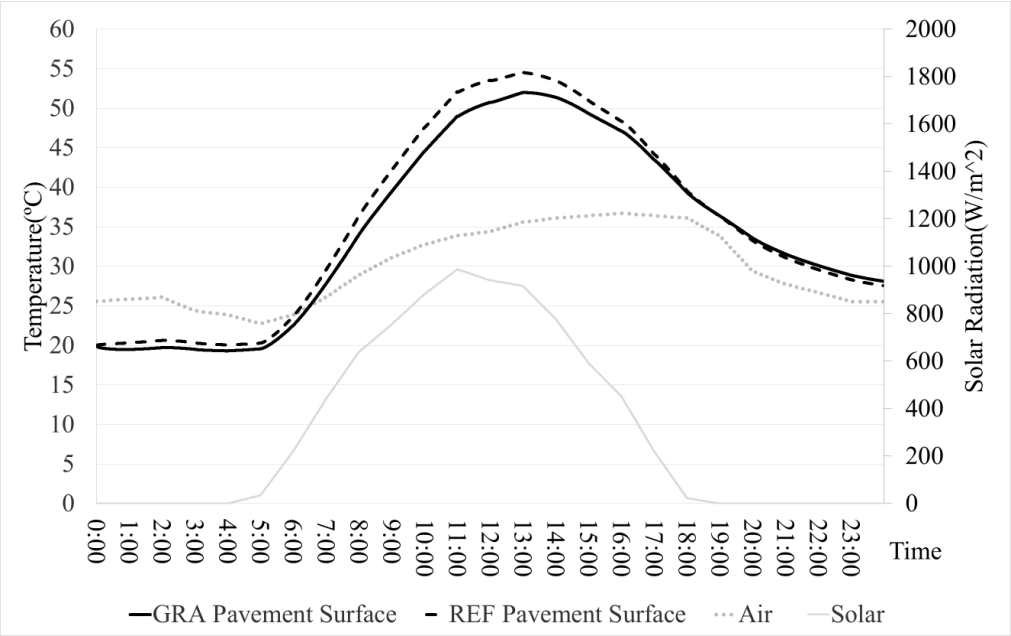

Figure 51. Comparison of surface temperature of graphite and reference AC (summer)

Winter prediction

Daily temperature variation

The temperature variations with time in winter are shown in Figure 52~55. The trend of the temperature variation is similar to the summer prediction, the pavement surface temperature in winter is above the air temperature for all the analysis duration.

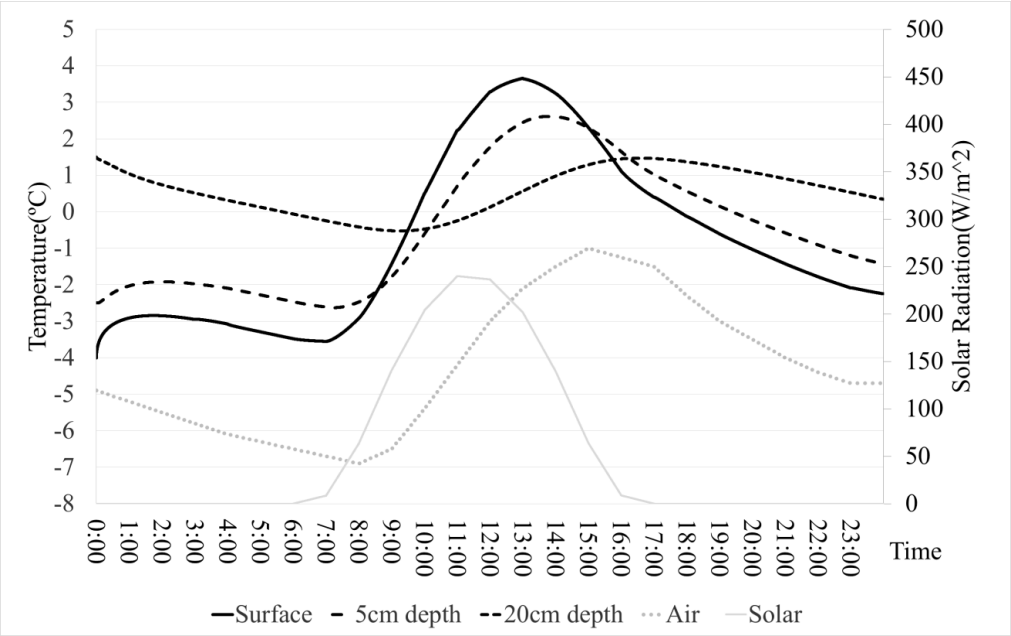

Figure 52. Predicted temperature variation with time in D-5 reference AC pavement (winter)

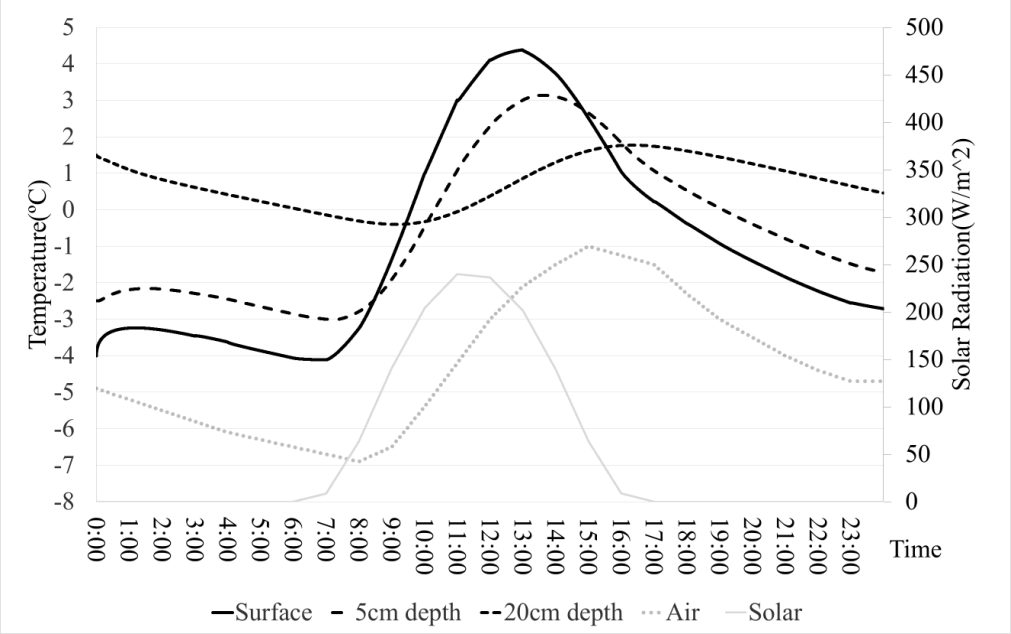

Figure 53. Predicted temperature variation with time in D-5 EPP AC pavement (winter)

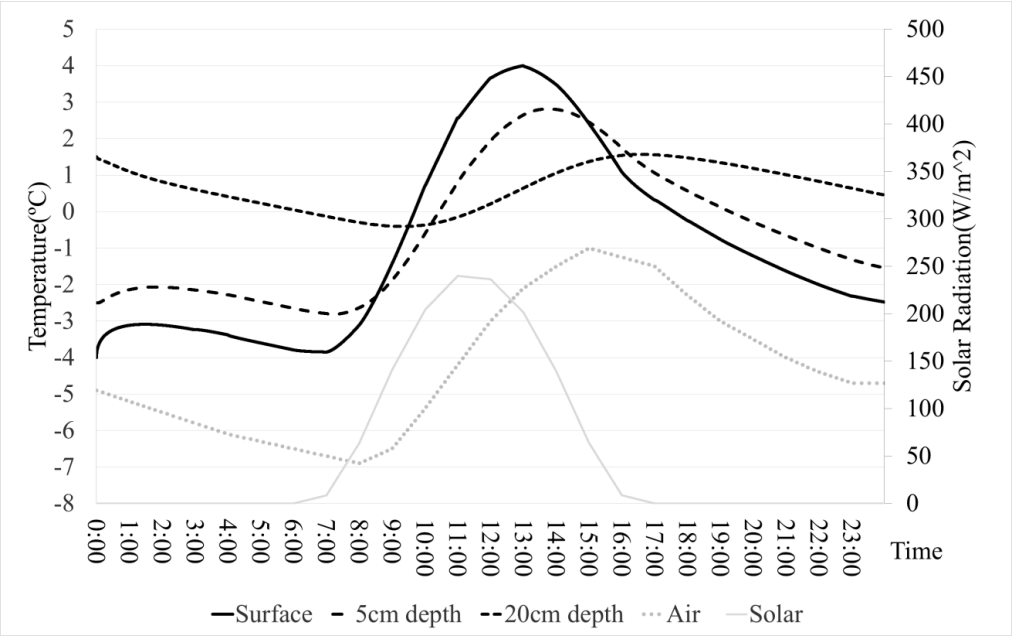

Figure 54. Predicted temperature variation with time in D-6 reference AC pavement (winter)

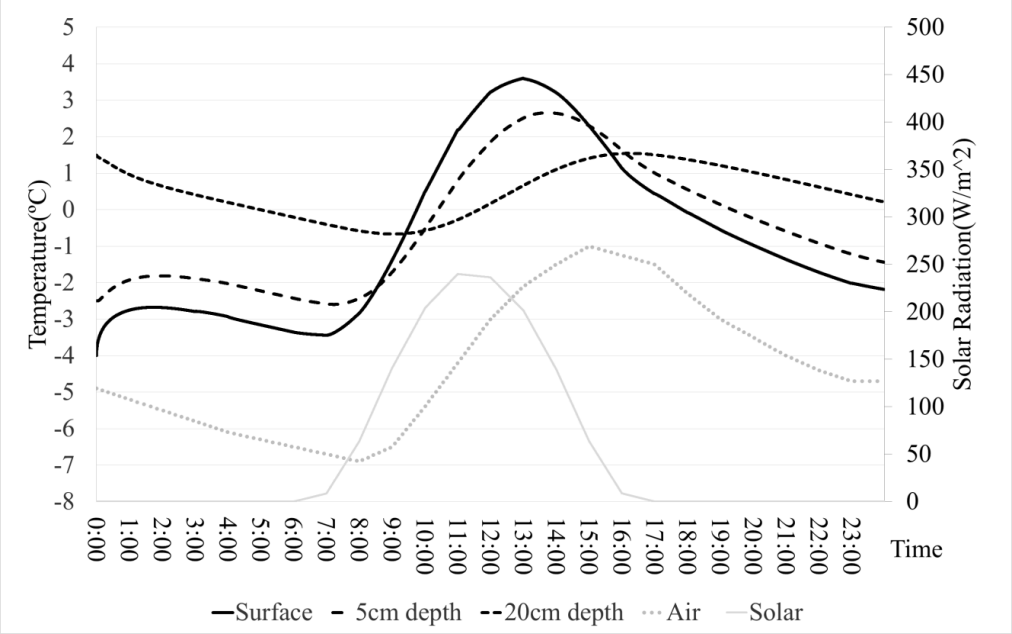

Figure 55. Predicted temperature variation with time in D-6 graphite AC pavement (winter)

Temperature gradient

Temperature profiles of winter prediction are presented in Figure 56~59. As time passed, the pavement surface temperature starts to go up. Solar energy transfers downward from the surface and temperature gradient becomes smaller. Similar to the summer case, an arc forms because the solar energy is strong in the noon and the heat could not transfer in time. At 16:00pm, another arc develops in the gradient curve as the surface starts to cool down.

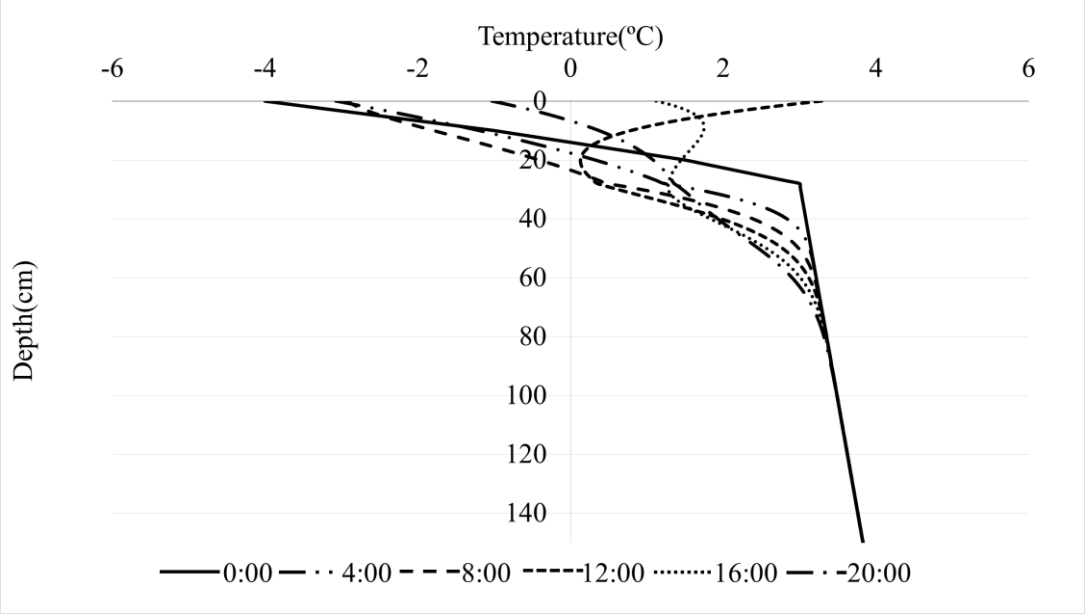

Figure 56. Predicted temperature profile in D-5 reference AC pavement (winter)

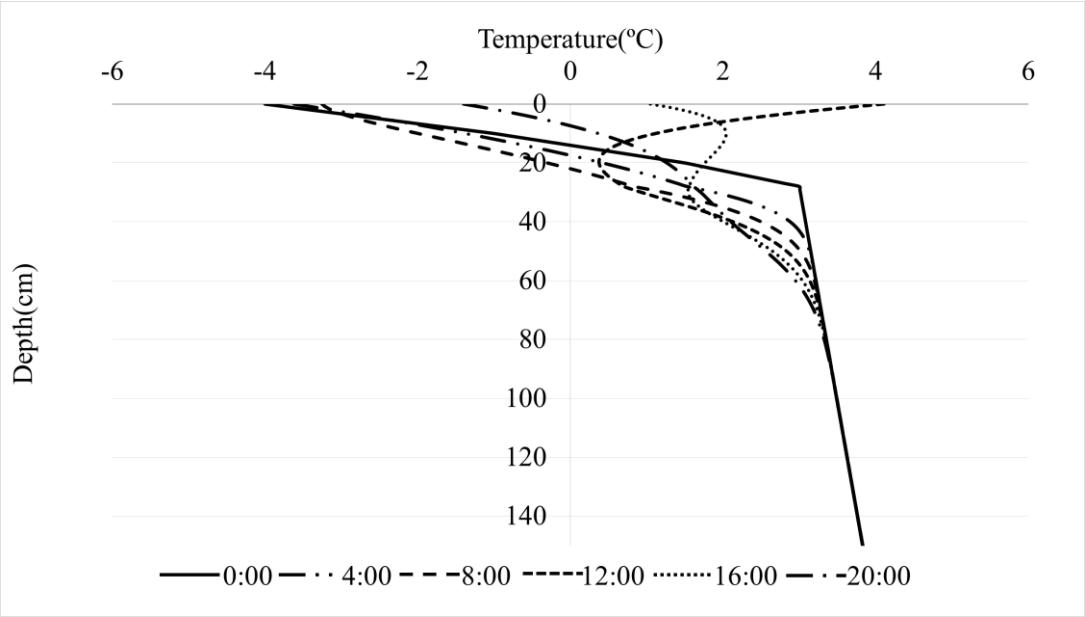

Figure 57. Predicted temperature profile in D-5 EPP AC pavement (winter)

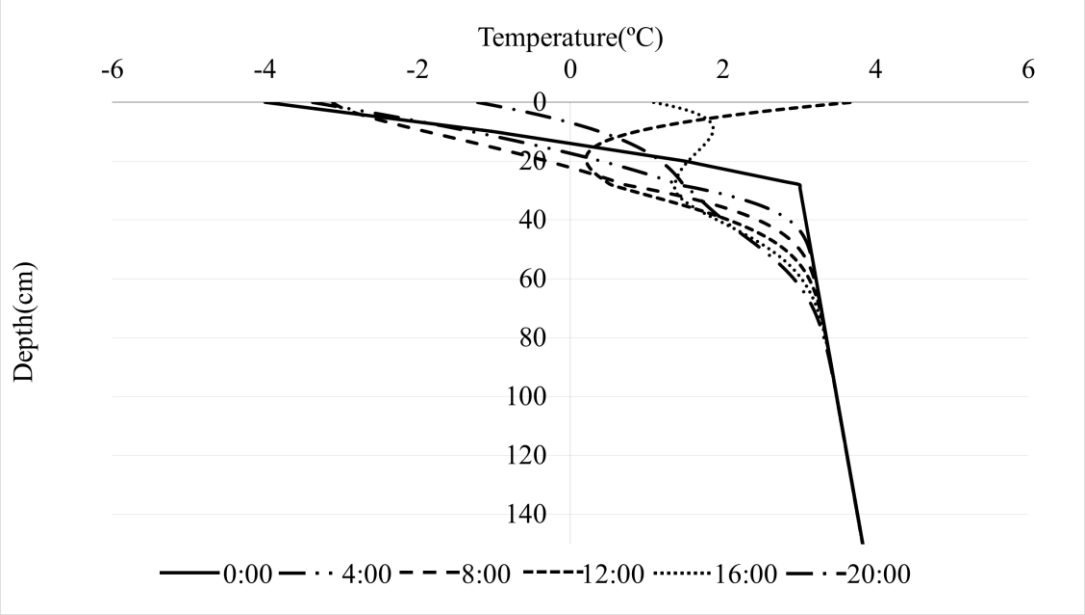

Figure 58. Predicted temperature profile in D-6 reference AC pavement (winter)

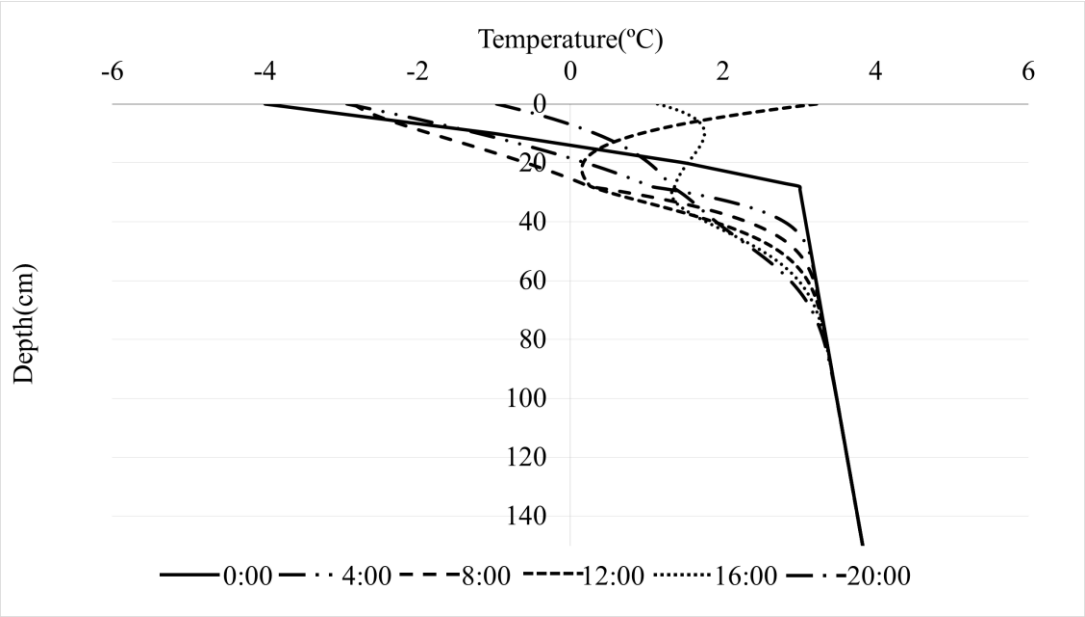

Figure 59. Predicted temperature profile in D-6 graphite AC pavement (winter)

Comparison of pavement surface temperature

Pavement surface temperature varies during 24 hours. In the night, the temperature drops rapidly, the surface minimum temperature is crucial to ice formation: the higher the minimum temperature, the harder the ice layer will form. In the daytime, the solar heats the pavement and temperature rises. Surface maximum temperature, which occurs in the noon, directly affects pavement snow and ice melting ability, with higher maximum temperature, the snow and ice melts more easily. Figure 60 and Figure 61 compare the winter prediction results of pavement surface temperatures. Figure 60 indicates that addition of EPP increased the temperature variation, this added more difficulties to pavement deicing because lower temperature in the night would demand more deicing agent. Besides, decreasing pavement minimum temperature (occurrs at 7:00) will lead to

more low temperature cracking. However, in the daytime, pavement containing EPP asphalt concrete layer has higher peak temperature, making it easier for melting snow and ice. Conversely, graphite modified asphalt concrete will both improve pavement deicing ability and reduce low temperature cracking because pavement minimum temperature increases, but will have worse snow and ice removal application because of its lower maximum temperature in the noon, as indicated in Figure 61.

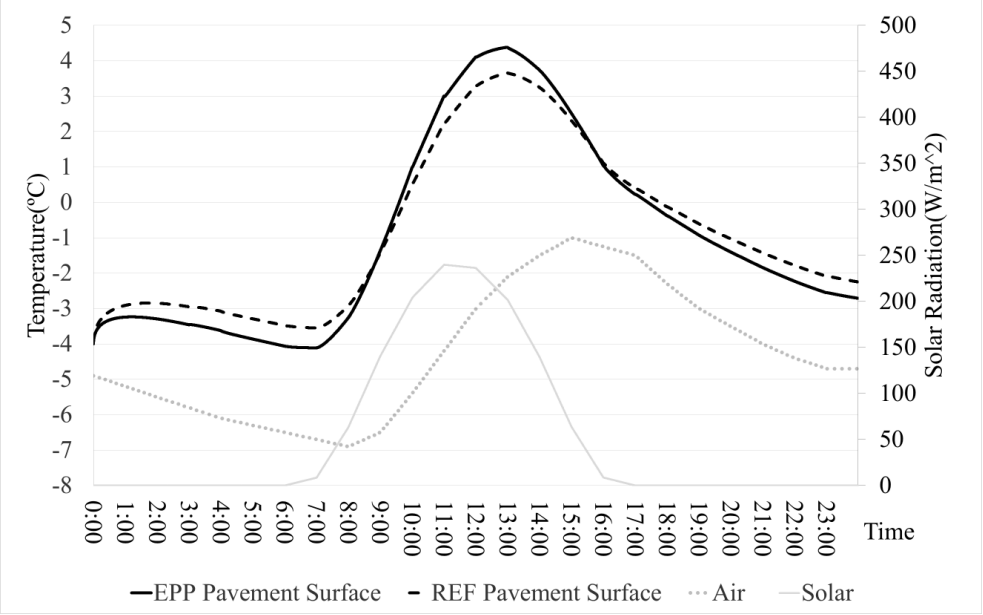

Figure 60. Comparison of surface temperature of EPP and reference AC (winter)

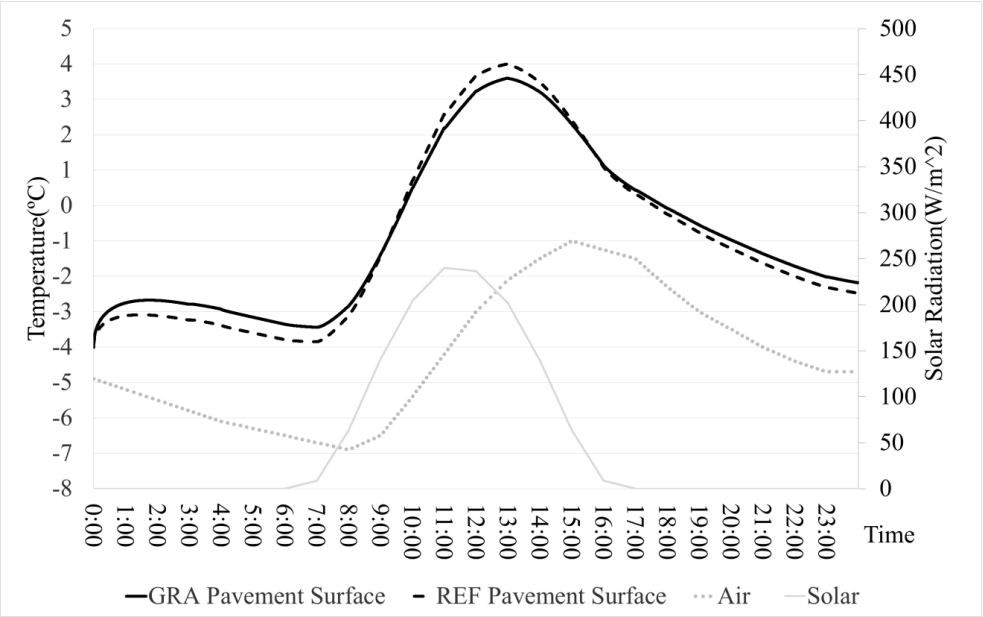

Figure 61. Comparison of surface temperature of graphite and reference AC (winter)

Sensitivity analysis

To further study the impact of each thermal property on pavement surface temperature separately, a sensitivity analysis is carried out. In this analysis, the weather data inputs and initial pavement temperature profile are followed as winter simulation, the AC layer material thermal properties vary independently, as listed in Table 11 and Table 12.

Table 11. Sensitivity analysis on thermal conductivity

Layer	Thermal Conductivity ($W/m \times K$)	Volumetric Heat Capacity ($MJ/m^3 \times K$)
Assumed Layer	0.5/1.0/1.5/2.0/2.5/3.0	2.0
Subgrade	1.0	2.85

Table 12. Sensitivity analysis on heat capacity

Layer	Thermal Conductivity ($W/m \times K$)	Volumetric Heat Capacity ($MJ/m^3 \times K$)
Assumed Layer	2.0	1.0/1.5/2.0/2.5/3.0
Subgrade	1.0	2.85

Figure 62 and Figure 63 showed the analysis results. It is concluded that:

1)When thermal conducitivity (k) increases, pavement maximum surface temperature decreases, but minimum surface temperature increases. This is because higher thermal conductivity reduces the surface temperature by allowing the heat absorbed from solar to be transferred rapidly to the deep ground during daytime. This heat then transfers back to the surface faster because of good conduciton and the minimum surface temperature increases during night (Gui et al. 2007).

2) When heat capacity (c) increases, pavement maximum surface temperature decreases, while minimum surface temperature increases. This conclusion is obvious because heat capacity is the measurable physical quantity of heat required to change the temperature, the higher the heat capacity, the better the material will resist temperature change.

That is to say by either increasing thermal conductivity or heat capacity, pavement surface variation will decrese. The conclusion matches the simulation results from Gui et al. (2007).

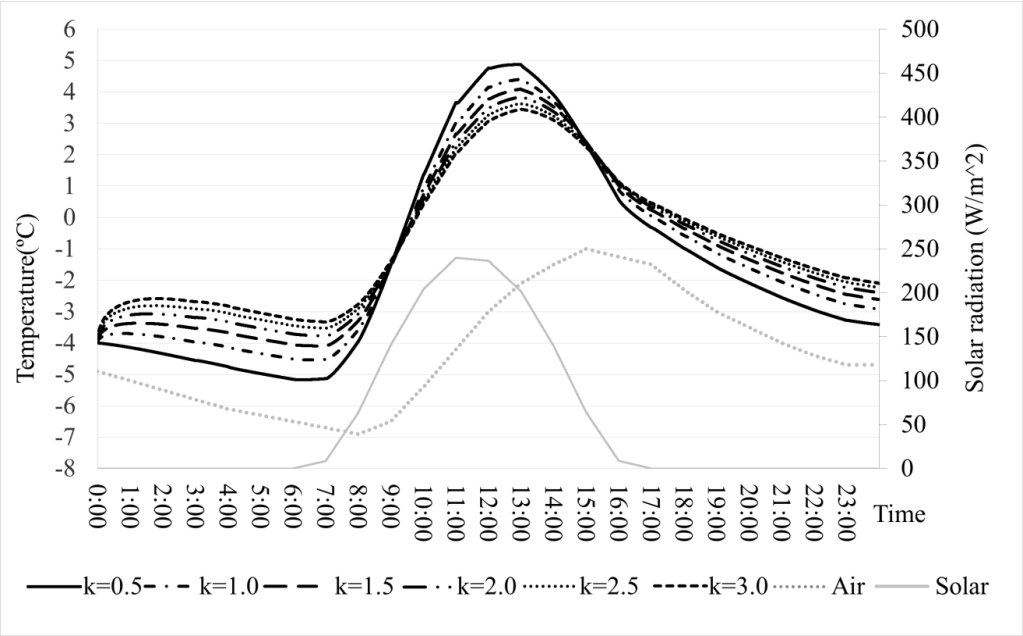

Figure 62. Sensitivity analysis on thermal conductivity

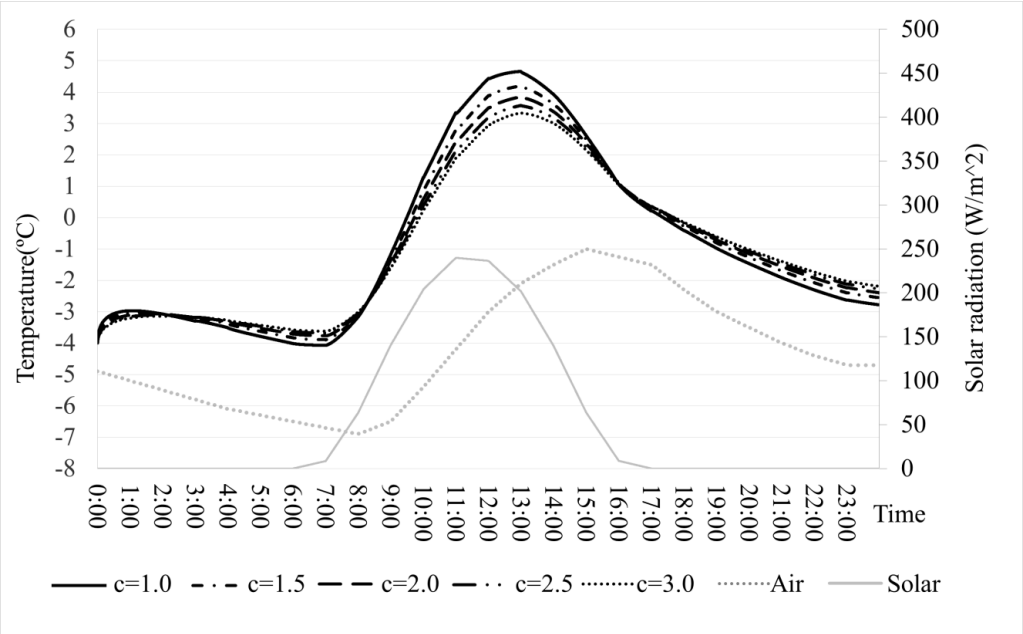

Figure 63. Sensitivity analysis on heat capacity

5.2 Numerical Analysis of Bridge Deck

Regarding the bridge model, the deck is assumed to have two layers. The top layers is 10-cm thick-reference/modified asphalt concrete, the bottom layer is 20cm thick plain concret layer, which remains unchanged for different cases. Different from pavement simulation, at the bottom of the deck, it also exchanges heat by convection and emission. The model is explained as Figure 64. Equations 17~22 described in *Section 3* are used to calculate the bridge deck temperature variation with time.

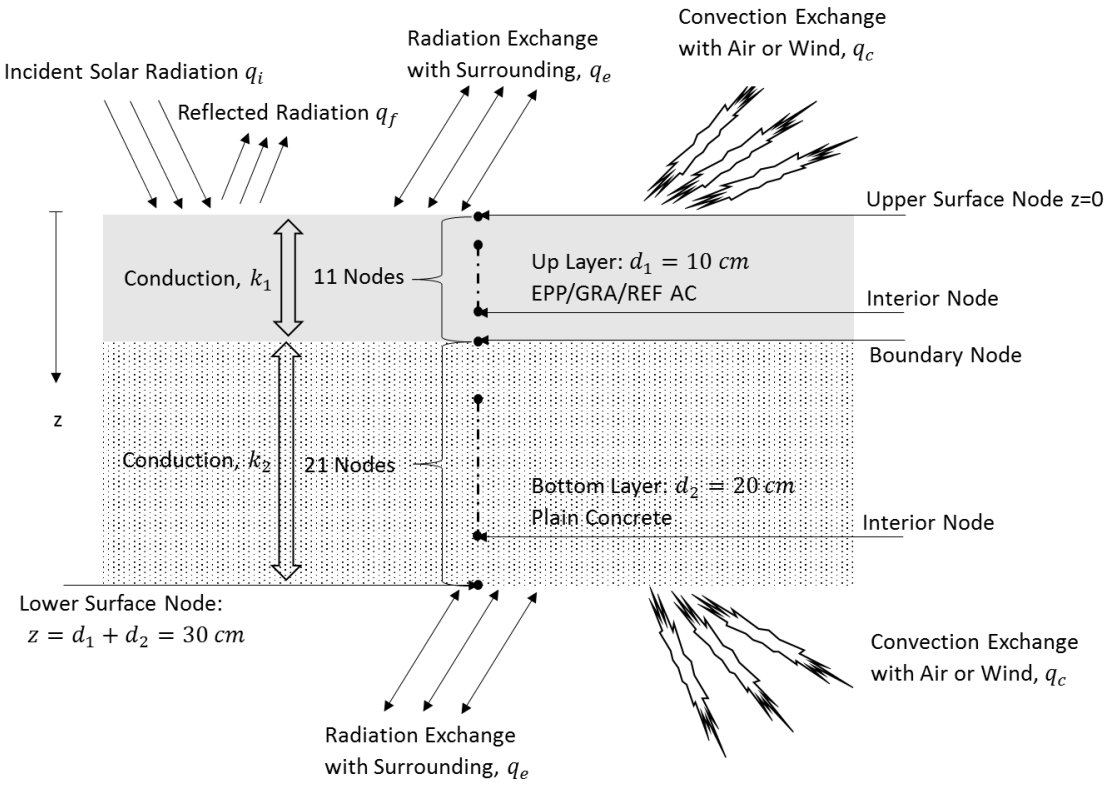

Figure 64. Bridge deck heat transfer model

5.2.1 Simulation Input

Climatic data input, time increment, depth increment, surface absorptivity and emissivity remain same with pavement simulation. The emissivity at bottom of the bridge is selected as 0.75, which is typical value for cement concrete material (Hermansson 2001). The initial temperature profile of bridge deck is based on author's assumption. For the summer prediction, the initial temperature of each node is set as 26ºC. For the winter, -3ºC was used. The materials thermal properties inputs are listed in Table 13.

Table 13. Thermal properties inputs of bridge layers

Case		**Layer**	**Thermal Conductivity ($\mathbf{W/m \times K}$)**	**Volumetric Heat Capacity ($\mathbf{MJ/m^3 \times K}$)**
Comparison 1	#1	D-5 Ref AC	2.431	2.009
	#2	D-5 EPP AC	1.643	1.473
Comparison 2	#3	D-6 Ref AC	1.936	1.807
	#4	D-6 Graphite AC	2.768	1.895
All Bridge Decks		**Plain Concrete**	**2.13**	**1.61**

Note: The thermal properties of plain concrete was tested by Dr. Chang-Seon Shon from Texas A&M Transportation Institute via TPS 2500S.

5.2.2 Simulation Results

The simulation results for 48-hour analysis duration of temperature distributions are presented as follows:

Summer prediction

Comparison of deck surface and bottom temperature

The surface and bottom temperature variations with time of bridge deck containing different asphalt concrete layer are compared in Figure 65 and Figure 66. From the figures, it is found that although boundary condition at the bottom of the bridge deck and pavement are different, the temperature variation with time at the surface of the deck has the similar trend with pavement: adding EPP increases maximum surface temperature while adding graphite decreases the temperature. The maximum reduction in pavement surface temperature is obtained as 1.87ºC according to the simulation. Considering the bottom temperature distribution, the effects of additives added in the top layers turn out to be negligible.

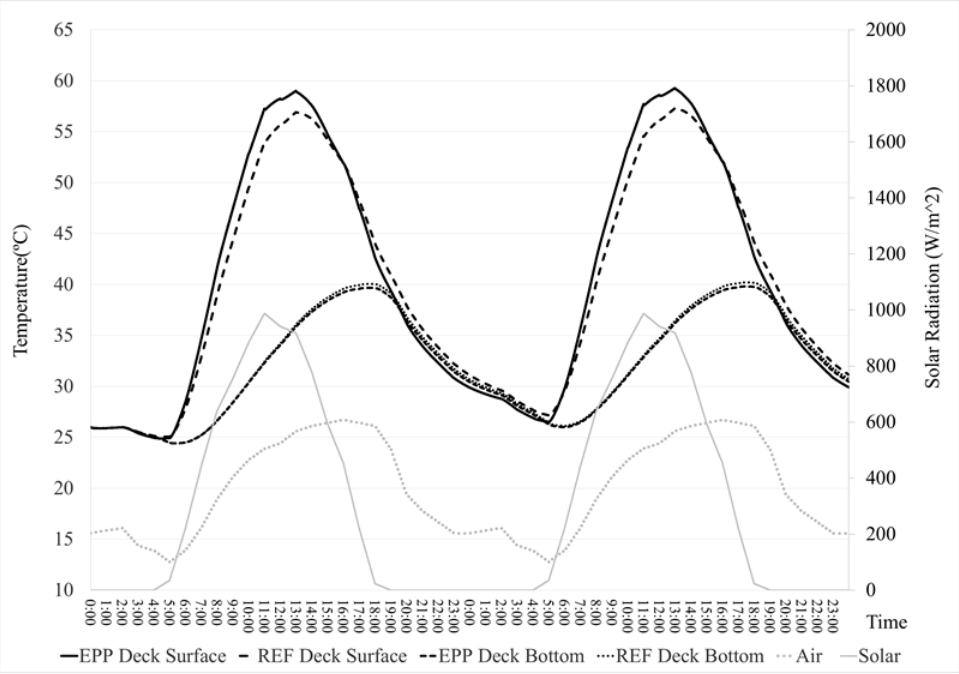

Figure 65. Comparison of surface and bottom temperatures of EPP and reference AC (summer)

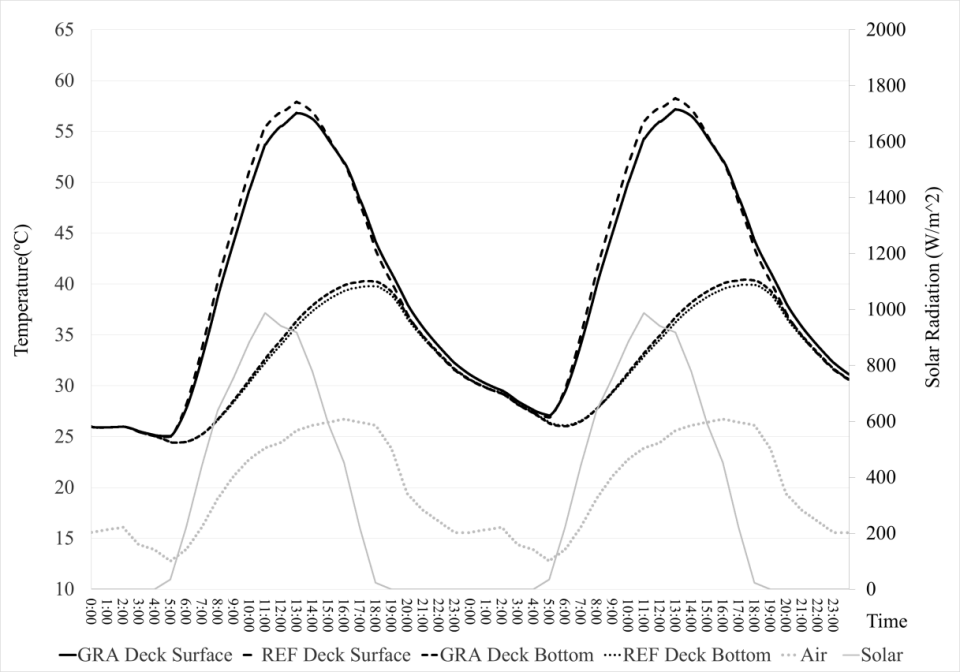

Figure 66. Comparison of surface and bottom temperatures of graphite and reference AC (summer)

Comparison of temperature profile in deck

Temperature profiles between pavements containing modified asphalt concrete layer and plain asphalt concrete layer at the time where min/max surface temperatures occur are compared in Figure 67 and Figure 68. Figure 67 shows temperature gradient in EPP asphalt concrete is bigger than reference one, this is because EPP has a lower thermal conductivity. Similarly, higher thermal conductivity leads to a smaller gradient in the graphite AC, as shown in Figure 68.

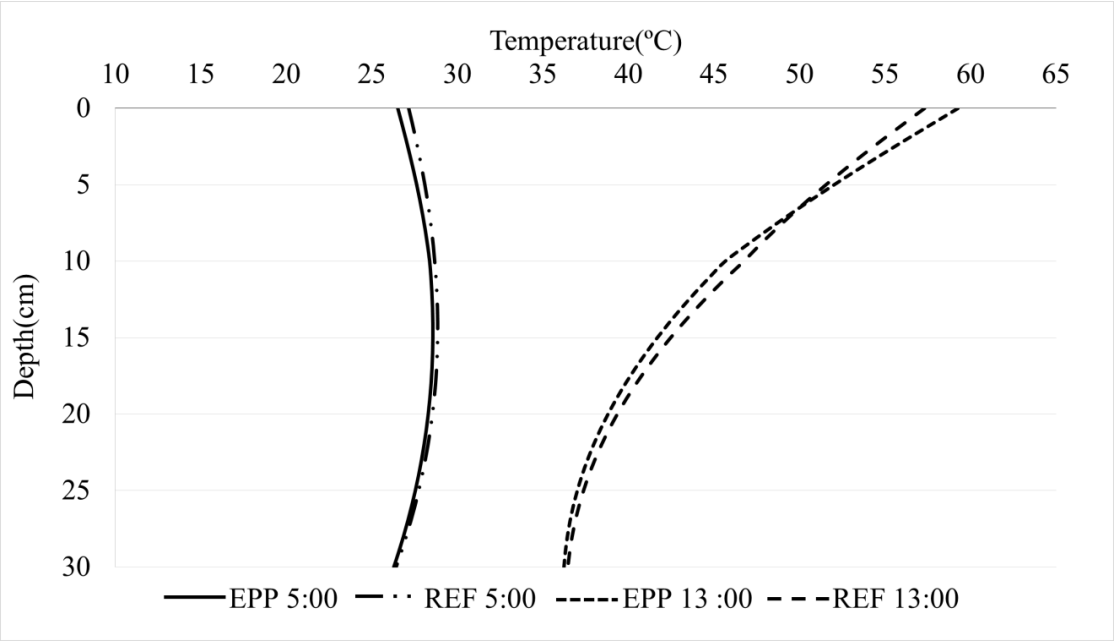

Figure 67. Comparison of temperature profiles of EPP and reference AC (summer)

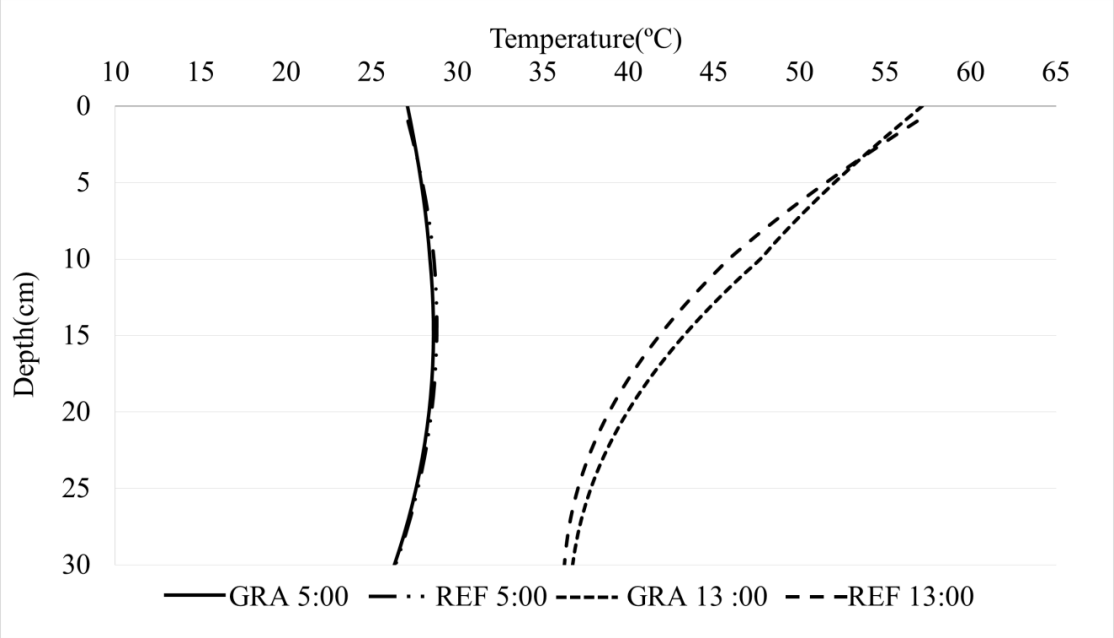

Figure 68. Comparison of temperature profiles of graphite and reference AC (summer)

Winter prediction

The temperature variations with time are compared in Figure 69 and Figure 70, and comparisons of temperature profiles are plotted in Figure 69 and Figure 70, they all have confirmed the conclusion that bottom boundary condition didn't change the trend of surface temperature distributions. It should be noted that although adding EPP decreases minimum surface temperature of bridge, which means decreased deicing ability, the maximum surface temperature increases as well. Compared to a 0.31ºC reduction in minimum temperature, the increase of maximum temperature of bridge by adding EPP is much higher (1.03ºC), this will contribute to a better ice and snow melting ability during day time. Regarding graphite case, although the minimum temperature increases a little bit (0.19ºC) in the night, the pavement becomes colder during daytime.

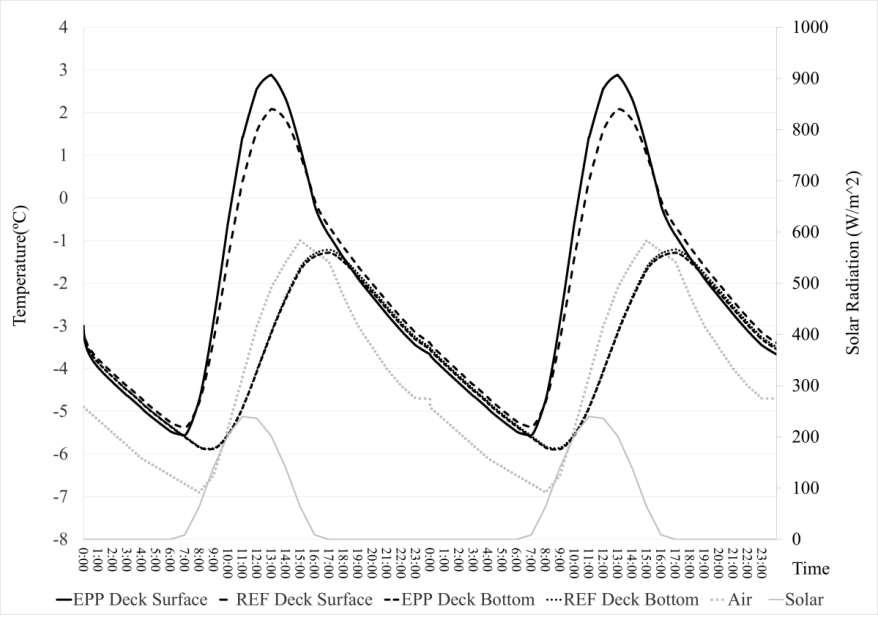

Figure 69. Comparison of surface and bottom temperatures of EPP and reference AC (winter)

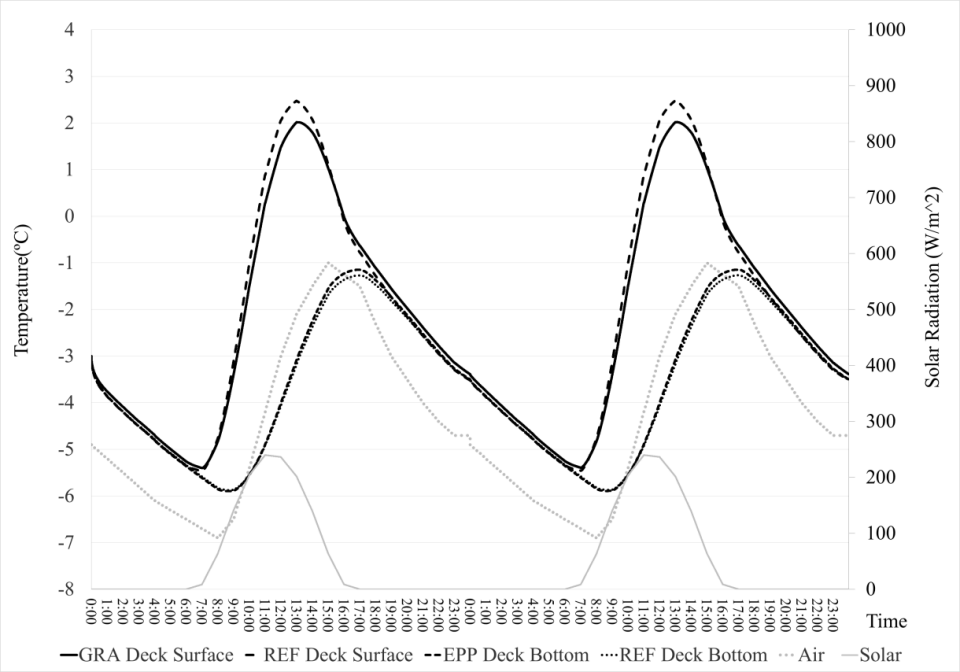

Figure 70. Comparison of surface and bottom temperatures of graphite and reference AC (winter)

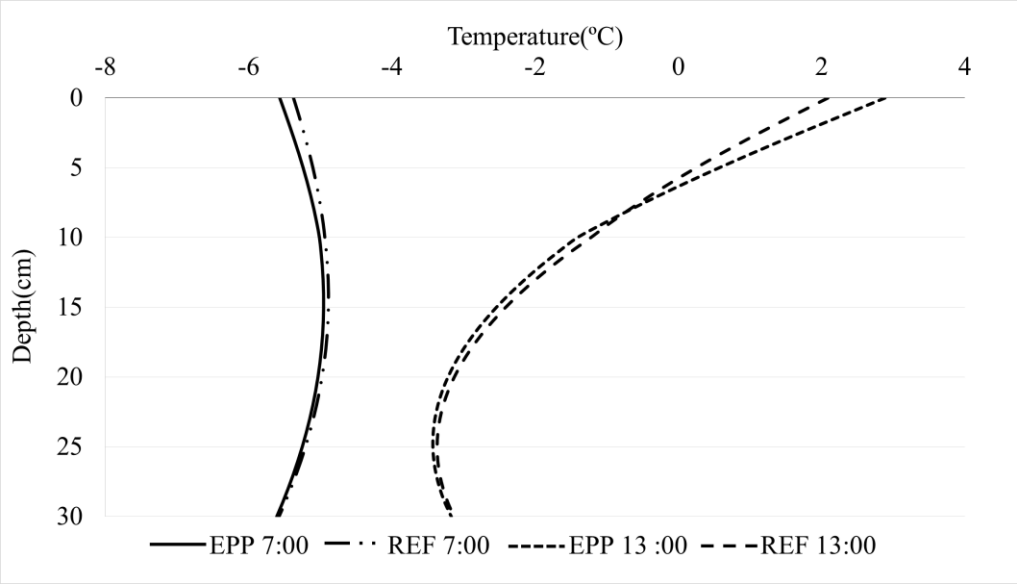

Figure 71. Comparison of temperature profiles of EPP and reference AC (winter)

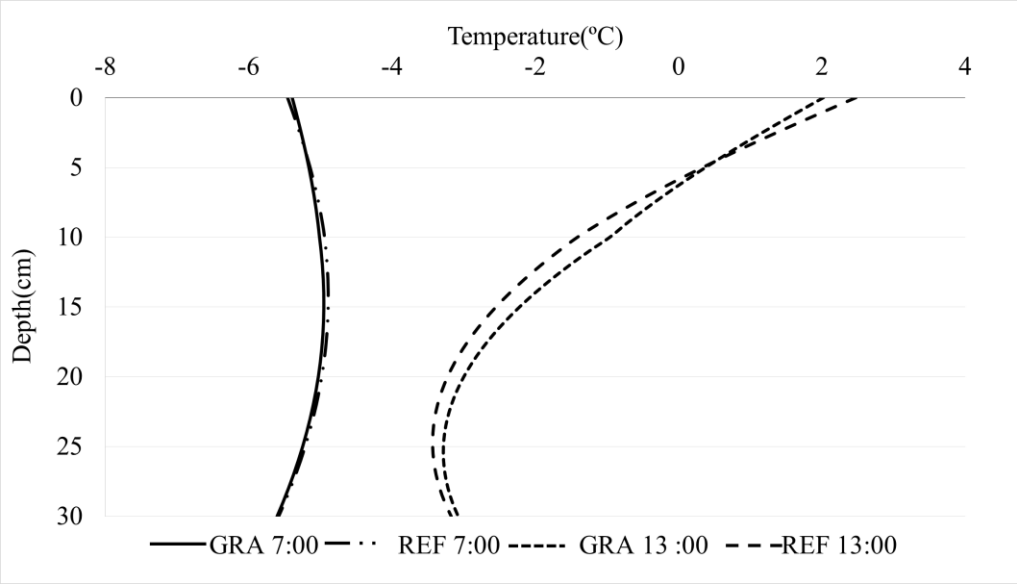

Figure 72. Comparison of temperature profiles of EPP and reference AC (winter)

A summary of simulation results with the probable thermal application of the additives is listed in Table 14.

Table 14. Summary of simulation results with probable thermal application

Structure	Season	Additives	Change in max surface temperature	Change in Min surface temperature	Mitigation of T-related problem
Pavement	Summer	EPP	+5.15	-0.83	N.A
		Graphite	-3.10	+0.57	Urban heat island effect
	Winter	EPP	+0.82	-0.58	Snow/Ice melting
		Graphite	-0.44	+0.45	Ice formation
Bridge	Summer	EPP	+3.36	-1.76	N.A
		Graphite	-1.87	+0.98	Urban heat island effect
	Winter	EPP	+1.03	-0.31	Snow/Ice melting
		Graphite	-0.61	+0.19	Ice formation

Note: The change is by comparison of the corresponding reference case. An increase is signed +, a decrease is signed –

5.3 Case Study: Heat Transfer of Construction Wall of Buildings

Previous study showed that adding EPP to asphalt concrete decreased both thermal conductivity and heat capacity of the mixture, leading to an increase of pavement surface temperature variation. The simulation clearly manifests that EPP modified asphalt concrete has pros and cons in deicing or mitigating urban heat island effect applications for both pavement and bridge. However, EPP has potential application for wall insulation. As a matter of fact, the construction wall of buildings requires good insulation so that it can improve energy efficiency. Because of thermal conductivity reduction caused by addition of EPP, modified concrete could be a potential choice of wall material to block the heat transfer between the domain inside building and outside building, the idea is shown in Figure 73.

In this case study, the theoretical background of heat transfer of wall system is introduced. Based on the basic heat transfer theory, a simple calculation is carried out by the author, and the feasibility of selecting EPP concrete as construction wall material is evaluated.

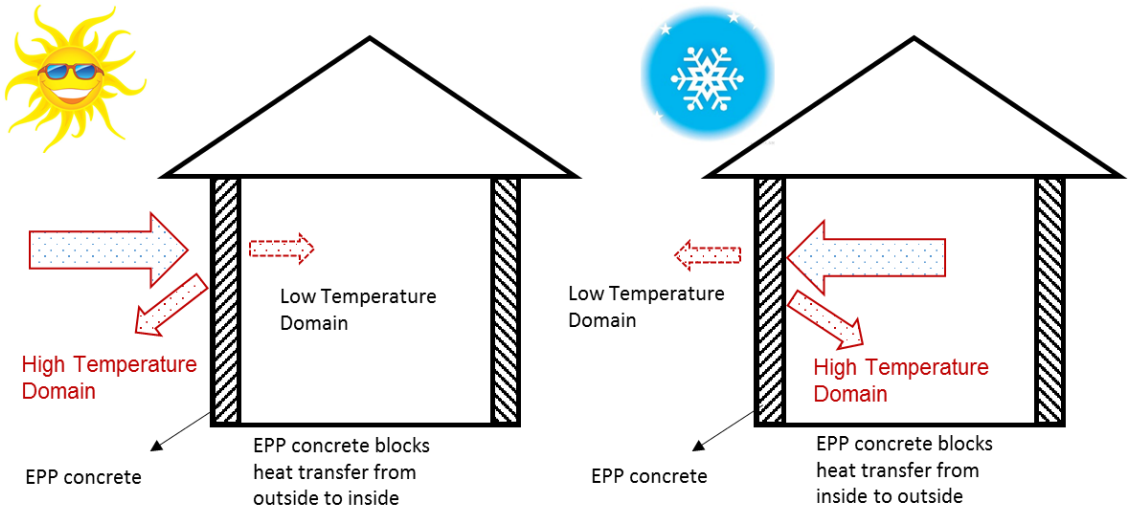

Figure 73. Using EPP concrete as wall insulator

5.3.1 Theoretical Background

In this case study, the heat transfer problem is simplified as one dimensional steady state model. The wall heat transfer system consists of three elements: two convection elements on each side of wall and one heat conduction element within in the wall. The wall is assumed to have homogenous material with constant thermal conductivity, each face is held at a constant uniform temperature.

Analogy between thermal and electrical concepts

The heat flow transfer model can be analogical to the electrical circuit model where heat flow (q) is represented by current, temperature (T) is represented by voltage and heat source are represented by constant current source. In case of the wall model, the convection elements are connected with wall conduction element in series. Radiation is

not considered in this study. The sketch of the heat transfer model of wall is explained in Figure 74.

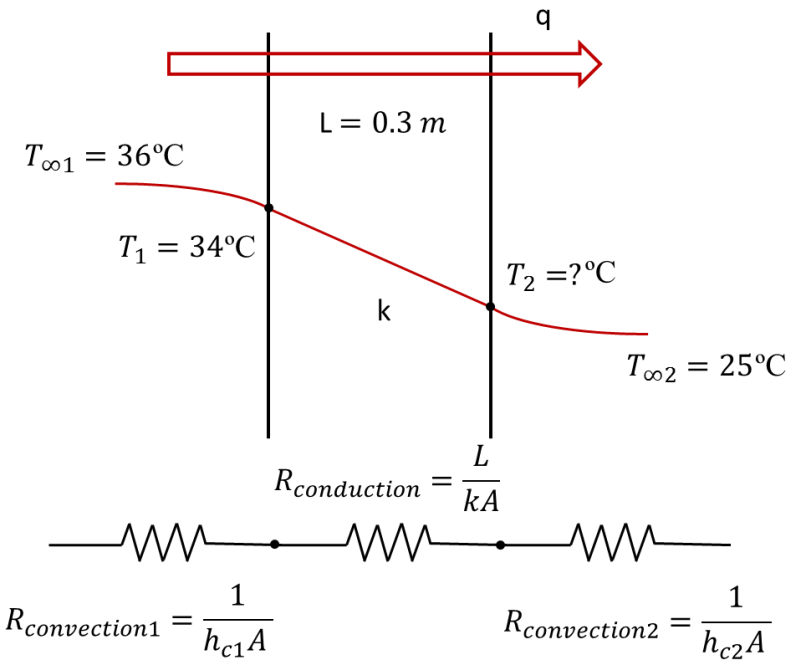

Figure 74. One dimensional steady state heat transfer model of wall

Thermal resistance concept

Like electrical resistance, the thermal resistance (R) is a measurement of a temperature difference by which an object or materials resists a heat flow.

Convection Resistance

The convection transfer can be explained as

$$q = h_c A_s (T_s - T_\infty) \quad (27)$$

Equation 27 can be written as:

$$q = \frac{T_S - T_\infty}{R_{convection}} \quad (28)$$

By comparing Equation 27 and Equation 28, the convection resistance is defined as:

$$R_{convection} = \frac{1}{h_c A_s} \quad (29)$$

In heat transfer at a boundary (surface) within a fluid, the Nusselt number (Nu) is written as:

$$Nu = \frac{h_c L}{k} \quad (30)$$

Where

L is characteristic length

k is thermal conductivity of the fluid

h_c is convective heat transfer coefficient of the fluid

Therefore, the average convective heat transfer coefficient ($\overline{h_c}$) for isothermal surface is:

$$\overline{h_c} = \frac{\overline{Nu}k}{L} \quad (31)$$

In natural convectional heat transfer, Rayleigh number (Ra) is obtained using:

$$\text{Ra} = \text{Gr} \times \text{Pr} \quad (32)$$

Where

Gr is Grashof number

Pr is Prandtl numer

The Grashof number is calculated as:

$$Gr = \frac{g\beta(T_S - T_\infty)L^3}{\upsilon^2} \quad (33)$$

Where

g is the acceleration of gravity

υ is kinematic viscosity

β is the coefficient of volume expansion, for ideal gas, $\beta = \frac{1}{T}$

The Nusselt number of the air is determined as follows (Pitts and Sissom 1998):

1) If $10^{-1} < Ra < 10^{4}$,

Nu is determined using Chart: *Correlation for heated vertical plate (McAdams 1954)* by correlating with Ra.

2) If $10^{4} < Ra < 10^{12}$,

$$\overline{Nu} = C(Ra)^{a} \tag{34}$$

Where

$C = 0.59$, $a = 1/4$ when $10^{4} < Ra < 10^{9}$

$C = 0.13$, $a = 1/3$ when $10^{9} < Ra < 10^{12}$

The properties values of gases including υ and Pr at atmospheric pressure can be checked in Holman (1997) at the mean film temperature $T_f = \frac{T_s + T_\infty}{2}$.

Conduction Resistance

One dimensional steady state conduction in a plane wall of homogeneous material having constant thermal conductivity and with each side held at a constant uniform temperature can be expressed as

$$q = kA\frac{(T_1 - T_2)}{L} \tag{35}$$

k is thermal conductivity of the wall material

A is the cross section area of the wall

T is the uniform surface temperature

Equation 35 gives:

$$q = \frac{(T_1 - T_2)}{R_{conduction}} \tag{36}$$

Where conduction resistance is defined as:

$$R_{conduction} = \frac{L}{kA} \tag{37}$$

5.3.2 Calculation

In this case study, it is assumed that a 0.3m thick plane wall has a 3m×3m cross section. The air temperature outside is 36ºC and the room temperature inside remains 25ºC by air conditioner. The temperature of the wall outer surface is 32ºC (Figure 75). The wall materials are selected as plain concrete and EPP modified concrete as two different cases, with the thermal conductivity listed in Table 15.

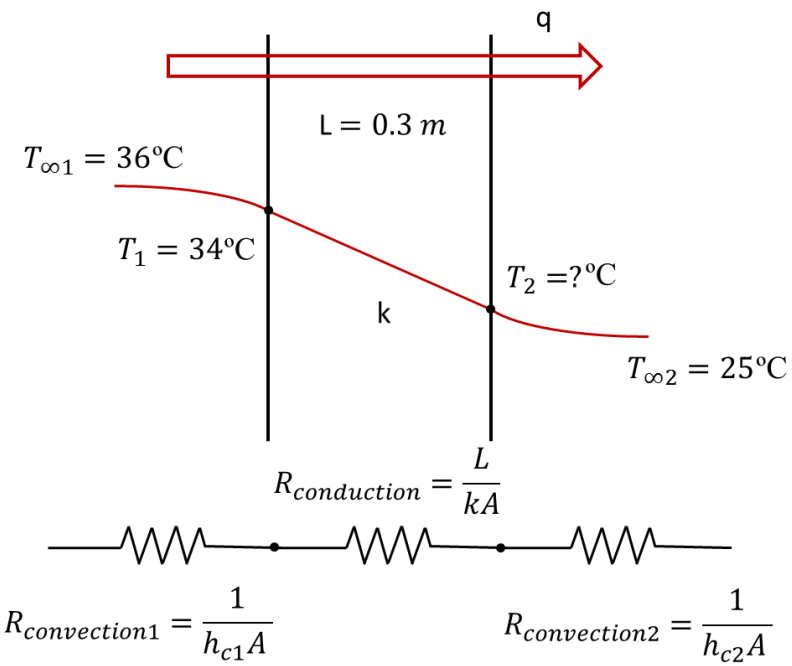

Figure 75. Case study problem explanation

Table 15. Thermal conductivity of wall material

Case	Type	Thermal Conductivity ($W/m \times K$)
#1	Plain concrete	2.13
#2	EPP modified concrete	1.25

The heat transferred by the air conditioner for two different case is calculated as follows, respectively:

The heat transfer follows:

$$q_{tr} = h_{c1}A(T_{\infty 1} - T_1) = \frac{kA}{L}(T_1 - T_2) = h_{c2}A(T_2 - T_{\infty 2}) \quad (38)$$

Mean film temperature outside is:

$$T_{f1} = \frac{T_1 + T_{\infty 1}}{2} = \frac{32+36}{2} = 34\ ^{o}\text{C} = 308\ \text{K} \quad (39)$$

Air properties at 308K is evaluated as: $k_{308} = 0.02685\ \ \text{W/m} \times \text{K}$, $\upsilon_{308} = 16.5012 \times 10^{-6}\ m^2/s$, $\beta_{308} = 0.00325\ T^{-1}$ $Pr_{308} = 0.705$ from Holman (1997).

Therefore, Grashof number for the air outside the wall is given by:

$$Gr_1 = \frac{g\beta(T_{\infty 1} - T_1)L^3}{\upsilon^2} = \frac{9.8 \times 0.00325 \times 4 \times 3^3}{(16.5012 \times 10^{-6})^2} = 1.26 \times 10^{10} \quad (40)$$

And Rayleigh number is

$$Ra_1 = \text{Gr} \times \text{Pr} = 1.26 \times 10^{10} \times 0.705 = 8.906 \times 10^9 \quad (41)$$

As $10^9 < Ra_1 < 10^{12}$, the air is turbulent, gives:

$$\overline{Nu_1} = C(Ra_1)^a = 0.13 \times (8.906 \times 10^9)^{1/3} = 269.47 \quad (42)$$

The convective heat transfer coefficient of the air outside the wall is obtained as:

$$\overline{h_{c_1}} = \frac{\overline{Nu}k_a}{L} = \frac{269.47 \times 0.02685}{3} = 2.41\ W/m^2 \times K \quad (43)$$

Hence, the heat transferred to the wall by convection is calculated by:

$$q_{tr} = h_{c1}A(T_{\infty 1} - T_1) = 2.41 \times 3 \times 3 \times (36 - 32) = 86.82\ \text{W} \quad (44)$$

Case 1 Plain concrete: k=2.13 $W/m \times K$

The conductive heat transfer in the wall gives:

$$q_{tr} = \frac{kA}{L}(T_1 - T_2) \quad (45)$$

Therefore,

$$T_2 = T_1 - \frac{q_{tr} \times L}{k \times A} = 32 - \frac{86.82 \times 0.3}{2.13 \times 3 \times 3} = 30.64\ ^{o}\text{C} \quad (46)$$

Mean film temperature inside is:

$$T_{f2} = \frac{T_2 + T_{\infty 2}}{2} = \frac{30.64 + 25}{2} = 27.82\ ^{o}\text{C} = 301.82\text{K} \quad (47)$$

Air properties at 302K is evaluated as: $k_{302} = 0.02639\ \text{W/m} \times \text{K}$, $\upsilon_{302} = 15.5928 \times 10^{-6} m^2/s$, $\beta_{302} = 0.00331 T^{-1}$, $Pr_{302} = 0.7076$ from Holman (1997).

Grashof number for the air inside the wall is given by:

$$Gr_2 = \frac{g\beta(T_2 - T_{\infty 2})L^3}{\upsilon^2} = \frac{9.8 \times 0.02639 \times (30.64 - 25) \times 3^3}{(15.5928 \times 10^{-6})^2} = 1.620 \times 10^{11} \quad (48)$$

And Rayleigh number is

$$\text{Ra}_2 = \text{Gr}_2 \times \text{Pr}_2 = 1.620 \times 10^{11} \times 0.7076 = 1.146 \times 10^{11} \quad (49)$$

As $10^9 < Ra_2 < 10^{12}$, the air is turbulent, gives:

$$\overline{Nu_2} = C(Ra_2)^a = 0.13 \times (1.146 \times 10^{11})^{1/3} = 631.48 \quad (50)$$

The averaged convective coefficient is:

$$\overline{h_{c2}} = \frac{\overline{Nu} k_a}{L} = \frac{631.48 \times 0.02639}{3} = 5.55\ W/m^2 \times K \quad (51)$$

The heat flow transferred by convection inside the wall is:

$$q_{conv2} = h_{c2} A(T_2 - T_{\infty 2}) = 5.55 \times 3 \times 3 \times (30.64 - 25) = 281.97\ \text{W} \quad (52)$$

To keep the net heat flow inside the wall same as the heat flow transferred to the wall from outside, the flow transferred by air conditioner is:

$$\Delta q = q_{conv2} - q_{tr} = 281.97 - 86.82 = 195.14\text{W} \quad (53)$$

Case 2 EPP concrete: k=1.25 $W/m \times K$

Followed as case 1 and using k=1.25W/m × K in equation 41, the inner surface temperature of the wall is calculated as 29.68ºC. The heat flow transferred by air conditioner is $\Delta q = 130.01$W.

Summary of calculations

Table 16 and Figure 76 and Figure 77 summarize the calculation results. From Figure 68, the temperature of inner surface of the plain concrete wall is calculated as 30.64C. Given the room temperature at 25ºC, 281.97W of heat flow is transferred by convection. To maintain the steady state, the air conditioner need to remove 195.14W heat flow. When modified the concrete with EPP and increased the insulation of the wall, the calculated the inner surface temperature reduces to 29.68ºC, around 1C cooler compared to the plain case. And the heat transferred by air conditioner is 130.01W, saving around 33% energy, as shown in Figure 77.

Table 16. Calculation results

Case	Thermal conductivity k (W/m × K)	Wall inner surface temperature T_2 (ºC)	Heat transferred by air conditioner Δq (W)
#1Plain Concrete	2.13	30.64	195.14
#2 EPP Concrete	1.25	29.68	130.01

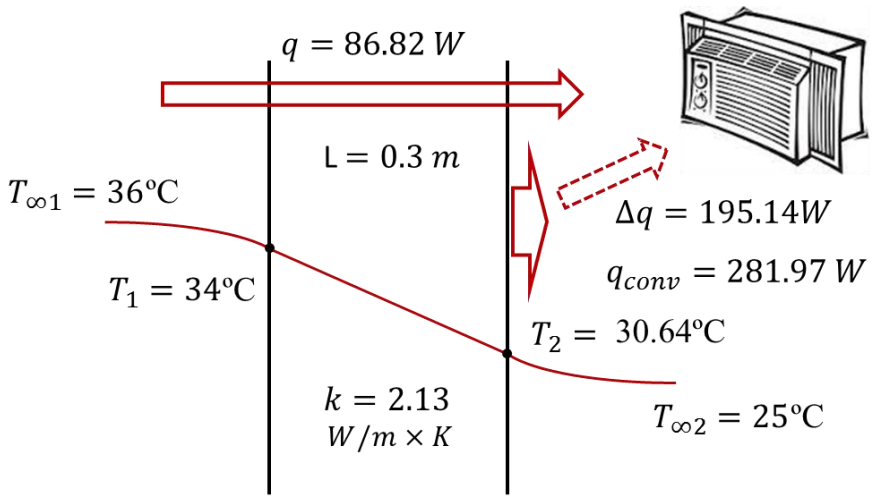

Figure 76. Heat transfer of plain concrete wall

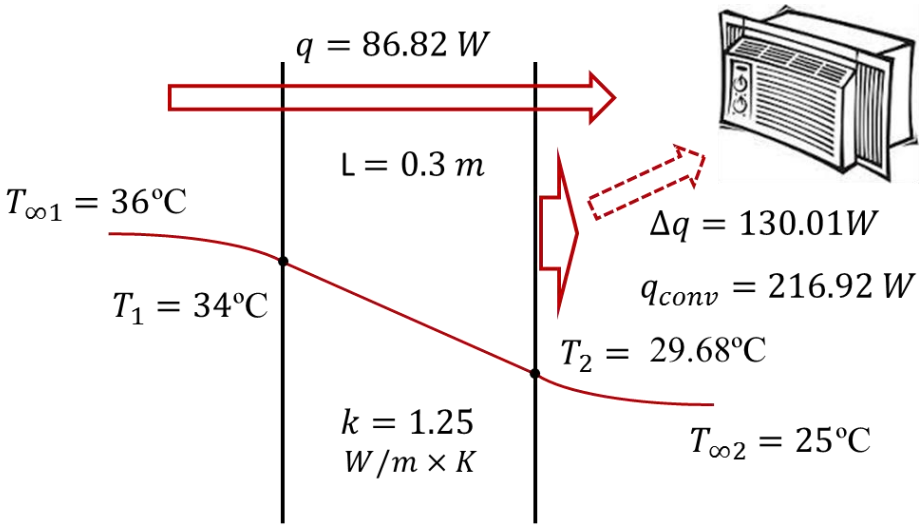

Figure 77. Heat transfer of EPP modified concrete wall

5.4 Summary of the Simulation Results

Simulation results with the major conclusion are summarized in Table 17.

Table 17. Summary of the simulation results with the potential thermal applications

Structures	Material Properties Comparison (SI Uints)	Season	Simulation results	Potential Thermal Applications
Pavement & Bridge	Reference AC: D-5:k=2.431 c=2.009× 10^6 D-6:k=1.936 c=1.807× 10^6 EPP Modified AC D-5:k=1.643 c=1.473× 10^6 Graphite Modified AC D-6:k=2.768 c=1.895× 10^6	Summer	1. EPP modified asphalt concrete layer increases pavement/bridge surface temperature variation while adding graphite decreases the variation. 2. Graphite AC layer reduces surface maximum temperature by 3.1ºC for pavement, and 1.9ºC for bridge, while EPP AC layer increases maximum temperature by 5.2ºC for pavement , and 3.4ºC for bridge, compared to their corresponding reference case.	Adding graphite into asphalt mixture benefits mitigating urban heat island effect for pavement and bridge
		Winter	1. Graphite AC layer increases minimum surface temperature by 0.5ºC, and 0.2ºC for bridge, while EPP AC layer decreases minimum temperature by 0.6ºC for pavement, and 0.3ºC for bridge, compared to their corresponding reference case. 2. Adding EPP increases maximum surface temperature by 0.8ºC for pavement, and 1.0ºC for bridge.	Adding graphite into asphalt concrete benefits deicing for pavement and bridge, adding EPP benefits snow and ice removal for pavement and bridge.

Table 17. Summary of the simulation results with the potential applications (continued)

Structures	Material Properties Comparison (SI Uints)	Season	Simulation results	Potential Thermal Applications
Pavement	Sensitivity Analysis: Thermal conductivity : k= 0.5/1.0/1.5/2.0/2.5/3.0 c=2.0× 10^6 Heat capacity: k=2.0 c=1.0/1.5/2.0/2.5/3.0 × 10^6	Winter	By either increasing thermal conductivity or heat capacity, pavement surface variation will decrese.	Higher thermal conductivity and higher heat capacity benefits pavement temperature distribution
Wall	Plain Concrete k=2.13 EPP Modified Concrete k=1.25	Summer	1. EPP concrete reduces wall inner surface temperature by around 1ºC compared to the plain concrete 2. EPP concrete saves 33% energy cost provided by air conditioner.	EPP concrete can serve as wall insulation

6. CONCLUSION AND FUTURE WORK

In this study, the use of the expanded polypropylene as a replacement of a part of aggregate and the graphite powder as a replacement of a part of filler in asphalt concrete were investigated. The heat susceptibility of the EPP beads was evaluated to confirm that the EPP does not melt during the mixing process of the hot mix asphalt concrete. The mechanical performance of the EPP and graphite modified asphalt concrete were examined via indirect tensile test. Their thermal properties were obtained using TPS machine.

Heat transfer through a pavement, bridge deck, and building wall were simulated, and the temperature distributions of different structures were evaluated using a discrete heat transfer model for non-steady state heat transfer (pavement and bridge deck) and heat equation for steady state heat transfer (building wall). The benefits and probable applications of thermally modified construction materials are discussed based on the numerical results.

Major findings from this study are summarized as follows:

1. It is hard to melt and mix EPP with asphalt binder, and the melted EPP in asphalt binder causes an exponential increase in viscosity. This implies that the EPP is better to be used as an aggregate replacement than a binder modifier.

2. The EPP has sufficient heat resistance for the mixing process. The EPP particles turned yellow and tended to stick together when placed in the oven during a whole night, but no change was observed during typical mixing hours and temperature. The EPP

modified asphalt mixtures are easy to compact, but a difficulty was found in controlling air void in the EPP asphalt concrete. The indirect tensile strength of the asphalt concrete containing the EPP is consistently lower than the control specimens.

3. Mixing graphite causes an increase in the mastic viscosity, and hence, compacting graphite modified asphalt concrete required more gyrations to control air voids. The asphalt concrete specimens containing appropriate amount of graphite (2.4-3.6% by the mixture volume) have higher IDT strength than the control specimens.

4. Thermal conductivity of asphalt concrete increases when the graphite content increases. The maximum increase in thermal conductivity is 43% with 4.8% volume content of graphite. No significant variation was observed in volumetric heat capacity by adding graphite. On the other hand, adding EPP up to 18% by volume of the mixture results in the decrease of both thermal conductivity and volumetric heat capacity. The maximum reductions are 32% in thermal conductivity and 27% in heat capacity.

5. Adding graphite into asphalt concrete drops the daily maximum temperature and raises the daily minimum temperature on the pavement surface. In other words, the graphite modified asphalt concrete reduces the amplitude of daily temperature variation at the pavement surface. In the simulation of using Texas typical weather data, graphite modified asphalt concrete reduces the surface maximum temperature by 3.1ºC at the pavement, and 1.9ºC at the bridge deck during the summer. This will be beneficial in mitigating urban heat island effect and saving energy for cooling. During the winter, adding graphite increases the minimum surface temperature by 0.5ºC at the pavement and 0.2ºC at the bridge deck, which can reduce the use of deicing agent. On the other hand,

the asphalt concrete with low thermal conductivity and heat capacity (the EPP modified) increases the temperature amplitude at pavement/bridge surface. In the simulation for the winter at Canada, the maximum surface temperature increases by 0.8ºC at the pavement and 1.0ºC at the bridge deck. This implies that the EPP modified concrete is a thermal insulator rather than a conductor. The beneficial application of the EPP modified concrete can be a concrete wall of the buildings, which will increase the temperature difference between the interior and exterior of the wall, and may save the energy for cooling and heating of buildings.

The following future work is recommended:

1. Adding graphite benefits pavement and bridge temperature distributions, helping with mitigation of heat island effect. Meanwhile, graphite is also used to impart electrical conductivity into pavement so that pavement has potential for various multifunctional applications such as self -healing, self-sensing, snow and ice removal, and energy harvesting (Baranikumar 2013). Combining the thermal and electrical applications is expected to bring additional benefits.

2. In terms of thermal effect, adding more graphite will bring a higher thermal conductivity, and be more effective in reducing the amplitude of temperature variation at pavement surfaces. On the other hand, when the graphite volume fraction exceeds 3.6%, the strength reduction is observed. To obtain higher thermal conductivity without the loss of mechanical performances, a combined use of steel fibers, graphite, and conductive aggregates will be investigated as the next step.

3. The EPP modified cementitious concrete has application potential to be used as a building insulation. However, the efficiency in energy and cost, and the structure performances of the EPP modified concrete should be evaluated for the practical application.

REFERENCES

Abtahi, S. M., Esfandiarpour, S., Kunt, M., Hejazi, S. M., and Ebrahimi, M. G. (2013). "Hybrid reinforcement of asphalt-concrete mixtures using glass and polypropylene fibers." *Journal of Engineered Fabrics & Fibers (JEFF)*, 8(2), 25-35.

Ahmed, Z., Marukic, I., Zaghloul, S., and Vitillo, N. (2005). "Validation of enhanced ntegrated climatic model predictions with New Jersey seasonal monitoring data." *Transportation Research Record: Journal of the Transportation Research Board*, 1913, 148-161.

Al-Hadidy, A., and Yi-Qiu, T. (2009). "Mechanistic approach for polypropylene-modified flexible pavements." *Materials & Design*, 30(4), 1133-1140.

Baranikumar, A. (2013). "Imparting electrical conductivity into asphalt composite using graphite.", M.S. thesis, Texas A&M University, College Station, TX.

Barber, E. S. (1957). "Calculation of maximum pavement temperatures from weather reports." *Highway Research Board Bulletin*(168), 1-8.

Chen, M., Wan, L., and Lin, J. (2012). "Effect of phase-change materials on thermal and mechanical properties of asphalt mixtures." *Journal of Testing and Evaluation*, 40(5), 746-753.

Chen, M., Wu, S., Wang, H., and Zhang, J. (2011). "Study of ice and snow melting process on conductive asphalt solar collector." *Solar Energy Materials and Solar Cells*, 95(12), 3241-3250.

Chen, M., Wu, S., Zhang, Y., and Wang, H. (2010). "Effects of conductive fillers on temperature distribution of asphalt pavements." *Physica Scripta*, T139(2010), 014046.

Chen, Y. (2013). "Deicing mechanism for crumb rubber asphalt pavement." *Journal of Central South University (Science and Technology)*, 44(5), 2073-2081.

Chen, Z., Wu, S. P., Chen, M. Z., and Wang, J. G. (2009). "Evaluation on solar heat reflective coatings to reduce asphalt concrete temperature." *Materials Science Forum*, 620, 181-184.

Dawson, A. R., Dehdezi, P. K., Hall, M. R., Wang, J., and Isola, R. (2012). "Enhancing thermal properties of asphalt materials for heat storage and transfer applications." *Road Materials and Pavement Design*, 13(4), 784-803.

Design, S. M. (1996). "Superpave series No. 2 (SP-2)." *Asphalt Institute, Lexington, KY*.

Fan, W., Kang, H., and Zheng, Y. (2010). "Experimental study of pavement performance of basalt fiber-modified asphalt mixture." *Journal of Southeast University (English Edition)*, 26(4), 614-617.

Gibson, R. F. (2010). "A review of recent research on mechanics of multifunctional composite materials and structures." *Composite Structures*, 92(12), 2793-2810.

Guan, B., Bo, G., Biao, M., and Fang, Q. (2011). "Application of asphalt pavement with phase change materials to mitigate urban heat island effect" *Proc., International Symposium on Water Resource and Environmental Protection*, IEEE, Beijing, China, 2389-2392.

Gui-juan, Z. (2010). "Test on evaluation index of deformation performance for polyester fiber reinforced asphalt concrete." *Proc., International Conference on Intelligent System Design and Engineering Application (ISDEA)*, IEEE, Changsha, China, 561-564.

Gui, J., Phelan, P. E., Kaloush, K. E., and Golden, J. S. (2007). "Impact of pavement thermophysical properties on surface temperatures." *Journal of Materials in Civil Engineering*, 19(8), 683-690.

Hermansson, A. (2000). "Simulation model for calculating pavement temperatures including maximum temperature." *Transportation Research Record: Journal of the Transportation Research Board*, 1699, 134-141.

Hermansson, A. (2001). "Mathematical model for calculation of pavement temperatures: Comparison of calculated and measured temperatures." *Transportation Research Record: Journal of the Transportation Research Board*, 1764, 180-188.

Holman, J. (1997). *Heat transfer*, McGraw-Hill, NY.

Houle, K. M., Roseen, R. M., Ballestero, T. P., Briggs, J. F., and Houle, J. J. (2009). "Examinations of pervious concrete and porous asphalt pavements performance for stormwater management in Northern climates." *Proc., World Environmental and Water Resources Congress*, ASCE, Kansas City, MO, 1105-1122.

Khan, A., and Mrawira, D. (2008). "Influence of selected mix design factors on the thermal behavior of lightweight aggregate asphalt mixes." *Journal of Testing and Evaluation*, 36(6), 492-499.

Mallick, R., Chen, B.-L., and Bhowmick, S. (2009). "Harvesting energy from asphalt pavements and reducing the heat island effect." *International Journal of Sustainable Engineering*, 2(3), 214-228.

MatWeb, LCC (2014). " Graphite, carbon, C." Thermal properties, <http://www.matweb.com/ > (April 20, 2014).

MatWeb, LCC (2014). " Portland Cement. " Thermal properties, <http://www.matweb.com/ > (April. 20, 2014).

McAdams, W. H. (1954). *Heat transmission*, McGraw-Hill, NY.

Minhoto, M. J., Pais, J. C., Pereira, P. A., and Picado-Santos, L. G. (2005). "Predicting asphalt pavement temperature with a three-dimensional finite element method." *Transportation Research Record: Journal of the Transportation Research Board*, 1919, 96-110.

Mrawira, D. M., and Luca, J. (2002). "Thermal properties and transient temperature response of full-depth asphalt pavements." *Transportation Research Record: Journal of the Transportation Research Board*, 1809, 160-171.

Othman, A. M. (2010). "Impact of polypropylene application method on long-term aging of polypropylene-modified HMA." *Journal of Materials in Civil Engineering*, 22(10), 1012-1018.

Park, P., Rew, Y., and Baranikumar, A. (2014). *Controlling conductivity of asphalt concrete with graphite*, Final Report for Southwest Region University Transportation Center (SWUTC), Texas A&M Transportation Institute, College Station, TX.

Pitts, D. R., and Sissom, L. E. (1998). *Schaum's outline of theory and problems of heat transfer*, McGraw-Hill, NY.

Rapp, D., and Hoffman, A. (1977). "On the relation between insolation and climatological variables—III. The relation between normal incidence solar intensity, total insolation, and weather at Fort Hood, Texas." *Energy Conversion*, 17(4), 163-172.

Roberts, F. L., Kandhal, P. S., Brown, E. R., Lee, D.-Y., and Kennedy, T. W. (1996). *Hot mix asphalt materials, mixture design and construction*. NAPA Education Foundation, MD.

Sebaaly, P., Lake, A., and Epps, J. (2002). "Evaluation of low-temperature properties of HMA mixtures." *Journal of Transportation Engineering*, 128(6), 578-586.

Solaimanian, M., and Kennedy, T. W. (1993). "Predicting maximum pavement surface temperature using maximum air temperature and hourly solar radiation." *Transportation Research Record: Journal of the Transportation Research Board*, 1417, 1-11.

Song, J. X., Chang, C. L., and Yang, H. R. (2011). "Comparing tests on water relating stability of polyester and polyacrylonitrile fiber reinforced asphalt mixture." *Advanced Materials Research*, 287, 742-746.

Tapkın, S. (2008). "The effect of polypropylene fibers on asphalt performance." *Building and Environment*, 43(6), 1065-1071.

Weather Source, LLC (2014), " Past weather reports. " Official weather: Fort Hood", <www.weathersource.com>(April. 22, 2014).

Wu, S. (2009). "Laboratory study on solar collector of thermal conductive asphalt." *International Journal of Pavement Research and Technology*, 2(4), 130-136.

Wu, S. P., Li, B., Wang, H., and Qiu, J. (2008). "Numerical simulation of temperature distribution in conductive asphalt solar collector due to pavement material parameters." *Materials Science Forum*, 575, 1314-1319.

Xie, J. G., Yang, Z. X., Fang, X. Q., and Hu, Y. (2011). "The Performance of low-heat accumulation asphalt mixture and the evaluation model of its thermal effect on cities." *Advanced Materials Research*, 287, 1795-1804.

Xiong, R., Chen, S., Guan, B., Cong, P., and Ma, L. (2011). "High temperature stability of brucite fiber-reinforced asphalt concrete." *Proc., Third International Conference on Transportation Engineering (ICTE)*, ASCE, Chengdu, China, 2002-2007.

Yavuzturk, C., Ksaibati, K., and Chiasson, A. (2005). "Assessment of temperature fluctuations in asphalt pavements due to thermal environmental conditions using a two-dimensional, transient finite-difference approach." *Journal of Materials in Civil Engineering*, 17(4), 465-475.

Yeh, P. H., Nien, Y. H., Chen, J. H., Chen, W. C., and Chen, J. S. (2005). "Thermal and rheological properties of maleated polypropylene modified asphalt." *Polymer Engineering & Science*, 45(8), 1152-1158.

Yunus, A. C. (2003). *Heat transfer: a practical approach*, 2nd Ed., McGraw-Hill, NY.

Zhao, L. H., Xu, G., and Zhao, J. (2011). "Research of the low temperature crack resistance for the mineral fiber rein-forced asphalt mixture." *Applied Mechanics and Materials*, 97, 172-175.

Zhao, X. H., and Zhang, X. D. (2011). "The research on the anti-icing and pavement performance of the chloride-stored asphalt mixture." *Applied Mechanics and Materials*, 97, 321-326.

APPENDIX

A1. Sieve Analysis of Aggregates

- D-5 Gradation

Table 18. Aggregate gradation of D-5 mixture

Sieve size (mm)	*% Passing Aggregate*	*% Remain Aggregate*	*Specification D-5 mix*
19	100	0	100
12.5	95	5	90-100
9.5	82	7	
4.75	55	23	44-74
2.36	34	25	28-58
1.18	22	20	
0.6	16	8	
0.3	12	4	5-21
0.15	6	3	
0.075	5	0	2-10

Nominal maximum size: 9.5mm

Maximum size: 12.5mm

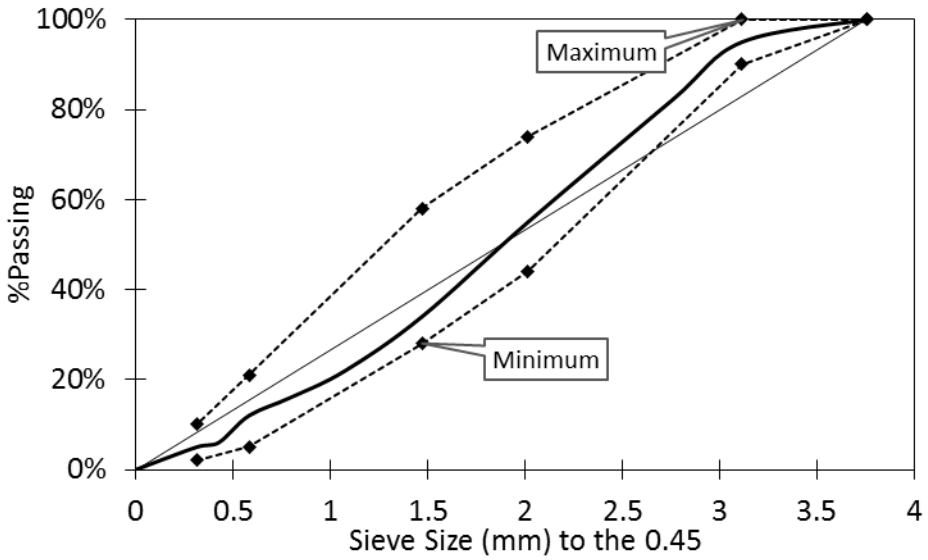

Figure 78. Sieve analysis of D-5 mix

- D-6 Gradation

Table 19. Aggregate gradation of D-6 mixture

Sieve size (mm)	*% Passing Aggregate*	*% Remain Aggregate*	*Specification D-6 mix*
19	100	0	
12.5	99.9	0	100
9.5	95.3	5	90-100
4.75	68.1	20	55-85
2.36	50.8	15	32-67
1.18	35.3	25	
0.6	21.0	15	
0.3	11.5	8	7-23
0.15	7.2	7	
0.075	6.1	0	2-10

Nominal maximum size: 4.75mm

Maximum size: 9.5mm

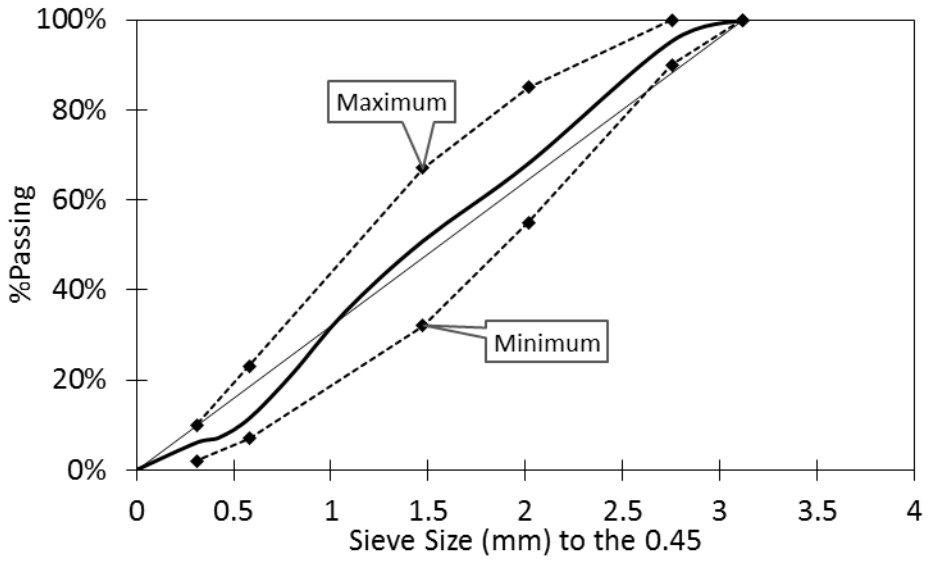

Figure 79. Sieve analysis of D-6 mix

A2. Determination of Binder Content

- D-5: 4.37% for 4% Air Void

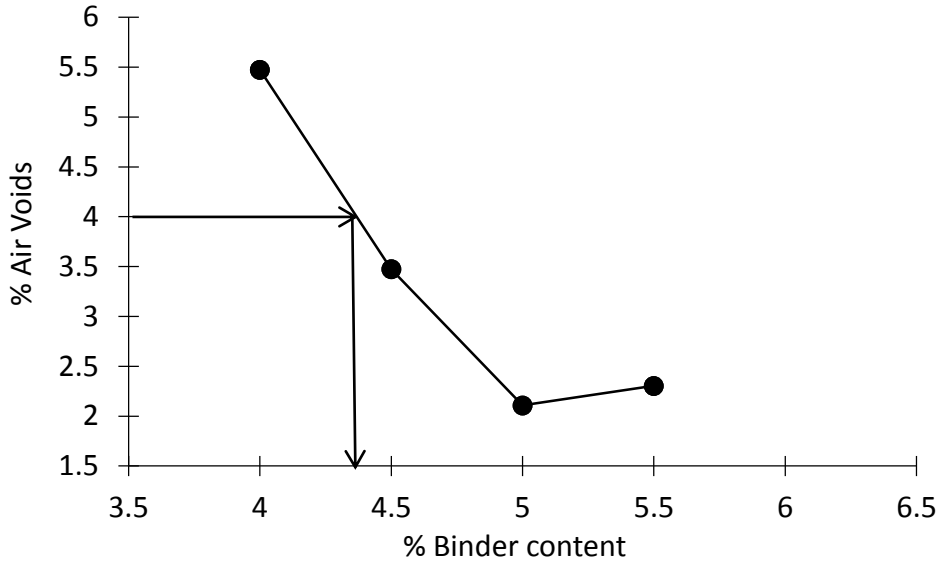

Figure 80. Air voids versus % binder content of D-5 mixture

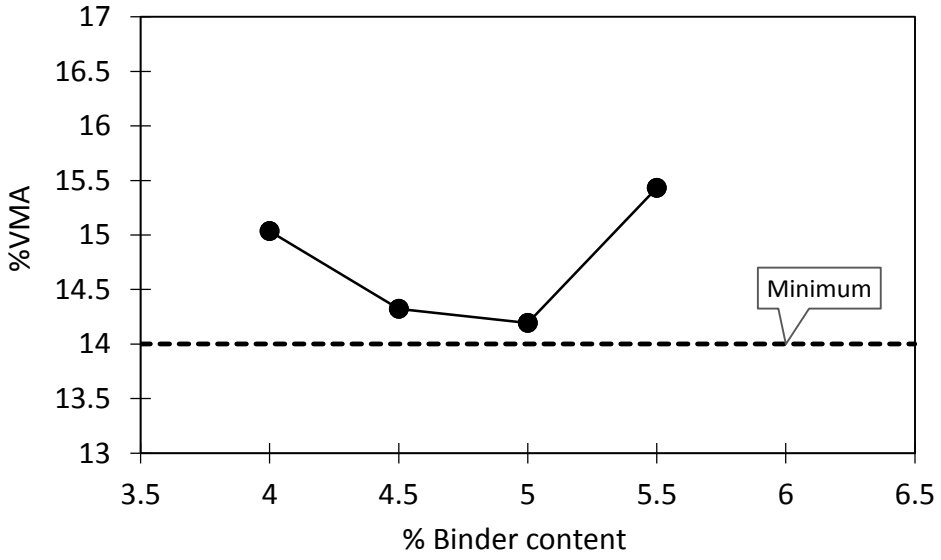

Figure 81. VMA versus % binder content of D-5 mixture

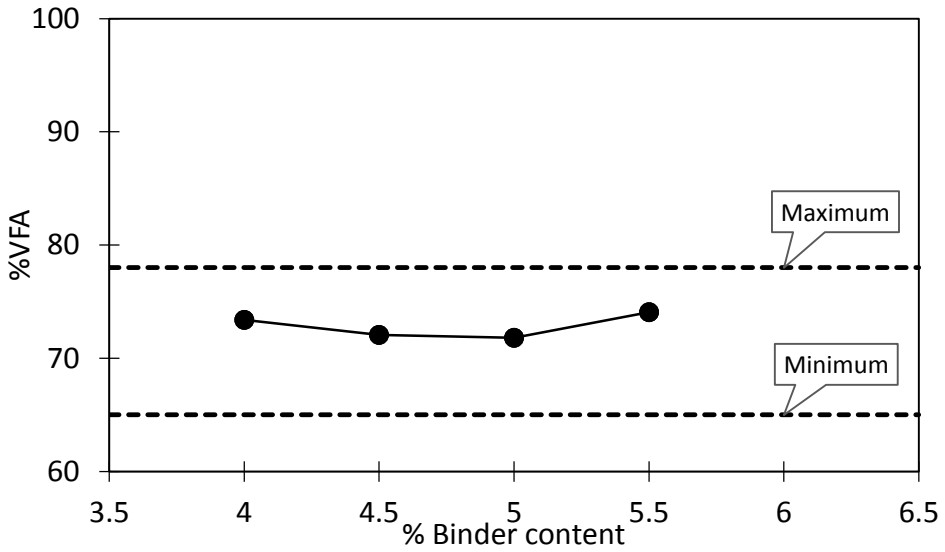

Figure 82. VFA versus % binder content of D-5 mixture

- D-6: 5.3% for 4% Air Void

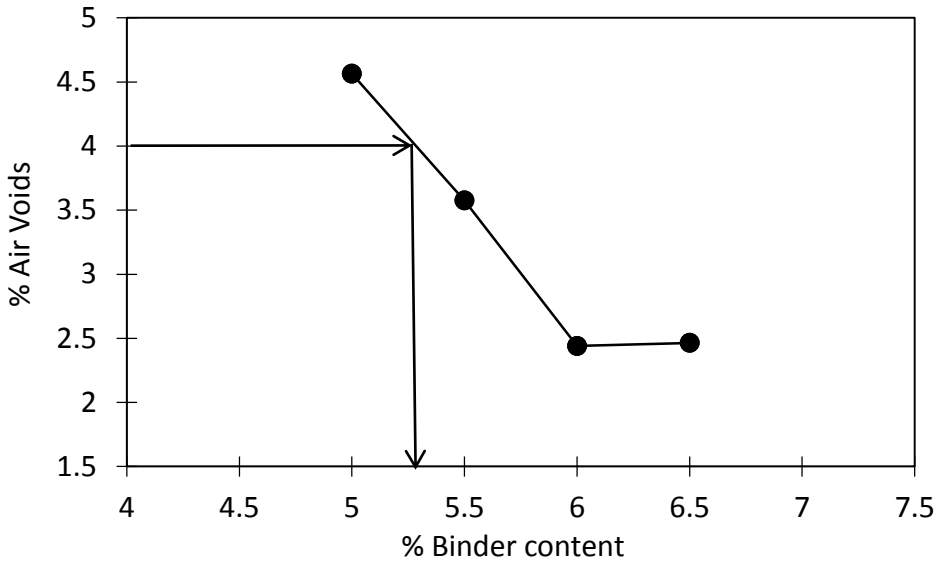

Figure 83. Air voids versus % binder content of D-6 mixture

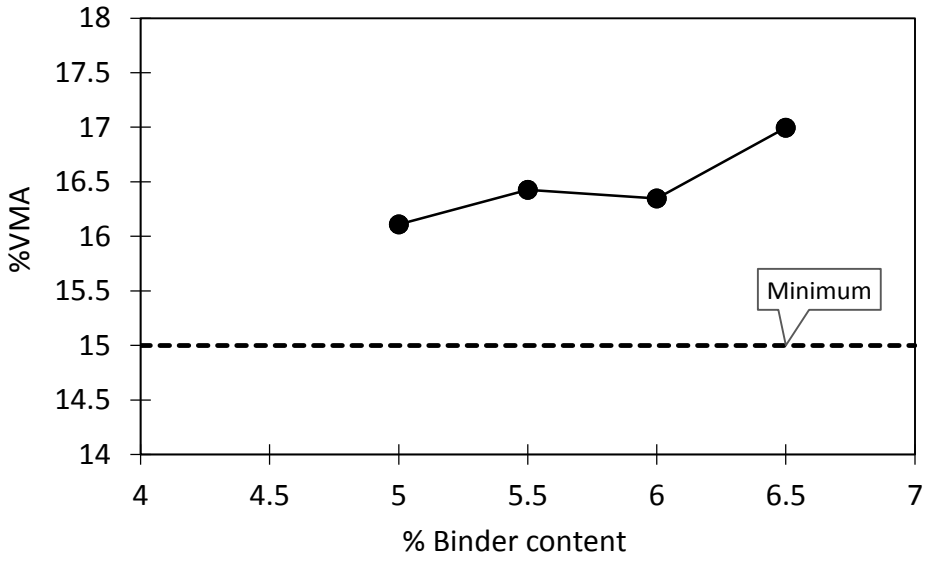

Figure 84. VMA versus % binder content of D-6 mixture

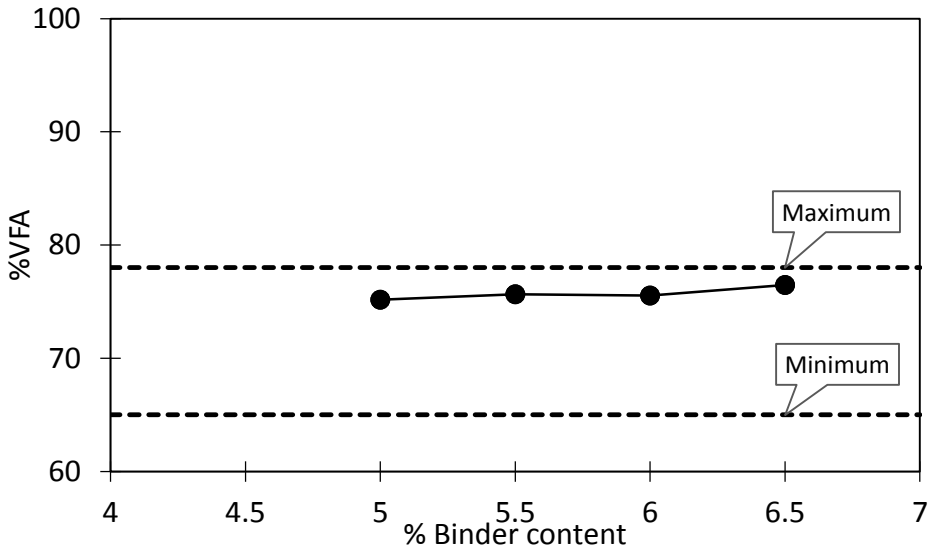

Figure 85. VFA versus % binder content of D-6 mixture

A3. Volumetric Parameters of Modified Asphalt Concrete Specimens

Table 20. Volumetric parameters of EPP modified asphalt concrete (D-5)

Specimens	*Wt in air*	*Wt under Water*	*Wt of SSD*	*Gmb*	*Gmm*	*AV*	*Gyrations*	*Purpose*
REF-D-5-AC								
1	3911.0	2268.4	3921.1	2.37	2.45	3.54	258	IDT
2	3910.1	2266.0	3919.3	2.36	2.45	3.60	258	IDT
3	3912.1	2268.5	3920.3	2.37	2.45	3.46	210	TP
REF-D-5-GC								
1	3907.3	2265.0	3912.1	2.37	2.45	3.30	115	IDT
2	3910.3	2278.4	3923.4	2.38	2.45	3.11	115	IDT
EPP-20%-AC								
1	3902.1	2258.2	3906.7	2.37	2.43	2.83	54	IDT
2	3845.9	2206.5	3852.6	2.34	2.43	4.09	30	IDT
3	3802.6	2165.6	3811.4	2.31	2.43	5.15	25	TP
EPP-60%-AC								
1	3764.2	2130.3	3771.7	2.29	2.39	4.17	11	IDT
2	3790.5	2160.8	3796.8	2.32	2.39	3.17	16	IDT
3	3766.2	2140.6	3773.6	2.31	2.39	3.62	11	TP
EPP-100%-AC								
1	3644.7	2029.4	3657.1	2.24	2.38	5.92	5	IDT
2	3621.8	2016.4	3638.9	2.23	2.38	6.21	5	IDT
3	3418.0	1896.9	3436.8	2.22	2.38	6.74	4	TP
EPP-10%-GC								
1	3863.0	2246.4	3868.8	2.38	2.44	2.53	115	IDT
2	3873.8	2257.6	3879.3	2.39	2.44	2.22	115	IDT
3	3870.3	2259.4	3874.8	2.40	2.44	1.92	115	Stored
EPP-20%-GC								
1	3850.7	2259.0	3852.5	2.42	2.43	0.40	115	IDT
2	3841.3	2249.0	2844.4	2.40	2.43	0.76	115	IDT
3	3839.2	2249.2	3841.8	2.41	2.43	0.64	115	Stored
EPP-40%-GC								
1	3778.3	2211.0	3778.5	2.41	2.39	-0.73	115	IDT
2	2785.6	2213.4	3786.2	2.40	2.39	-0.58	115	IDT
3	3783.0	2212.5	3783.6	2.40	2.39	-0.62	115	IDT
EPP-60%-GC								
1	3735.9	2180.0	3736.6	2.40	2.37	-1.16	115	IDT
2	3708.8	2162.5	3710.4	2.40	2.37	-1.00	115	IDT
3	3382.1	1864.2	3382.8	2.23	2.37	6.12	115	Discarded
EPP-80%-GC								
1	3775.1	2195.0	3776.2	2.39	2.36	-1.11	115	IDT
2	3730.7	2171.4	3732.0	2.39	2.36	-1.24	115	IDT
3	3460.4	2012.3	3461.2	2.39	2.36	-1.15	115	Stored

Table 21. Volumetric parameters of graphite modified asphalt concrete (D-6)

Specimens	*Wt in air*	*Wt under Water*	*Wt of SSD*	*Gmb*	*Gmm*	*AV*	*Gyrations*	*Purpose*
REF-D-6-AC								
1	3911.0	2268.4	3921.1	2.37	2.45	3.54	258	IDT
2	3910.1	2266.0	3919.3	2.36	2.45	3.60	258	IDT
3	3912.1	2268.5	3920.3	2.37	2.45	3.46	210	IDT
GRA-10%-AC								
1	3902.1	2258.2	3906.7	2.37	2.43	2.83	54	IDT
2	3845.9	2206.5	3852.6	2.34	2.43	4.09	30	IDT
3	3802.6	2165.6	3811.4	2.31	2.43	5.15	25	TP
GRA-15%-AC								
1	3764.2	2130.3	3771.7	2.29	2.39	4.17	11	IDT
2	3790.5	2160.8	3796.8	2.32	2.39	3.17	16	IDT
3	3766.2	2140.6	3773.6	2.31	2.39	3.62	11	TP
GRA-20%-AC								
1	3644.7	2029.4	3657.1	2.24	2.38	5.92	5	IDT
2	3621.8	2016.4	3638.9	2.23	2.38	6.21	5	IDT
3	3418.0	1896.9	3436.8	2.22	2.38	6.74	4	TP

A4. Indirect Tensile Test Results

Table 22. IDT strength of EPP modified asphalt concrete

Sample	S_T *(MPa)*
REF-D-5-AC	
1	1.18
2	1.27
REF-D-5-GC	
1	1.05
2	1.10
EPP-20%-AC	
1	1.20
2	1.04
EPP-60%-AC	
1	0.90
2	1.14
EPP-100%-AC	
1	1.06
2	0.97
EPP-10%-GC	
1	1.05
2	1.09
EPP-20%-GC	
1	1.17
2	1.26
EPP-40%-GC	
1	1.13
2	1.13
EPP-60%-GC	
1	1.25
2	1.29
EPP-80%-GC	
1	1.14
2	1.19

Table 23. IDT strength of graphite modified asphalt concrete

Sample	S_T *(MPa)*
REF-D-6-AC	
1	1.12
2	1.04
3	1.21
GRA-10%-AC	
1	0.97
GRA-15%-AC	
1	1.06
GRA-20%-AC	
1	1.27
2	1.43
3	1.32
GRA-25%-AC	
1	1.53
2	1.73
3	1.46
GRA-30%-AC	
1	1.50
2	1.50
3	1.63
GRA-35%-AC	
1	1.11
GRA-40%-AC	
1	0.90

A5. Thermal Properties of Modified Asphalt Concrete

Table 24. Thermal properties of EPP modified asphalt concrete

Specimen	*Thermal Conductivity* $(W/m \times K)$	*Volumetric Heat Capacity* $(MJ/m^3 \times K)$	*Specimen*	*Thermal Conductivity* $(W/m \times K)$	*Volumetric Heat Capacity* $(MJ/m^3 \times K)$
REF-D-5			REF-D-5		
1	2.189	1.838	7	2.475	2.258
2	2.259	1.871	8	2.294	1.834
3	2.326	2.072	9	2.532	1.861
4	2.658	2.258	10	2.427	1.828
5	2.669	2.402	11	2.454	1.853
6	2.419	2.029	12	2.469	1.999
EPP-20%-AC			EPP-20%-AC		
1	2.186	1.928	7	2.364	1.804
2	2.190	1.967	8	2.380	2.011
3	2.362	2.100	9	2.346	1.895
4	2.293	1.981	10	2.422	2.216
5	2.124	1.870	11	2.135	1.813
6	2.127	2.277	12	2.082	1.963
EPP-60%-AC			EPP-60%-AC		
1	1.889	1.987	7	2.152	2.003
2	1.889	1.945	8	2.214	2.194
3	1.899	1.583	9	2.075	1.661
4	1.849	1.485	10	2.154	2.129
5	1.831	1.715	11	1.848	1.249
6	1.825	1.634	12	1.925	1.523
EPP-100%-AC			EPP-100%-AC		
1	1.645	1.21	7	1.673	1.278
2	1.942	1.718	8	1.458	1.514
3	1.561	1.578	9	1.457	1.474
4	1.662	1.882	10	1.571	1.727
5	1.797	1.592	11	1.604	1.125
6	1.764	1.49	12	1.584	1.082

Table 25. Thermal properties of graphite modified asphalt concrete

Specimen	*Thermal Conductivity* $(W/m \times K)$	*Volumetric Heat Capacity* $(MJ/m^3 \times K)$	*Specimen*	*Thermal Conductivity* $(W/m \times K)$	*Volumetric Heat Capacity* $(MJ/m^3 \times K)$
REF-D-6			REF-D-6		
1	1.989	2.098	7	1.846	1.867
2	1.961	1.957	8	1.835	1.700
3	1.819	1.677	9	2.012	1.635
4	1.834	1.822	10	2029	2.149
5	2.087	1.514	11	1.853	1.799
6	2.084	1.543	12	1.887	1.922
GRA-10%-AC			GRA-10%-AC		
1	1.974	1.849	7	1.982	1.954
2	1.948	1.962	8	1.984	2.067
3	1.895	1.840	9	1.812	1.514
4	1.902	1.862	10	1.792	1.119
5	1.944	2.097	11	2.007	2.065
6	1.946	2.251	12	2.061	2.382
GRA-15%-AC			GRA-15%-AC		
1	2.055	1.970	7	1.995	1.841
2	2.052	1.901	8	2.155	2.212
3	2.348	2.189	9	2.008	1.689
4	2.354	2.297	10	1.993	1.671
5	2.470	2.813	11	2.114	2.182
6	2.057	2.010	12	2.109	2.121
GRA-20%-AC			GRA-20%-AC		
1	2.135	1.819	7	2.160	1.256
2	2.126	1.739	8	2.223	1.611
3	2.479	1.918	9	2.287	1.659
4	2.372	1.673	10	2.295	1.702
5	2.244	1.795	11	2.632	2.156
6	2.189	1.693	12	2.639	2.269

Table 25. Thermal properties of graphite modified asphalt concrete (continued)

Specimen	*Thermal Conductivity* $(W/m \times K)$	*Volumetric Heat Capacity* $(MJ/m^3 \times K)$	*Specimen*	*Thermal Conductivity* $(W/m \times K)$	*Volumetric Heat Capacity* $(MJ/m^3 \times K)$
GRA-25%-AC			GRA-25%-AC		
1	2.730	2.285	7	2.507	1.825
2	2.601	2.401	8	2.477	1.754
3	2.393	1.769	9	2.505	1.875
4	2.277	1.504	10	2.504	1.908
5	2.334	1.759	11	2.666	1.906
6	2.426	2.127	12	2.681	2.018
GRA-30%-AC			GRA-30%-AC		
1	2.402	1.555	7	2.567	1.801
2	2.690	1.950	8	2.819	2.132
3	2.575	1.656	9	2.370	1.517
4	2.579	2.017	10	2.404	1.734
5	2.596	2.187	11	2.701	2.251
6	2.530	1.657	12	2.637	2.096
GRA-35%-AC			GRA-35%-AC		
1	2.837	2.038	7	2.880	2.189
2	2.788	1.925	8	2.632	1.558
3	2.367	1.422	9	2.726	2.022
4	2.422	1.726	10	2.603	1.753
5	2.494	1.508	11	2.528	1.524
6	2.811	2.525	12	2.609	1.712
GRA-40%-AC			GRA-40%-AC		
1	2.610	1.553	7	2.987	2.348
2	2.635	1.631	8	2.969	2.360
3	2.538	1.285	9	2.776	1.934
4	3.035	2.764	10	2.803	2.011
5	2.757	1.562	11	2.686	1.924
6	2.831	1.718	12	2.589	1..648